Engin. Library
Aud O
MAY 28 1932

U. S. DEPARTMENT OF COMMERCE

BUREAU OF STANDARDS JOURNAL OF RESEARCH

Vol. 8 MAY, 1932 No. 5

CONTENTS

RP. No.	TITLE AND AUTHOR	Page
434.	A contribution relative to the structure of collagen. John Beek, jr	549
435.	Graphical determination of polar pattern of directional antenna systems. G. L. Davis and W. H. Orton	555
436.	Manufacture of calcium gluconate by the electrolytic oxidation of dextrose. Horace S. Isbell, Harriet L. Frush, and F. J. Bates	571
437.	Simplified automatic Wilson chamber. L. F. Curtiss	579
438.	Ionization of normal decane from petroleum by distillation and equilibrium melting. Johannes H. Bruun and Mildred M. Hicks-Bruun	583
439.	A laboratory apparatus for the continuous extraction of liquids by low boiling solvents. R. T. Leslie	591
440.	Volume changes of cast irons during casting. E. J. Ash and C. M. Saeger, jr	601
441.	A study of the delta lactones by the oxidation of aldoses with bromine water. Horace S. Isbell	615
442.	Effect of antimony on the mechanical properties of a bearing bronze (Cu 80 : Sn 10 : Pb 10). C. E. Eggenschwiler	625
443.	Investigation of the method of determining the relation of statical hysteresis and flexural stress by measurement of the decrement of a freely-vibrating U bar. G. H. Keulegan	635
444.	An unrecognized property of the reversible pendulum. Paul R. Heyl	657
445.	A method for the accurate determination of cobalt in magnetic and high-speed tool steels. James I. Hoffman	659

BUREAU OF STANDARDS JOURNAL OF RESEARCH

CONTENTS OF RECENT NUMBERS

December, 1931 (Vol. 7, No. 6)

RP387. The life of the saggar as affected by varying certain properties. R. A. Heindl and L. E. Mong. Price, 10 cents.

RP388. Thermal expansion of heat-resisting alloys: Nickel-chromium, iron-chromium, and nickel-chromium-iron alloys. Peter Hidnert. Price, 25 cents.

RP389. The physical properties of cast stone. John Tucker, jr., G. W. Walker, and J. Arthur Swenson. Price, 5 cents.

RP390. Investigations of Kennelly-Heaviside layer heights for frequencies between 1,600 and 8,650 kilocycles per second. T. R. Gilliland, G. W. Kenrick, and K. A. Norton. Price, 10 cents.

RP391. Determination of insoluble matter in shellac. C. C. Hartman. Price, 5 cents.

RP392. Derivatives of 4-glucosido-mannose. Horace S. Isbell. Price, 10 cents.

RP393. Thermal expansions of gasolines from 0° to 30° C. C. S. Cragoe and E. E. Hill. Price, 5 cents.

RP394. Tests of integral and surface waterproofings for concrete. C. H. Jumper. Price, 10 cents.

RP395. The effect of pH on the photochemical decomposition of silk. Milton Harris and Daniel A. Jessup. Price, 5 cents.

January, 1932 (Vol. 8, No. 1)

RP396. The preparation of crystalline methyl-*d*-gulosides by means of coordination compounds with calcium chloride. Horace S. Isbell. Price, 5 cents.

RP397. International comparison of X-ray standards. Lauriston S. Taylor. Price, 10 cents.

RP398. Volumetric determination of pentoses and pentosans. G. M. Kline and S. F. Acree. Price, 5 cents.

RP399. A method for determining the volume changes occurring in metals during casting. C. M. Saeger, jr., and Eugene J. Ash. Price, 10 cents.

RP400. Registration of cathode rays by thin films of metals and metal compounds. Warren W. Nicholas and C. G. Malmberg. Price, 5 cents.

RP401. Effect of casting temperature and of additions of iron on bearing bronze (Cu 80 : Sn 10 : Pb 10). C. E. Eggenschwiler.

RP402. Ultrasonic measurements of the compressibility of solutions and of solid particles in suspension. Chester R. Randall. Price, 10 cents.

RP403. On elimination of liquid potentials with potassium chloride and ammonium chloride. G. M. Kline, M. R. Meacham, and S. F. Acree. Price, 5 cents.

RP404. An electrostatic voltmeter. Warren W. Nicholas Price, 5 cents.

RP405. The heats of combustion of methyl and ethyl alcohols. Frederick D. Rossini.

RP406. A clock-controlled constant-frequency generator. A. B. Lewis.

February, 1932 (Vol. 8, No. 2)

RP407. Deteriorative effect of sulphur dioxide upon paper in an atmosphere of constant humidity and temperature. Arthur E. Kimberly.

RP408. Tensile properties of rail steels at elevated temperatures. G. Willard Quick.

RP409. The resistance to impact of rail steels at elevated temperatures. G. Willard Quick.

RP410. Kaolins; effect of firing temperature on some of their physical properties. R. A. Heindl, W. L. Pendergast, and L. E. Mong.

Research papers, where price is given, are already available, and others will be available in the near future as separates for purchase from the Superintendent of Documents, United States Government Printing Office, Washington, D. C.

U. S. DEPARTMENT OF COMMERCE
R. P. LAMONT, Secretary
BUREAU OF STANDARDS
GEORGE K. BURGESS, Director

BUREAU OF STANDARDS JOURNAL OF RESEARCH

May, 1932
Vol. 8, No. 5

UNITED STATES
GOVERNMENT PRINTING OFFICE
WASHINGTON: 1932

For sale by the Superintendent of Documents, Washington, D. C. - - - - - - - - - $3 per year on Subscription

For a partial list of previous research papers appearing in BUREAU OF STANDARDS JOURNAL OF RESEARCH see pages 2 and 3 of the cover

A CONTRIBUTION RELATIVE TO THE STRUCTURE OF COLLAGEN

By John Beek, jr.

ABSTRACT

The quantity of gaseous hydrogen chloride reacting with collagen was measured, under various conditions by three methods. The seven combining weights thus obtained, together with two similar values for gelatin, are used to find the number of nitrogen atoms in the unit of structure of the collagen. This number is found to be 38, or possibly a multiple of 38.

CONTENTS

		Page
I.	Introduction	549
II.	Methods and results	550
III.	Discussion of results	552
IV.	Conclusions	553

I. INTRODUCTION

A study of the fundamental principles governing tanning processes requires a more definite knowledge of the structure of collagen, the chief constituent of hides.

Collagen is generally considered to be a chemical species in the classical sense, but the evidence on this point is not conclusive. The work of Thomas [1] and Kelly on the reactions of collagen with chromium and iron salts shows that it is probable that collagen is a definite substance.

This research was undertaken in connection with the problem of determining the combining weight of collagen with acids in dilute aqueous solution. It is believed that a knowledge of the number of nitrogen atoms occurring in a unit of the collagen structure would facilitate the accurate determination of this combining weight, as it is the nitrogen-containing groups which react basically in collagen. If a definite integral value is obtained for this number it is simultaneously demonstrated that collagen is a chemical species. Thus it is unnecessary to prove independently that collagen is a definite substance if a positive result is obtained in a research on one of its structural characteristics.

If the combining ratios in a series of compounds formed from collagen could be shown to bear a stoichiometrical relation to the nitrogen content of the collagen, some factor of the number of nitrogen atoms in a structural unit of the collagen would be known.

In the present work the quantity of HCl gas which reacts with collagen is determined under various conditions. It is demonstrated that a whole-number relation exists among the various combining ratios which are obtained. As Bancroft [2] has shown that gaseous

[1] Ind. Eng. Chem., vol 14, p. 621, 1922; and Ind Eng. Chem. vol, 20, p. 632, 1928.
[2] J. Phys. Chem., vol. 34, pp. 449 and 753, 1930.

HCl reacts only with the nitrogen- containing groups in polypeptides, and that not more than 1 mol of HCl per nitrogen atom reacts, it is possible to calculate from the above series of results the number of nitrogen atoms in a unit of the collagen structure.

II. METHODS AND RESULTS

The collagen used in this work was prepared in this laboratory. Steer hide was treated as suggested by Dr. J. A. Wilson,[3] except that instead of shredding the material after splitting it was cut into small pieces and deashed by putting it in water and adding hydrochloric acid until the solution remained acid to methyl red. The collagen was then washed thoroughly. Ammonia was then added until the solution remained basic to methyl red, after which the washing was repeated. This process was continued until the collagen had been in acid solution three times and in basic solution three times. The resulting collagen contained 17.8 per cent N, 0.02 per cent ash, and 0.02 per cent Cl.

The results of the determinations are expressed in terms of the fraction of the total nitrogen which reacted with HCl. The letter f will be used to denote this fraction. The values of f are calculated by taking the ratio of the number of gram atomic weights of chlorine, in the sample after the reaction, to the number of gram atomic weights of nitrogen in the sample.

A description of the methods used in making the determinations follows:

1. A sample of collagen was dried at 100° C. for 2 days, and then allowed to remain in an atmosphere of hydrogen chloride for 151 days at room temperature (15° to 35° C.). At the end of this time the hydrogen chloride was swept with a stream of air out of the vessel containing the collagen, the collagen salt was dissolved in cold water, and the chloride was titrated with $AgNO_3$ solution, using $(NH_4)_3\ AsO_4$ as an indicator. The value of f was 0.395.

2. A sample of collagen was dried over P_2O_5 for 2 months and then put in an atmosphere of HCl for 45 days. The total chloride in the sample was then determined as in method 1. The value of f was 0.398.

3. A sample of collagen dried over P_2O_5 for 44 days was kept in an atmosphere of HCl for 3 days. At the end of this period the rate of combination of the HCl with the collagen was so low as not to be easily measurable by the volume change. The sample was transferred to a vessel containing sodium in an atmosphere of hydrogen. The sample was suspended on a glass rod passing through the top of the vessel, so that it could be weighed without making a large opening. The pieces of sodium were cut at intervals of about 10 days in order to expose fresh surfaces to the atmosphere in the vessel. After 49 days, the rate of loss of weight of the collagen sample being less than 0.1 mg per day, the sample was dissolved in water and the chloride titrated with $AgNO_3$, as in method 1, above. This gave 0.107 as the value of f.

4. The sodium from the vessel used in experiment 3 was put with the adhering salts, into an atmosphere of moist air and left until no metallic sodium remained. The resulting sodium salts were dissolved in water, and the chloride titrated as in methods 1 and 2 above. The quantity given by this titration was added to that of experiment 3,

[3] The Chemistry of Leather Manufacture, vol. 1, p. 90.

giving the total chloride in the collagen sample when it was put in the vessel with the sodium. The resulting value of f was 0.317.

5. This method is similar to that employed by Dr. W. D. Bancroft [4] in measuring the quantity of HCl reacting with various proteins over a range of pressure. It consists essentially in admitting successive quantities of HCl into an evacuated vessel containing the protein, and measuring the equilibrium pressure in the vessel after each addition. These measurements permit the construction of a phase diagram for the 2-component system over the range of pressure studied. Not enough data were obtained to make possible the construction of a complete phase diagram for the samples used, but definite regions in which the quantity of HCl combined did not vary with the pressure were established at values of f, of 0.184, and 0.236. The corresponding pressures were in the region of 12 and 30 mm, respectively. The value 0.236 was obtained in two separate determinations.

6. A sample of leather tanned with chestnut wood extract was used in this determination. The grain and flesh surfaces were split off, after which the material was washed in a shaking machine with about 30 changes of distilled water, and then in a water reflux apparatus for a month. The leather contained 9.82 per cent nitrogen. A dropping funnel of 60 ml capacity with the stem cut off about 5 cm from the stopcock, was used as a container for the sample, which weighed about 4.3 g. The bulb, containing the sample (dried at 100° C.) was filled with HCl. After 12 days the pressure was reduced to 15 mm, and repeatedly brought to that value, as the leather gave off HCl, until the pressure remained constant at that point. The container was then weighed, with the gas at 15 mm pressure and the leather in it. The process was then repeated. The two weights checked to within 3 mg, giving a value of 0.343 for f, after correction for the HCl taken up by the tannin.

7. Deashed gelatin was used for this determination. The sample was used without drying, containing 13.7 per cent moisture. It was put in an atmosphere of HCl for seven days, after which the total chloride was determined as in method 1. The result was $f = 0.633$.

8. This is the same as method 7 except that the sample was heated at 180° C. for two days before being put in HCl. The result was $f = 0.105$.

The work on gelatin is included because of the close relation between collagen and gelatin.

Table 1 gives the experimental results.

TABLE 1.—*Showing the fraction of the total N reacting with HCl*

No.	f
1	0.395
2	.398
3	.107
4	.317
5-(1)	.184
5-(2)	.236
5-(3)	.236
6	.343
7	.633
8	.105

[4] See footnote 2, p. 549.

III. DISCUSSION OF RESULTS

The whole number relation among the results may be shown by dividing all the values of f by the smallest value. For cases in which the values apparently occur in pairs, the mean of the two is taken, and later used with a weight of two. The resulting quotients fall approximately on quarters of integers. Thus, if they are multiplied by four they are approximately integers, which may be denoted as a_1, a_2, etc. Then all of the ratios f/a are about equal, and represent the smallest fraction of the nitrogen which was found to react. The weighted mean of the values of this smallest fraction will be called f_o. The numerical values of the quantities which have been discussed are presented in Table 2.

The deviation of the values of f/f_o from the corresponding values of a determines the probability that the relationship apparently found was a result of chance coincidence. This probability is found to be 2.2×10^{-9}, which indicates that the relationship is a result of the chemical nature of the collagen.

TABLE 2.—*Showing the whole-number relation among the experimental results*

f	Weight	$\frac{f}{0.106}$	a	f/a	f/f_o
0.633	1	5.97	24	0.02637	24.00
.397	2	3.75	15	.02647	15.05
.343	1	3.24	13	.02638	13.01
.317	1	2.99	12	.02642	12.02
.236	2	2.23	9	.02622	8.95
.184	1	1.74	7	.02629	6.98
.106	2	1.00	4	.02650	4.02

f_o=0.02638.

The reciprocal of f_o is the number of nitrogen atoms occurring in a unit of the collagen structure, or a factor of this number. As the reciprocal of 0.02638, the value found for f_o, is 37.91, 38 may be taken tentatively as the integer in question. The per cent of difference between $1/f_o$ and 38 is slightly less than the probable percentage of error in the value of f_o, calculated from the distribution of the values f/a.

As there is a possibility that some integer other than 38 might fit the results better than 38, a comparison was made of all integers less than 76 to determine the probability that they were not the correct numbers. The result for 38 was 1.1×10^{-5} times that for 55, the integer of this group having the next highest probability of being correct. The work was not carried further than for 75 because 38 gave a satisfactory correspondence with the experimental results.

According to Hofmeister's [5] analysis, collagen contains 50.75 per cent carbon and 17.86 per cent nitrogen, which gives the atomic ratio of carbon to nitrogen as 3.318. Thus, if there are 38 nitrogen atoms in a unit of the collagen, there are (38) (3.318) atoms of carbon in the same unit. This product is 126.08, which is sufficiently close to the integer 126 to provide a check on the determination of 38 as the number of nitrogen atoms.

Belden [6] has measured the combination of gaseous HCl with gelatin. He found a combining weight of 332 for gelatin, which corresponds

[5] Z. physiol. Chem., vol. 2, p. 299, 1878.
[6] J. Phys. Chem., vol. 35, p. 2164, 1931.

to a value of 0.237 for f. This checks the value of 0.236 obtained in the present work, for the fraction of the total nitrogen in collagen reacting under the same conditions. Belden also made this measurement on gelatin hydrolysate, the result being 285 to 290 mg of HCl combined per gram of gelatin. This checks the value given in this paper for the air-dry gelatin which was kept in HCl at about atmospheric pressure for seven days, this value being 293 mg of HCl per gram of gelatin.

The work of Thomas [7] and Kelly must also be considered in connection with the results in this paper. The equivalent weights of collagen calculated from the results given in their papers are given in Table 3, together with the corresponding values of f and a. The values of $a/38$ are given for comparison with the observed values of f. The fifth combining weight in the table is not given by Thomas and Kelly, but represents a maximum in the quantity of iron fixed by collagen in one of their experiments. The value of 94 from the work on chromium salts, reported by the authors, was derived from a similar maximum.

TABLE 3.—*Combining weights of collagen with chromium and iron*

[Data of Thomas and Kelly]

Combining weight	f	$a/38$	a
94	0.836	0.842	32
187	.421	.421	16
380	.207	.211	8
750	.105	.105	4
299	.263	.263	10

It should be noted that a necessary condition for the existence of the relation found among the experimental results is that the amount of physical adsorption taking place under the conditions of the experiments is negligible.

IV. CONCLUSIONS

1. Collagen, as prepared for this work, is a chemical species.

2. The number of nitrogen atoms in a unit of the structure of collagen is 38 or a multiple of 38. The corresponding number of carbon atoms is 126.

WASHINGTON, February 26, 1932.

[7] See note 1, p. 549.

GRAPHICAL DETERMINATION OF POLAR PATTERNS OF DIRECTIONAL ANTENNA SYSTEMS

By G. L. Davies and W. H. Orton

ABSTRACT

This paper describes graphical methods for the determination of polar patterns of directional antenna systems. These methods are less tedious and more generally applicable than computation from available mathematical equations.

At any distant point, the relative phases of the disturbances from the individual antennas of an array are dependent upon the differences in the paths from the antennas to the point, and upon the relative phases of the antenna currents. The path differences may be readily constructed on a scale drawing of the array, and by means of a special protractor these path differences are converted to phase angles for the construction of a vector diagram representing the disturbances at the field point. The resultant of this vector diagram gives the field intensity at that point. Such diagrams for a number of points equidistant from the array give the relative field intensities in various directions and thus enable a polar pattern to be drawn.

As illustrations, the polar patterns of two very simple arrays are determined; a broadside array of two antennas spaced one-half wave length and carrying equal equiphased currents; and an end-on array of two antennas spaced one-quarter wave length and carrying equal currents in time quadrature.

By a principle for the addition of the directive patterns of groups of antennas, the work involved in determining patterns of arrays containing a large number of antennas may be greatly simplified. This method also permits ground effects to be readily included, the image current being calculated by means of equations given by Wilmotte.

CONTENTS

	Page
I. Introduction	555
II. General method	556
III. Applications of method	559
IV. Conclusion	569

I. INTRODUCTION

During the course of a study of the characteristics of directional antenna systems, undertaken in connection with experimental work on the use of a high-frequency beam as an aid in the blind landing of aircraft, it was found that existing mathematical methods for plotting the polar patterns of antenna arrays were in many cases quite tedious. Furthermore, most of the equations now available apply only to somewhat restricted classes of arrays, so that, in order to plot the directional pattern of an array not included in such classes, it was necessary first to develop the equation of the pattern. A definite need was felt for a rapid and less tedious method of determining these diagrams. The graphical methods [1] presented here were found to save much time and labor and to be quite general in their application to what may be termed planar arrays; that is, arrays whose individual antennas are so arranged that their midpoints lie in the same plane.

The mathematical equations available for the computation of directional diagrams have been developed by numerous investigators,

[1] A graphical treatment from a somewhat different viewpoint appeared in Marconi Review No. 33, pp. 11-18, November-December, 1931, while the present paper was in press.

notably Foster,[2] Fleming,[3] Green,[4] Wilmotte,[5] and Southworth.[6] Wells[7] has given a graphical method based on Green's analysis. This method, however, is subject to important limitations which, although not mentioned by Wells, are evident from the analysis given by Green.

II. GENERAL METHOD

All methods for the determination of polar patterns of antenna arrays involve the calculation of the vector sum of the effects, at a distant point, due to the individual antennas or elements of the array. For simplicity, the present discussion is limited to planar arrays in which the elements are parallel and one-half wave length long.

The radiation from an isolated half-wave antenna, in a plane perpendicular to the antenna, is equal in all directions; that is, the polar pattern is a circle. In a plane containing the antenna, the radiation is approximately represented by the polar pattern $r = \cos\theta$, the direction $\theta = 0$ being perpendicular to the antenna. This pattern consists of two circles each tangent to the other and to the antenna.

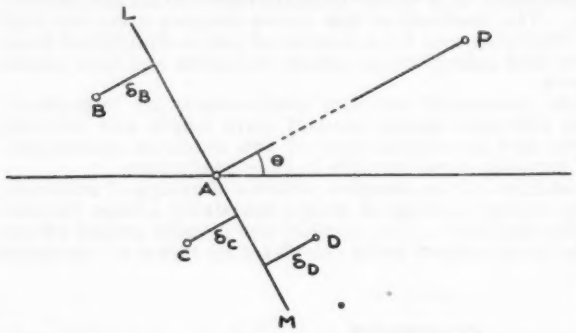

FIGURE 1.—*A group of four point-sources and their respective retardations δ in the direction of P*

For the purposes of analysis, the half-wave elements of a planar array may be considered equivalent to point sources located at their centers. The individual directivity of these elements in their containing plane will be accounted for and discussed later.

In Figure 1, antennas are located at A, B, C, D, the currents in them being considered, for the moment, as equiphased. If P (r, θ) is taken to be sufficiently distant, the lines joining it with A, B, C, and D, are sensibly parallel. Under this condition, periodic disturbances originating at any point on the line LM perpendicular to AP will be in phase at P. This phase is taken as a reference. Then a disturbance originating at a point, such as D, on the near side of LM will have a positive phase angle, while one originating at a point, such as B or C, on the far side of LM will have a negative phase angle. This phase angle, which will be denoted by ϕ is equal to $2\pi\frac{\delta}{\lambda}$, where λ is the wave length and δ is the path difference; that is, the distance from

[2] R. M. Foster, Directive Diagrams of Antenna Arrays, Bell System Tech. J., vol. 5, p. 292, April, 1926.
[3] J. A. Fleming, Approximate Theory of the Flat Projector (Franklin) Aerial Used in the Marconi Beam System of Wireless Telegraphy, Experimental Wireless, vol. 4, p. 387, July, 1927.
[4] E. Green, Calculation of the Polar Curves of Extended Aerial Systems, Experimental Wireless, vol. 4, p. 587, October, 1927.
[5] R. M. Wilmotte, General Considerations of the Directivity of Beam Systems, J. I. E. E., vol. 66, p. 955, September, 1928. General Formulæ for the Radiation Distribution of Antenna Systems, J. I. E. E., vol. 68, p. 1174, September, 1930. The Radiation Distribution of Antennæ in Vertical Planes, J. I. E. E., vol. 68, p. 1191; September, 1930.
[6] G. C. Southworth, Certain Factors Affecting the Gain of Directive Antennas, Proc. I. R. E., vol. 18, p. 1502, September, 1930. Bell System Tech. J. vol. 10, p. 63, January, 1931.
[7] N. Wells, Beam Wireless Telegraphy, Elect. Rev., vol. 102; Part I, p. 898, May 25, 1928; Part II, p. 940, June 1, 1928.

the line LM to the antenna. The phase angle of the disturbance from B is therefore $\phi_B = -2\pi\frac{\delta^B}{\lambda}$, that from C is $\phi_C = -2\pi\frac{\delta^C}{\lambda}$, and that from D is $\phi_D = 2\pi\frac{\delta^D}{\lambda}$. The sign of δ, and, therefore, of ϕ may be readily determined by the following rule: Consider δ to be directed from the reference line LM (fig. 1) toward the antenna with which it is associated; then δ (and thus ϕ) is positive when it points toward P and negative when it points away from P.

Since the antenna currents were assumed to be equiphased these phase angles ϕ determine the directions of the rotating vectors representing the disturbances at P due to each antenna. The relative magnitudes of these vectors are determined by the amplitudes of the respective antenna currents. If an arbitrary length is chosen for one of the vectors (preferably the one representing the disturbance whose phase has been taken as reference), a vector diagram may be constructed whose resultant represents the electric field intensity at P due to the antenna array. If the antenna currents are not equiphased as assumed, then the direction of the vector at P representing the disturbance due to an element will be $\phi+\alpha$, where α is the phase angle of the current in that element with respect to the reference element and is positive for leading and negative for lagging phase angles. This construction is shown in Figure 2.

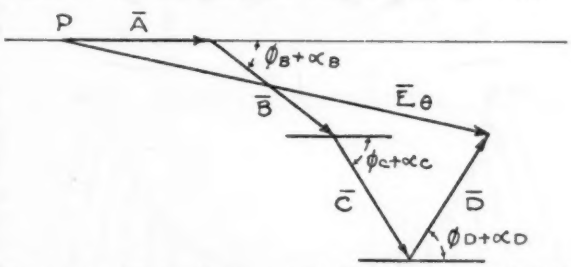

FIGURE 2.—*Vector diagram giving the resultant electric field intensity at P due to the four sources of Figure 1*

If such vector diagrams are drawn for a number of similar points, lying in the directions θ and equidistant from the array, the resultant values of electric field intensity plotted as radii, with the corresponding values of θ as angle, give a polar pattern which is the directional diagram of the array.

The values of the phase angles ϕ may be computed from the parameters of the array, but are more readily determined graphically. If the array is drawn to scale, unit length on the drawing being equal to one wave length, the lengths of the path differences δ will be equal to the phase angles ϕ expressed as a fraction of a complete revolution; that is, of 360°. Thus, if a unit length (that is, one wave length to the scale of the drawing of the array) is divided into 360 equal parts, each part equivalent to 1°, and the lengths of the path differences laid off on this scale, the angular values of ϕ may be read directly in degrees.

It has been found convenient to combine this (δ, ϕ) conversion scale with a protractor which is also fitted with a circular scale for the inclusion of α. Three (δ, ϕ) conversion scales are provided, corresponding to scales of 4, 8, and 12 inches, respectively, equal to one wave length in the scale drawing of the array. They occupy the lower

half while the time phase or α-scale occupies the upper half of the protractor as shown in Figure 3.

As an example of the use of the protractor, let it be required to find the angle $(\phi_B + \alpha_B)$ between **B** and **A** of Figure 2, where these vectors represent the effects at P of the elements B and A, respectively of Figure 1. Assume the current in B to be leading that in A by one-eighth period; that is, $\alpha = +T/8$. The center of the protractor is placed at the head of the reference vector **A** and the instrument rotated in a counter-clockwise direction until the action line of A (in this case its tail, extended if necessary) coincides with $T/8$ on the positive α-scale. With the instrument in this position, the length of δ_B, taken from Figure 1 (drawn to scale 4 inches $= \lambda$) with dividers, is laid off on the 4-inch scale from the origin for negative δ. The corresponding angle ϕ marks a point on the action line of the required vector **B** which is directed through the center of the protractor toward the ϕ-scale.

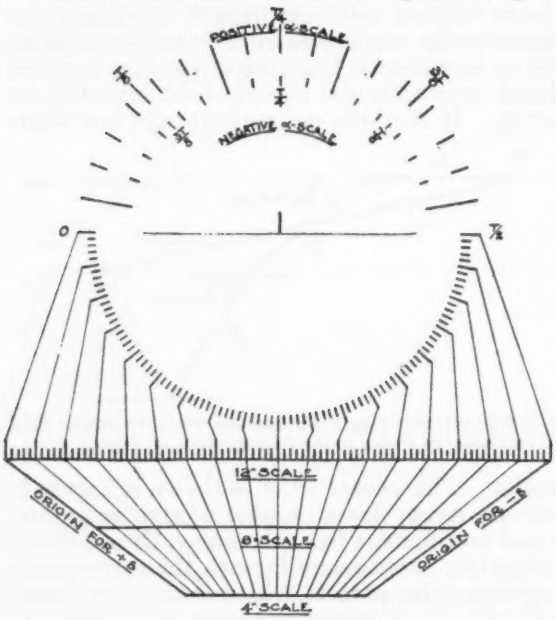

FIGURE 3.—*Special protractor for conveniently determining and combining the time phase angles α and the space phase angles φ in vector diagram*

If α had been negative the protractor with its center at the head of **A** would have been rotated in a clockwise direction until $T/8$ on the negative α-scale coincided with the action line of **A** (in this case the head of **A**, extended if necessary). With the instrument in this position a δ would have been laid off as before or in case δ_B had been positive, its length would have been laid off from the origin for $+\delta$. The corresponding angle ϕ in this case would determine a point on the action line of the required vector **B** directed from the ϕ-scale through the center of the protractor.

When path differences greater than $\frac{\pi}{2}$ occur, the following procedure is used: As many half-wave lengths as possible are measured along the path difference and the protractor (after it has been set for the proper time phase angle α) is rotated through 180° for each one-half wave length so measured. The remainder of the path difference (which is less than one-half wave length) is laid off on δ-scale as previously described.

III. APPLICATIONS OF METHOD

As illustrations of the method, the steps in plotting polar diagrams of two very simple arrays will be outlined here. The first array (shown in fig. 4) consists of two antennæ separated by a distance equal to one-half wave length and carrying equal equiphased currents. This is the simplest type of broadside array. The direction $\theta = 0°$ is perpendicular to the line joining the antennæ, and the antenna A is considered as the reference standard. This array has two axes of symmetry ($\theta = 0$ and $\theta = 90°$) so that it is necessary to determine the polar pattern for one quadrant only, the others being exactly similar.

A convenient method of determining the path differences δ_B for points P lying in different directions from the array is illustrated in Figures 4 and 5. It is evident from Figure 4 that the angle BMA is a right angle and that as P moves from the direction $\theta = 0°$ to $\theta = 90°$ the locus of M is a semicircle which circumscribes the right triangle BMA and has AB for its diameter. This construction is shown in Figure 5, where AB is drawn equal to one-half wave length to the scale chosen, and BM_{10}, BM_{20} are the required path differences when P lies in the directions $\theta = 10°$, $\theta = 20°$, etc.

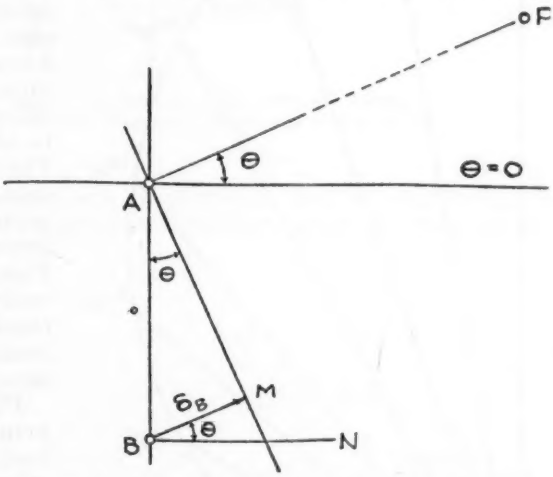

FIGURE 4.—*Arrangement of two equiphased antennæ with λ/2 spacing*

A length must now be chosen for the vector **A** which represents the electric field intensity at P due to the antenna A. Since there are two antennas with equal equiphased currents, the maximum possible field intensity is twice that due to A alone, so that the length used for **A** must be half of the maximum length of radius desired on the polar diagram. For diagrams of simple arrays, 4 inches is a convenient maximum; then **A** may be made 2 inches long. This length is laid off on a reference line, as in Figure 6, and the phase angles ϕ measured from its end, the values of ϕ being obtained from Figure 5 and converted to ϕ's by means of the protractor described. From the termination of **A**, vectors **B** of the same length as **A** are drawn, each corresponding to the proper phase angle ϕ_δ. The vector sums **A** + **B**, represented by the heavy lines in Figure 6, are the magnitudes of the radii of the directional diagram, so that these lengths from the vector diagram may be transferred directly to polar coordinate paper by means of dividers to give the polar pattern of the array. This is shown in Figure 7.

Another very simple array is the end-on array of two antennas in Figure 8. Here the antennas are separated by one-fourth wave length, and the currents in them are equal but in phase quadrature, the current in B leading that in A. The direction $\theta = 0$ lies in a line joining the two antennas, and the antenna A is again taken as reference. This array has but one axis of symmetry ($\theta = 0$), so that radiation in the directions $\theta = 0°$ to 180° must be determined.

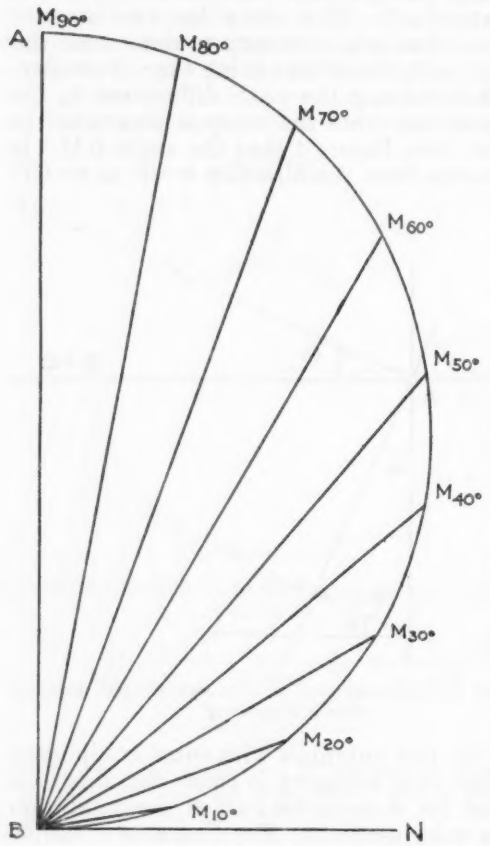

FIGURE 5.—*Section ABN of Figure 4 drawn to scale*

The lengths AMθ are the retardations in the directions θ from the array

As before, the values of δ are the lengths, between B and points M lying on a semicircle of diameter AB. Values of δ, as P moves in 10° steps through the first quadrant are shown in Figure 9. As P moves through the second quadrant δ changes sign but duplicates the δ-lengths of the first quadrant. All the required path differences may, therefore, be obtained from Figure 9. The vector diagrams for this case, drawn by means of the protractor are shown superimposed one on the other in Figure 10, where, to avoid confusion, only a few of the resultants are drawn. The resulting polar pattern is shown in Figure 11.

Figure 12 illustrates a principle which is very useful in the determination of polar patterns of arrays having a large number of elements. Let $\mathbf{E}$ represent the field intensity at P due to the group of elements AB, in which A has been taken as reference for the group, and let $\mathbf{E}'$ represent the field intensity of a similar group $A'B'$ in which A' has been taken as reference, then the vector sum $\mathbf{E}+\mathbf{E}'$ represents the effects at P of both groups. The angle between $\mathbf{E}$ and $\mathbf{E}'$ will be the sum of the time phase angle between the currents in A and A' and the space phase angle corresponding to the path difference δ'.

If the group $A'B'$ is not exactly similar to the group AB, account must be taken of the relative differences of phase of $\mathbf{E}$ and $\mathbf{E}'$ in different directions since, as may be seen from Figures 6 and 10, the angle between the vector resultants of these two dissimilar groups in the direction $\theta = 10°$ is not the same as the angle between them in the

direction $\theta = 20°$. These differences must be included in determining the phase angles between the vectors **E** and **E′** and are obtained from the vector diagrams for the two groups.

This method for adding the effects of groups of antennas is particularly valuable in determining the directional characteristics of

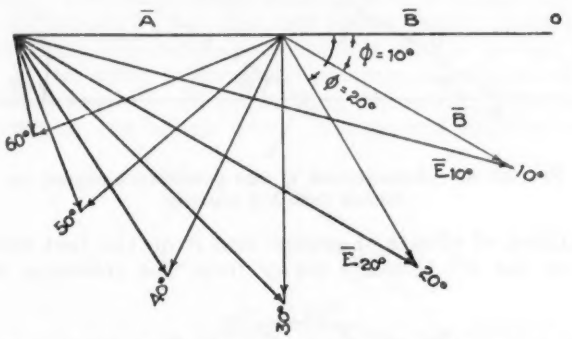

FIGURE 6.—*Vector diagrams showing how the effects of antennas A and B of Figures 4 and 5 are added at the points P_θ*

linear arrays of large numbers of antennas, and in calculating the effects of the ground. In the case of a linear array, the resultant due

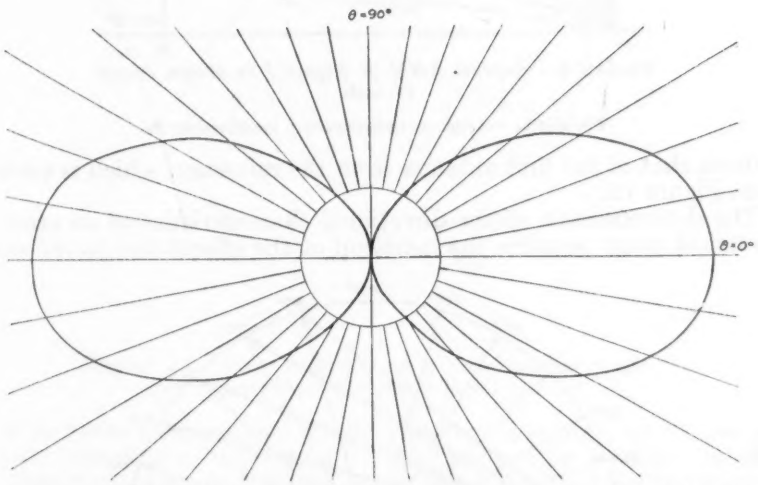

FIGURE 7.—*Polar pattern of an array consisting of two equiphased elements with λ/2 spacing*

to two antennas at one end of the array is first computed. Let the phase angle between these two components be ϕ_1, the resultant being denoted by $\mathbf{E}_1$. Then the effect due to the first four antennas may be obtained by adding to $\mathbf{E}_1$ another vector of equal length, the angle between the two being $2\phi_1$. This resultant is added to another of

equal length and an angle of $4\phi_1$ to give the resultant for the first eight antennas, and so on. This procedure follows from the method

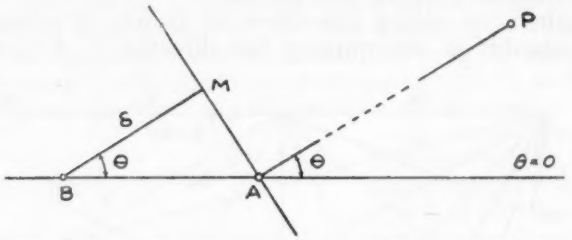

FIGURE 8.—*Arrangement of two quadrature-phased antennas with λ/4 spacing*

for the addition of effects of groups and from the fact that the path difference of the n^{th} antenna away from the reference is equal to

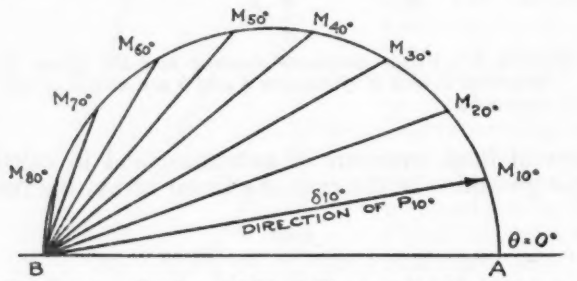

FIGURE 9.—*Section ABM of Figure 8 is shown drawn to scale*

The lengths AM_θ are the radiations δ_θ in the directions P_θ.

n times that of the first antenna from the reference, which is evident from Figure 12.

The determination of the directional characteristics of an array in a vertical plane requires the inclusion of the effects due to reflection

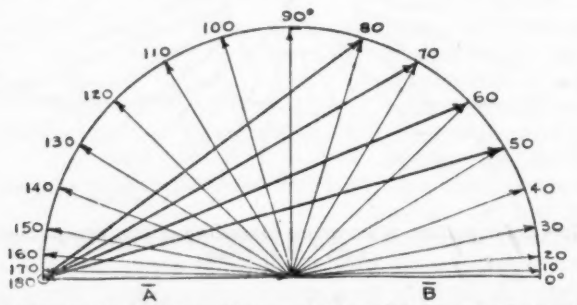

FIGURE 10.—*Vector diagrams showing how the effects of antennas A and B of Figures 8 and 9 are added at the points P_θ*

Only four of the resultants are shown.

from the earth. In this case, the polar pattern of the array is first determined neglecting the ground effects. Then the effects due to the image are added to those due to the array itself by the method

already described, the construction being indicated in Figure 13. It will be noted that the field intensity in a direction θ is determined by the addition, with proper phase angle, of the intensity due to the array in the direction θ and the intensity in the direction $-\theta$, the magnitude of the latter being multiplied by the reflection coefficient of the ground. The phase angle must include not only the angle due to the path difference δ', but also any phase change at reflection and the relative phase difference between the effects in the directions θ and $-\theta$. If the array is symmetrical about the line $\theta=0$, this last phase difference is zero. In calculating the magnitudes and phases of the currents in the image array, the ground may be considered

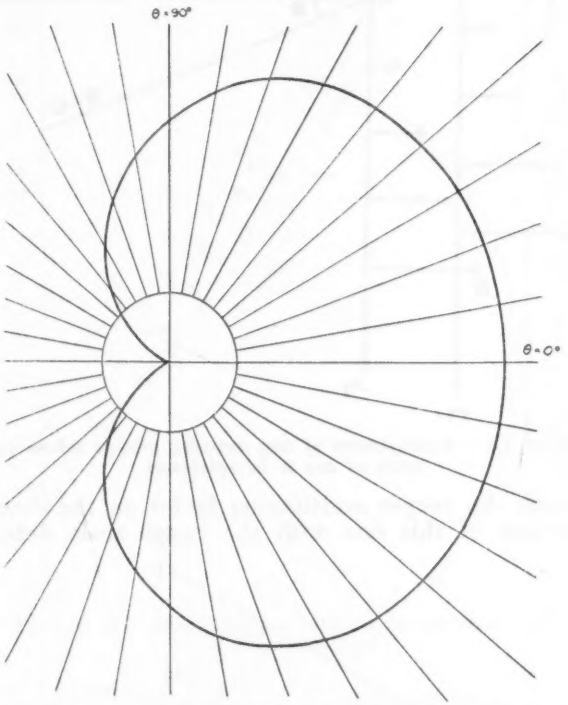

FIGURE 11.—*Polar pattern of an array consisting of two quadrature-phased elements with $\lambda/4$ spacing*

(1) as a perfect conductor, (2) as a perfect insulator, or (3) as an imperfect conductor, depending on the surrounding terrain. In the last case, equations and curves given by Wilmotte [8] are very convenient and have been applied here. The angle designated as θ by Wilmotte is the angle *Abc* of Figure 13. In most cases it may be considered equal to the complement of the angle θ of that figure.

To facilitate the determination of the vectors representing the image antenna effect, the multiplication chart shown in Figure 14 was made. It is an adaptation of the *Z*-type nomographic or align-

[8] R. M. Wilmotte, General Formulae for the Radiation Distribution of Antenna Systems, J. I. E. E., vol. 68, p. 1174, September, 1930.

ment chart. The length of vector due to the array is laid off from A on the antenna scale and from the terminus of this vector, a line is

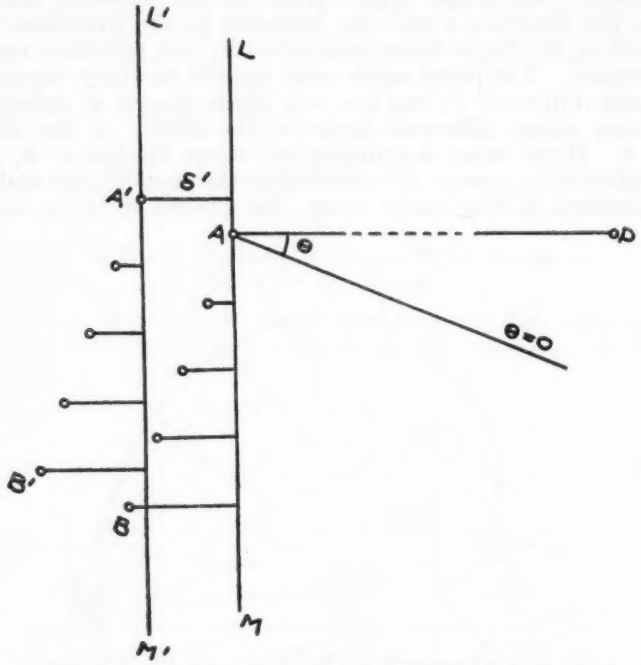

FIGURE 12.—*Arrangement of two antenna groups whose polar patterns are to be combined*

drawn through the proper multiplying factor on the diagonal scale. The intersection of this line with the image scale determines the

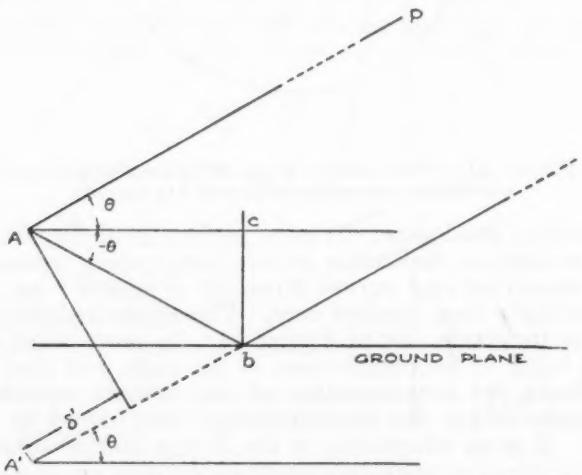

FIGURE 13.—*Construction for determining the effect of antenna image*

magnitude of the required vector. Practically, these multiplications can be carried out very rapidly with a divider and straightedge.

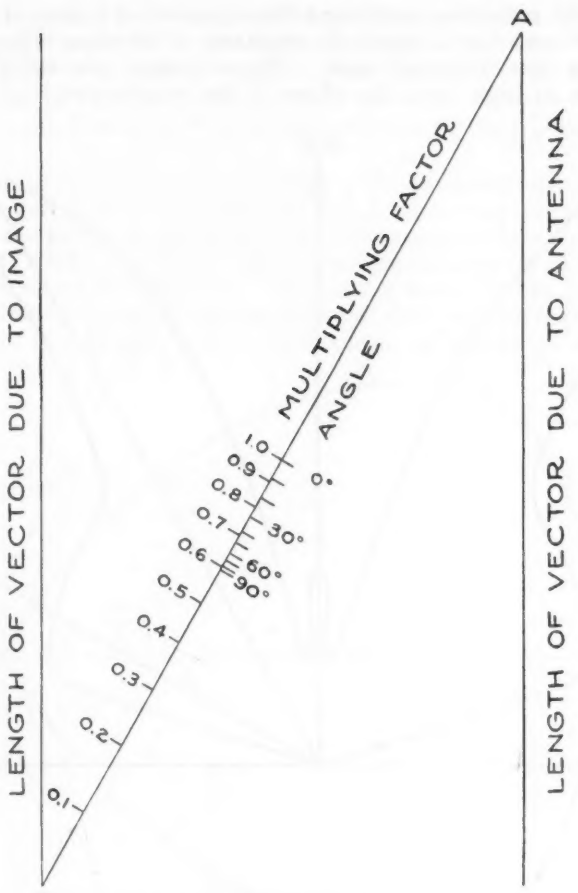

FIGURE 14.—*Multiplying chart for determining the effect of antenna image*

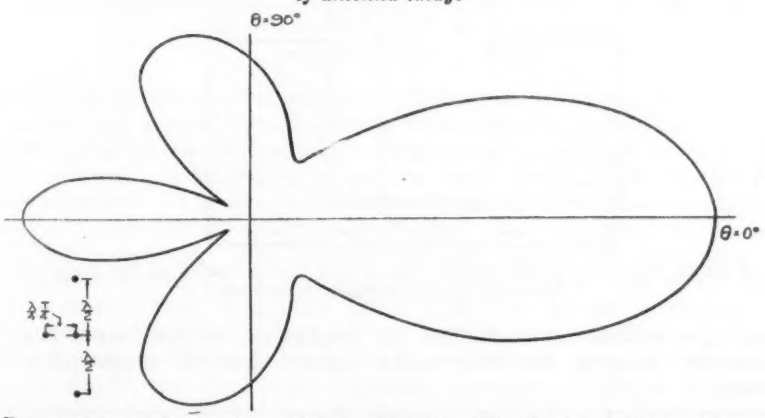

FIGURE 15.—*Polar pattern of four elements with phasing and spacing as indicated*

Effect of image is neglected

Values of the reflection coefficient for a number of values of θ between 0° and 90° and for a dielectric constant of 15 were computed and marked on the diagonal scale. These points are valid only for frequencies so high that the effect of the conductivity of the earth

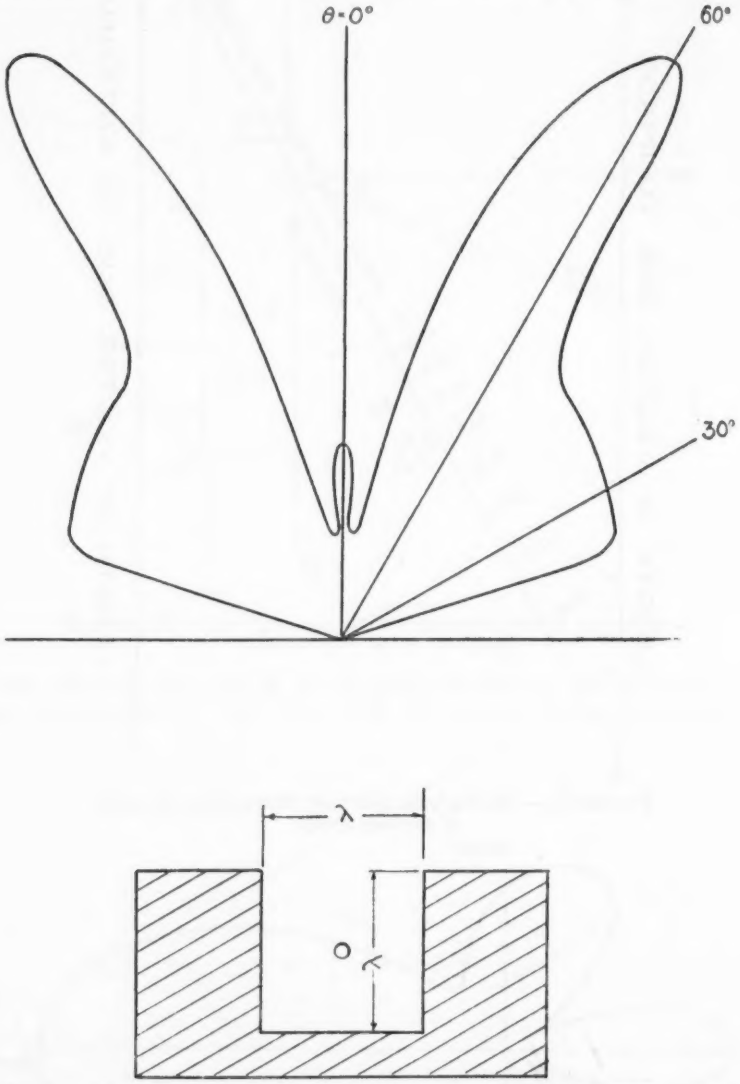

FIGURE 16.—*The polar pattern of a single source located at the center of a trough in an insulating medium*

upon the reflection coefficient is negligible, which according to Wilmotte,[9] is true for frequencies higher than 60 megacycles per second.

[9] See footnote 8, p. 563.

Figures 15 and 16 illustrate polar patterns obtained by methods described. The directive pattern of Figure 15 can be checked analytically from its equation, which in polar coordinates is

$$r=\sqrt{[1+2\cos(\pi\sin\theta)]^2+2\,[1+2\cos(\pi\sin\theta)]\sin\left(\frac{\pi}{2}\cos\theta\right)+1}$$

Figure 16 shows the radiation from a single source located at the center of cross section of a trough in an insulating medium. The width and the depth of the trough are each equal to one wave length.

Figures 17 and 18 illustrate the magnitude and nature of the effects of the earth in some instances. The first of these figures is the polar pattern in free space for an end-on array of eight antennas spaced one-fourth wave length and with a time phase difference of one-fourth

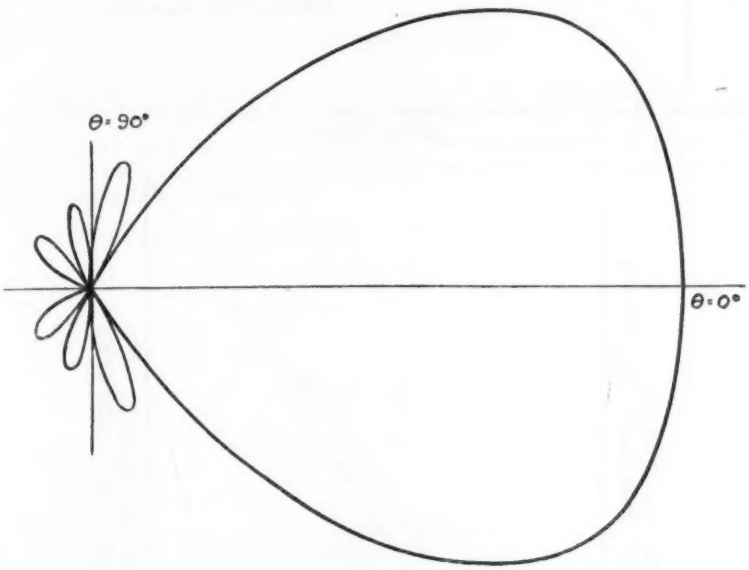

FIGURE 17.—*Polar pattern of an end-on array of 8 elements with λ/4 spacing and quarter-period phasing*

Image effects neglected.

period between adjacent antennas. This type of array is very closely similar to that selected by Dunmore [10] for a landing beam for aircraft. Figure 18 shows the pattern of the same array placed one wave length above ground. Wilmotte's equations were used to determine the image currents. The available observations on the radiation characteristics of the actual array indicate that the calculated pattern is very nearly correct. The differences may readily be attributed to differences between the actual and theoretical arrays, and to the fact that the actual array is slightly tilted, while the calculated diagram is based upon a horizontal array. It is evident that the major portion of the directive efficiency is due to the broadside effect of the array and its image, the horizontal extension serving merely to eliminate unwanted lobes. This is of course also evident from equations derived

[10] H. Diamond and F. W. Dunmore, A Radiobeacon and Receiving System for Blind Landing of Aircraft, B. S. Jour. Research, vol. 5 (RP238), p. 897, October, 1930.

by Wilmotte [11] which show that maximum directivity is obtained when the array is extended in a direction perpendicular to the desired

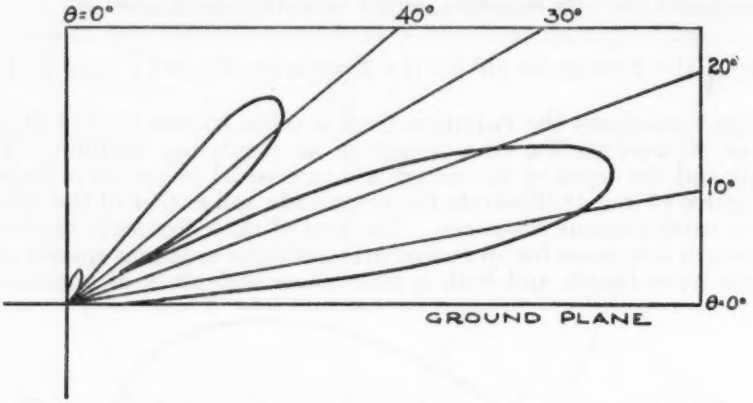

FIGURE 18.—*Polar pattern of same array as that of Figure 17, including effect of image*

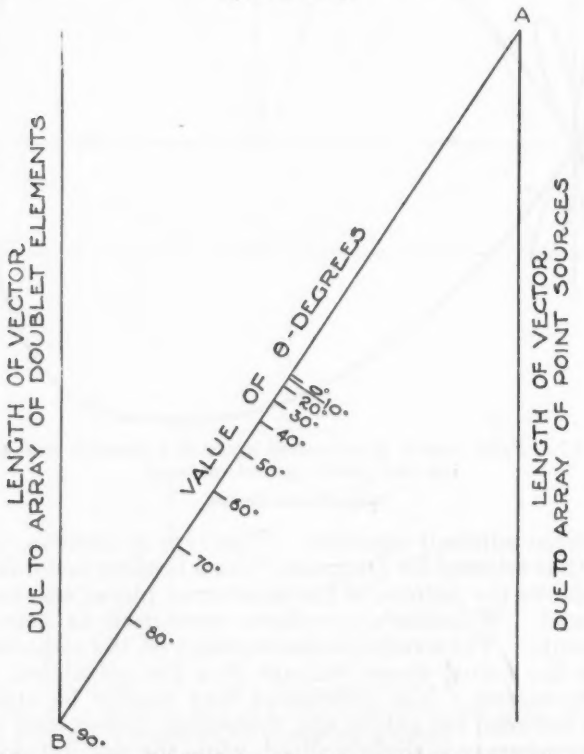

FIGURE 19.—*Multiplying chart for modifying the polar pattern of an array of point sources to include the directivity of doublet elements*

direction of maximum radiation. It will be noted also that the angle of elevation of the beam is dependent primarily upon the height of

[11] R. M. Wilmotte, General Considerations of the Directivity of Beam System. J. I. E. E., vol. 66, p. 955, September, 1928.

the array above ground, the effects of slight variations of the array from the horizontal being of the second order.

When the individual elements of the array have an inherent directivity of their own, the polar pattern of the array obtained by considering the elements as point sources must be modified to include this inherent directivity. Thus if the polar pattern in the containing plane of an array of half-wave antennæ is desired it is necessary to multiply each radius of the point source pattern by cos θ. This may be readily done by means of the Z-type chart shown in Figure 19, which is used in exactly the same way as the chart of Figure 14. The length of vector representing $\mathbf{E}$ at P_θ, from the point source array, is laid off from A on the right-hand vertical scale of the chart. Then the corresponding value of $\mathbf{E}'$ at P_θ, from the array of half-wave elements is obtained from the left-hand vertical scale.

IV. CONCLUSION

Graphical methods are well adapted to the determination of polar patterns of directional antenna systems. The labor involved is considerably less than that required for mathematical computation and is further reduced by the special protractor and graphical multiplication charts described.

WASHINGTON, March 9, 1932.

MANUFACTURE OF CALCIUM GLUCONATE BY THE ELECTROLYTIC OXIDATION OF DEXTROSE[1]

By H. S. Isbell, Harriet L. Frush, and F. J. Bates

ABSTRACT

In a previous paper the authors[2] described a simple method for the preparation of the calcium salts of the aldonic acids by electrolytic oxidation of the aldose sugars in the presence of a bromide and calcium carbonate. This method has been applied on a larger scale and has proved to be very satisfactory for the manufacture of calcium gluconate in considerable quantity. The principal products of the reaction are calcium gluconate, carbon dioxide, and hydrogen. The calcium gluconate which crystallizes from the electrolyte is collected upon a filter, and the mother liquors containing the bromide are returned to the cell after the addition of more dextrose and calcium carbonate. Since the process is continuous, the raw materials and electrical energy are readily available and cheap, and the product is obtained without any expensive evaporation or difficult steps, it is now possible to prepare calcium gluconate at a very reasonable cost.

CONTENTS

		Page
I.	Introduction	571
II.	Semicommercial manufacture of calcium gluconate	572
III.	Polarization and cracking of the electrodes	574
IV.	Recovery of the bromide	576
V.	Basic calcium gluconate	576

I. INTRODUCTION

Among the many sugar derivatives which hold promise for future development and industrial application are the monobasic sugar acids which are obtained by mild oxidation of the aldose sugars. Although these compounds have been known for a long time and have been of great importance in acquiring our present knowledge of the molecular structures of the various sugars, until recently they have received little attention from those interested in applied chemistry. Gluconic acid in particular should find many uses because it may now be prepared at low cost. The calcium salt of the acid has already found some application in the medicinal field, while the free acid offers many possibilities for the future. The sugar acids and their salts resemble the sugars, in that they form soluble complex compounds with numerous substances. Hence they are able to hold in solution many difficultly soluble substances, as, for example, certain amphoteric hydroxides. The sugar acids are also unique in that they form two anhydrides or lactones.[3] One of these is formed by condensation of the carboxyl group in gluconic acid with the hydroxyl on the fourth, or gamma carbon, and the other by condensation with the hydroxyl on the fifth, or delta carbon. These lactones are crystalline substances which should prove valuable additions to our

[1] Read at the meeting of the American Chemical Society, Buffalo, N. Y., September, 1931; and also published in Ind. Eng. Chem. vol. 24, p. 375, 1932.
[2] Isbell and Frush, B. S. Jour. Research, vol. 6 (RP328), p. 1145, 1930.
[3] Nef, Ann., vol. 403, p. 322, 1914.

supply of organic acids. Many uses for these weak organic acids or their lactones will undoubtedly be found when they are more readily available.

As may be seen from the following equation, the new process for the electrolytic oxidation of the aldose sugars, which has been developed by the authors,[4] is superior to the older method of bromine oxidation because the reaction product does not contain any objectionable substances derived from the oxidant:

$$\underset{\text{Dextrose}}{2C_6H_{12}O_6} + \underset{\text{Catalyst}}{CaCO_3 + CaBr_2} + H_2O \xrightarrow[\text{Electrolysis}^5]{} Ca(C_6H_{11}O_7)_2 + CaBr_2 + CO_2 + H_2$$

The bromide solution on electrolysis gives free bromine at the anode and hydrogen at the cathode. The bromine thus freed reacts with the sugar to give gluconic and hydrobromic acids. The calcium carbonate reacts with the acids as fast as they are formed and thus maintains a nearly neutral solution (about pH 6.2) in which the bromine combines as fast as it is liberated. The bromide is continuously regenerated; hence a small amount of it acts catalytically to facilitate the oxidation of a large quantity of the sugar. The amount of oxidation produced by a given quantity of current is very close to the theoretical. This shows that the reaction proceeds smoothly without the production of objectionable degradation products. The sugar is converted into the calcium salt of the sugar acid, and the only by-products are hydrogen and carbon dioxide which escape from the solution as gases.

II. SEMICOMMERCIAL PREPARATION OF CALCIUM GLUCONATE[6]

The adaptation of the electrolytic method for the production of calcium gluconate to a semicommercial scale was accompanied by very little difficulty such as is usually experienced in extending a laboratory method to a larger scale. This is due to the following facts: The process is unusually free from side reactions, the method does not necessitate careful control and can be applied efficiently under considerable variation of conditions, and the equipment is simple and easily constructed. The apparatus used in these studies is illustrated in Figure 1.

The outer jar is an ordinary 5-gallon water cooler. The solution is stirred with the mechanical stirrer shown in the center. There are four anodes and four cathodes, which are graphite rods 12 inches long and 1 inch in diameter. The cell was run at 10 amperes on an e. m. f. of 6 volts, and the temperature under these conditions was 55° C. On continuous operation at 20 amperes the temperature rose to 65° C. Although the cell ran satisfactorily at the higher rate it was usually run at 10 amperes; the current density was about 1.7 amperes per square decimeter of anode surface.

The cell was charged with 15 liters of water containing 2.7 kg of crystalline anhydrous dextrose, 0.75 kg of calcium carbonate, and 375 g

[4] See footnote 2, p. 571.

[5] The oxidation of two molecules of dextrose requires four Faradays of electricity.

[6] An application filed by one of the authors (H. S. I.) for a public-service patent covering this process has been placed in interference with applications filed by other parties. Those desiring to use the process are advised to await the outcome of the interference proceedings.

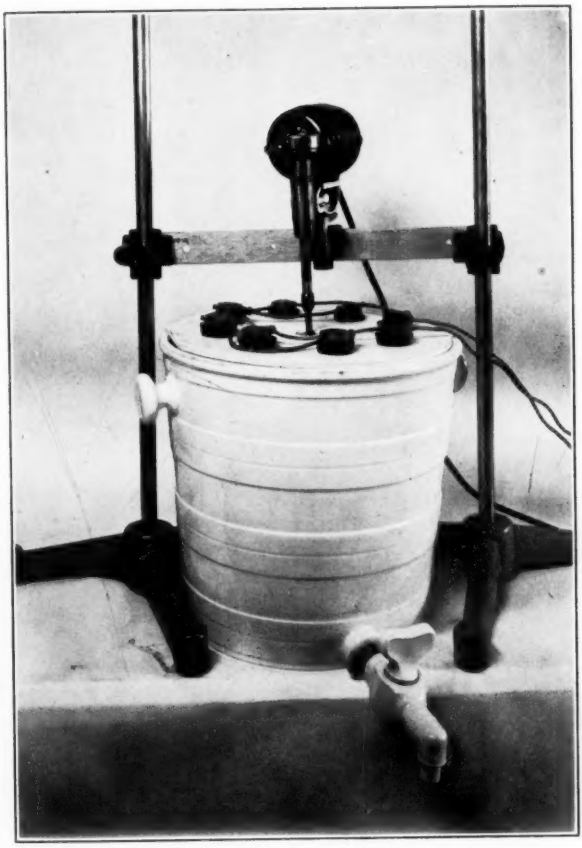

FIGURE 1.—*Electrolytic oxidation cell*

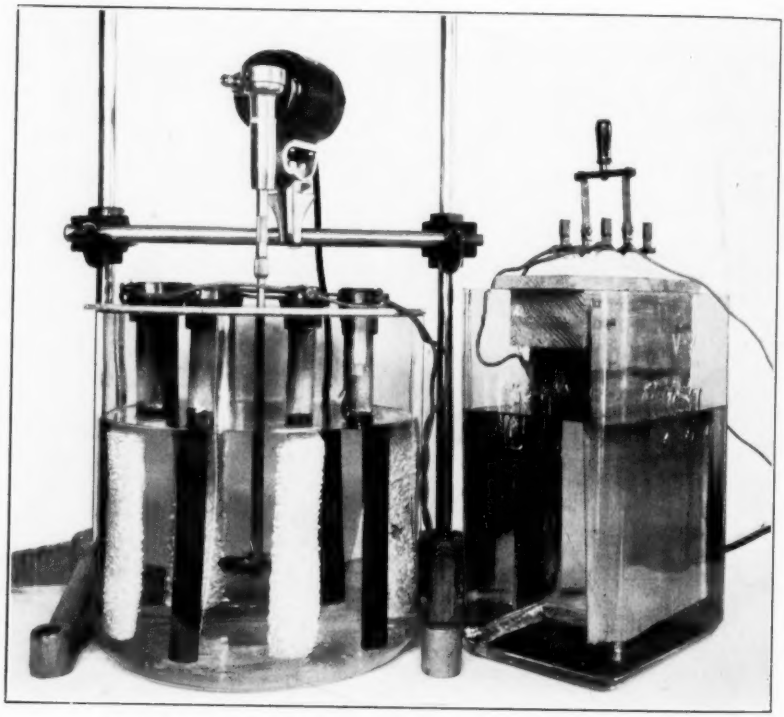

FIGURE 2.—*Cell showing calcareous deposit on cathodes*

of bromine.[7] The bromine reacts with the sugar and calcium carbonate to give calcium bromide and calcium gluconate. After oxidation had proceeded for three days at 10 amperes, considerable calcium gluconate crystallized from the electrolyte. A 5-liter portion was withdrawn and the calcium gluconate separated by filtration. The mother liquor and wash water were returned to the cell, together with 806 g of dextrose and 225 g of calcium carbonate. The oxidation was continued for 30 days with daily withdrawal of calcium gluconate and addition of dextrose and calcium carbonate in the amounts mentioned above. Each day's crop of calcium gluconate was recrystallized; the mother liquors from this recrystallization were used to wash the crude product obtained the following day, and were ultimately returned to the cell. A small amount of calcium carbonate reclaimed in the recrystallization was likewise returned. The volume of the electrolyte was kept at 15 liters, and occasionally the wash waters were concentrated in order to maintain this volume. At the end of the 30-day run, the entire electrolyte was filtered, and a sugar determination made upon the filtrate showed that 1.88 kg of sugar remained. The electrolyte was then returned to the cell, the required calcium carbonate added, and the amount of electricity (560 ampere hours) theoretically necessary to complete the oxidation of the remaining sugar was passed through. The calcium gluconate which crystallized was separated, and an additional yield was obtained on concentrating the mother liquors. After one recrystallization, these crops were combined with the previously recrystallized salt to give a total of 27.63 kg.

A quantity of calcium gluconate remained in the mother liquors and would not crystallize from the solution containing calcium bromide. This was reclaimed in part through precipitation as a basic calcium gluconate [8] by adding 1.5 kg of hydrated lime and heating to 70°. The basic salt was washed with lime water and then converted into the normal salt by removing the excess lime with carbon dioxide. The normal salt thus obtained after one recrystallization weighed 2.21 kg. The total yield of nearly pure calcium gluconate was 29.84 kg, or about 85 per cent of the theoretical.

At the end of the run the electrolyte was light colored and still in condition for continuing the process. In commercial operation it would be necessary to renew the elctrolyte occasionally. The frequency of renewal would depend upon the impurities in the raw materials and upon the operating conditions. Recovery of the bromide from the mother liquors will be discussed in Section IV.

As previously shown, under favorable conditions the sugar is nearly quantitatively oxidized. The experimental conditions in this case were not ideal, and there were relatively larger losses in handling and recrystallizing the material and in overoxidation than would occur in actual plant operation. Excess calcium gluconate caused the electrolyte to become thick enough to prevent thorough stirring, and some local overoxidation resulted. This difficulty would be overcome in a plant through continuous removal of the calcium

[7] The bromine reclaimed by one of the methods suggested in Section IV of this paper may be used. If the method yielding free bromine is employed, the bromine may be collected directly in the sugar solution. The resulting solution contains practically no free bromine, and hence is easily handled.

[8] The crude basic calcium gluconate obtained from the impure electrolyte after a washing with lime water may be used in a subsequent run in place of some of the calcium carbonate. The calcium gluconate is then recovered along with the crude oxidation product. However, in the event that the basic salt is very impure, it is probably better to prepare the normal salt by decomposition with carbon dioxide in the usual manner.

gluconate by a suitable filter. After one recrystallization the product usually contains a small quantity of calcium bromide. Although calcium gluconate is easily recrystallized from hot water, and calcium bromide is much more soluble than calcium gluconate, still the bulky nature of the calcium gluconate makes the removal of the last traces of the bromide difficult. This is the most troublesome step in the process, but with proper facilities for crystallizing and washing the salt in large quantity, it would be less burdensome.

In larger units, cooling coils would be necessary. In the experiments reported in this paper, no cooling device was used, but cooling is necessary when the described cell is run at its maximum capacity.

A small amount of foaming occurs during the reaction, but this does not cause any trouble provided the cell is not too full. The foaming may be reduced by the addition of a few drops of an antifoam compound, such as caprylic alcohol, although this is not necessary.

Costs for the production of calcium gluconate by this process depend largely upon the volume of production. Reliable figures can not be determined from the operation of a unit of the size outlined in this paper, but some idea of their magnitude may be obtained. A comparatively small initial investment is necessary as the equipment is simple and easily constructed. As shown in Table 1, the cost of the raw materials may be conservatively estimated at about $6 per 100 pounds. This estimate is based on current prices and the results obtained in the experimental run. The cost for electricity will depend largely on the location and operating conditions. The cell used in the run under discussion requires about 6 volts for a current of 10 amperes, and produces about 2 pounds of calcium gluconate per day; if the capacity is doubled by increasing the voltage to 12 volts, more energy is lost as heat. The most economical operating conditions, as well as the cost for electrodes, maintenance, operation, depreciation, etc., can not be determined at this time, but it is evident that calcium gluconate may be made by the new process at a very reasonable figure.

TABLE 1.—*Semicommercial manufacture of calcium gluconate*

	Chemicals actually used in experimental run		Chemicals required to produce 100 pounds of calcium gluconate.			
	Pounds	*kg*	*Pounds*			
Dextrose	59.3	26.9	90	at	$0.05	=$4.50
Calcium carbonate	16.1	7.3	25	at	.01	= .25
Bromine	.83	.375	1.25	at	.36	= .45
Electricity (for electrolysis only)	51 kw.-hr.		80 kw.-hr.	at	.01	= .80

Estimated cost of above items, $6.

Experimental run gave 29.84 kg (65.78 pounds) of calcium gluconate, $Ca(C_6H_{11}O_7)_2.2H_2O$ which is about 85 per cent of the theoretical yield.

III. POLARIZATION AND CRACKING OF THE ELECTRODES

In the course of the electrolytic oxidation the cathodes occasionally become coated with a calcareous deposit. The composition of this deposit varies considerably, but it always contains calcium carbonate, calcium hydroxide, calcium gluconate, and a small amount of material which reduces Fehling's solution. The coating is gen-

erally formed when dilute solutions are employed and is seldom found when the electrolyte contains considerable sugar or calcium gluconate. Presumably the sugar derivatives, by their solvent action, prevent the deposit of calcium hydroxide in the alkaline region immediately surrounding the cathode.

A typical cathode coating obtained with a dilute solution is illustrated in Figure 2. We have found that this deposit may be removed by reversing the current. The previously coated cathode then becomes the anode, and the hydrobromic acid formed in its vicinity quickly dissolves the deposit.

A number of experiments were made to determine the effect of reversing the direction of current upon the efficiency of the oxidation. The determinations were made on solutions containing 45 g of dextrose, 8 g of calcium bromide, and 25 g of calcium carbonate in 1 liter of water. The solution was electrolyzed in a flask fitted with graphite electrodes and a mechanical stirrer. A timing device was included in the circuit so that the direction of the current could be reversed at definite intervals. As shown in Table 2, reversing the current lowered the efficiency. With an alternating 60-cycle current, practically no oxidation occurred.

TABLE 2.—*Effect of reversing the direction of the current on the current efficiency*

Time (in minutes) between changes in the direction of the current	Current density	Current efficiency [1]
	Amperes/dm [2]	
1	1.6	39.4
1	3.2	53.5
25	1.6	80.1
400 (approx.) [3]	1.6	95.5
∞ [4]	1.6	94.7

[1] Current efficiency is the percentage of the sample found to have been oxidized after 13.4 ampere-hours. The quantity of electricity theoretically required for complete oxidation of the sample is 13.4 ampere-hours.
[2] The current was reversed whenever it was believed necessary to prevent the formation of a heavy deposit.
[3] The current was not reversed and consequently considerable deposit formed on the cathode.

It is apparent from the results given in Table 2 that the current should not be reversed except when it is necessary to clean the electrodes. If the proper conditions are maintained this is seldom required. In the continuous oxidation reported, the current was reversed three or four times at the beginning of the run.

Frequently, with concentrated solutions and high-current densities the anodes split longitudinally, but the cathodes are unaffected. The effect seems to be mechanical for the graphite is not corroded. The cracks usually are filled with crystalline material, and the difficulty occurs only during long continued oxidation. This suggests the explanation that the electrodes originally contained minute cracks in which calcium gluconate or some other substance collected, producing fractures in a manner analogous to the fracture of rocks by the freezing of water. This difficulty may be largely overcome by impregnating the electrodes with paraffin to fill up the minute cracks and thus prevent penetration by the electrolyte.

IV. RECOVERY OF THE BROMIDE

In a plant it would be necessary to recover the bromide from mother liquors which become contaminated by long-continued use. The simplest method consists in evaporating the residues to dryness and igniting to remove the organic matter. The ash which remains is largely calcium carbonate, oxide, and bromide, and hence it may be used in a subsequent electrolytic oxidation as a source of bromide. Frequently it contains objectionable impurities, in which case it requires further purification. The ash or residue may be extracted with water and the aqueous solution used directly; or the bromine may be liberated by electrolysis of the extract after acidification with sulphuric acid. In the latter case the free bromine is distilled into a dextrose solution containing calcium carbonate in suspension.

In the semicommercial experiment described in a previous section, the residues were ignited and the ash extracted with 2 liters of boiling water. The extract was acidified with sulphuric acid, and the bromine liberated by electrolysis. Platinum electrodes were used. Air was bubbled through the solution to aid in removing the bromine and the vapors were led into a solution containing 2.7 kg of dextrose, and 750 g of calcium carbonate in suspension. After all the bromine had been collected in the sugar solution it was transferred to the cell and used directly for the preparation of more calcium gluconate in manner analogous to that described above. The bromine recovered (and determined by bromide analysis upon the fresh electrolyte) was about 53 per cent of that originally used. This figure is not indicative of the efficiency of the method of recovery because of preventable losses in handling, and retention of the bromide in the calcium gluconate. In this connection it should be recalled that the cost of the bromine is only a small fraction of the total cost.

V. BASIC CALCIUM GLUCONATE

Although Fischer[9] reported in 1890 that gluconic acid forms a basic calcium salt, the compound has not been studied further nor its composition determined. The writers have found that the difficultly soluble basic salt obtained from calcium gluconate by the addition of hydrated lime may be used to advantage for the separation of calcium gluconate from impure solutions which will not yield the crystalline normal salt. As stated in a previous paragraph, it was used for this purpose in reclaiming calcium gluconate from the residual mother liquors. The product obtained was impure and contained an excess of lime. It is not necessary to prepare the pure salt when it is to be used for separating calcium gluconate, since the excess lime is removed later as the carbonate. However, in order to determine the composition of the substance it is necessary to obtain it pure. This may be accomplished by taking advantage of the fact that basic salts of this type are less soluble in hot water than in cold. The following procedure was used for preparing the basic salt of gluconic acid. To a solution of 100 g of pure calcium gluconate in 1,400 ml of water was added 600 ml of milk of lime prepared from 27 g of CaO. Both solutions were kept ice cold. The resulting mixture was filtered quickly on a large Büchner funnel with a coarse filter paper. After

[9] Fischer, Ber., vol. 23, p. 2615, 1890.

the addition of a small quantity of decolorizing carbon the solution was filtered again. The basic salt was precipitated by warming the clear filtrate on the steam bath. It was separated by filtration while hot, washed thoroughly with hot lime water, and finally with a small quantity of hot water, then dried to constant weight at 80° in vacuo (about 24 hours).

During its preparation it was protected as much as possible from the carbon dioxide of the air, and when dried was kept in small air-tight bottles until used. The crude basic calcium gluconate may be prepared with good yield, but the quantity of the pure salt obtainable by the above procedure varies considerably with the technique. As much as 40 g of the pure dry salt has been obtained, but in case the solution of calcium gluconate and the milk of lime are not cold, or an excess of lime is added, the basic salt may precipitate before the mixture can be filtered, and the yield from the filtrate is then very small.

Several preparations by the above procedure, dried to constant weight in vacuo at 80° C., gave consistent analyses, corresponding to the formula $Ca(C_6H_{11}O_7)_2.2CaO$. However, when dried at lower temperatures the salt appears to hold varying amounts of water. The calcium-oxide content usually ran a little low and the carbon somewhat high; this is probably caused by the absorption of a small amount of carbon dioxide during the preparation of the sample.

Analyses calculated for $Ca(C_6H_{11}O_7)_2.2CaO$: C, 26.55; H, 4.09; Ca, 22.16; CaO, 20.68. *Found:* C, 27.09, 27.09; H, 4.03, 4.07; Ca, 22.10; CaO, 20.30.

WASHINGTON, March 9, 1932.

SIMPLIFIED AUTOMATIC WILSON CHAMBER

By L. F. Curtiss

ABSTRACT

A description of a simplified form of exhaust or vacuum type Wilson cloud chamber, built for demonstrating ray tracks, is given. No vacuum pump or quick-acting valve is required. By introducing some refinements this design seems adaptable also to the automatic photography of ray tracks.

CONTENTS

	Page
I. Introduction	579
II. Description of chamber	580

I. INTRODUCTION

Of the many forms of the Wilson cloud chamber arranged for automatic operation, which have been devised, those operated on the exhaust, or "vacuum," principle of the original chamber built by C. T. R. Wilson, have proved most satisfactory. In this form the piston, forming the floor of the chamber, is pulled down by suddenly connecting the closed space beneath it with an evacuated chamber by means of a valve which can be opened instantaneously. The use of springs operating directly on the piston to produce the required motion does not give good results, since it is difficult to avoid a vibratory motion of the piston which interferes with the production of sharp tracks and may even cause the production of ghost tracks as the result of two rapidly succeeding expansions. Furthermore springs become troublesome to operate in the case of larger chambers where the tensions must be large to work against the back pressure of the atmosphere. Link motions and other direct mechanical drives which have been tried have failed to give sufficiently rapid expansion unless the piston is operated at the rate of 100 or more expansions per minute, which is entirely unsatisfactory for photographic purposes and leads to confusion of the observer where such apparatus is used to demonstrate ray tracks to those unfamiliar with their appearance. A further difficulty with rapidly successive expansions is that time is not allowed for temperature equilibrium to be restored, a requirement for sharp tracks.

The operation of chambers of the exhaust type requires an oil pump of fairly large capacity and a complicated valve mechanism. Whereas these items may not be serious disadvantages in the case of permanent laboratory equipment they make impractical the operation of small, more or less portable, chambers on this principle because of the bulk and cost of this accessory equipment. The writer has designed a small chamber of an exhaust type which eliminates the use of an oil pump or valve. It is therefore much more compact and portable than the usual form of chambers of this type. Likewise it is less expensive to build. These features make it particularly adaptable for the purpose of demonstrating ray tracks automatically. The

following description is based on a small chamber recently built in this laboratory for demonstrating ray tracks and no attempt has been made to include those refinements which would be required to adapt this design for automatic photography of ray tracks. It seems quite possible, however, by using more care in the construction, and altering slightly the method of driving the auxiliary piston, to use this form of chamber for more precise work.

II. DESCRIPTION OF CHAMBER

The complete apparatus, shown diagramatically in Figure 1, consists of two parts—the cloud chamber proper, where the ray tracks are produced, and an auxiliary chamber or cylinder which serves alternately to produce the vacuum and as a valve to connect the evacuated space with the inclosed air space below the piston of the cloud chamber. The piston in the auxiliary cylinder is driven directly from an eccentric driven by an electric motor through a reduction gear, not shown, at about 30 revolutions per minute. This rate of

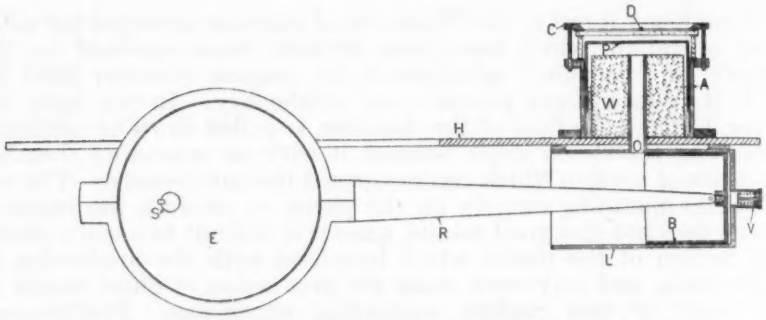

FIGURE 1.—*Sectional diagram of simplified chamber*

production of expansions is satisfactory for demonstration. To adapt this chamber for photographic work, however, a much slower rate would be necessary. This would entail more careful workmanship in making the auxiliary cylinder and a different type of mechanical drive for its piston.

The details of the apparatus are shown in section in Figure 1. The cloud chamber consists of a glass-walled cylindrical chamber closed on top by the glass disk, *D*, through which the ray tracks are observed. This disk is clamped down by screws through the metal ring, *C*, rubber gaskets being inserted in all joints to make them air-tight. The floor of the cloud chamber is formed by the "floating" piston, *P*, made of thin aluminum and working in an oil seal, as shown, within the brass cylinder, *A*. To reduce the volume of air which must be exhausted from the space below *P*, the usual practice of inserting a paraffined cylindrical wooden block, *W*, is followed. The auxiliary cylinder, *L*, is mounted horizontally beneath the base plate, *H*. It is provided with a close fitting brass piston, *B*, which is driven by the eccentric, *E*, mounted on the shaft, *S*. The eccentric and piston are connected by the rod, *R*. At the rate of operation indicated above, it is not necessary that the piston, *B*, be fitted to its cylinder, *L*, with great care since a fairly heavy lubricating oil may be used and a slight leak past this piston is not serious.

A description of the cycle of operation will help to make clear the function of the various parts of the apparatus. Starting with the piston, B, in the position indicated in Figure 1, as the eccentric, E, rotates this piston will be drawn forward in its cylinder, L, producing a vacuum in the space behind the piston. At the instant the rear edge of the piston passes the orifice, O, this evacuated space is suddenly connected with the air space below the main piston, P, causing it to be drawn rapidly down against the wooden block, W. This produces the expansion in the cloud chamber required for the formation of ray tracks. As the eccentric continues to rotate, the piston, B, returns to its initial position which again opens the orifice, O, to atmospheric pressure, permitting the piston, P, to rise to its initial position ready for another expansion. As this cycle is repeated, air would accumulate

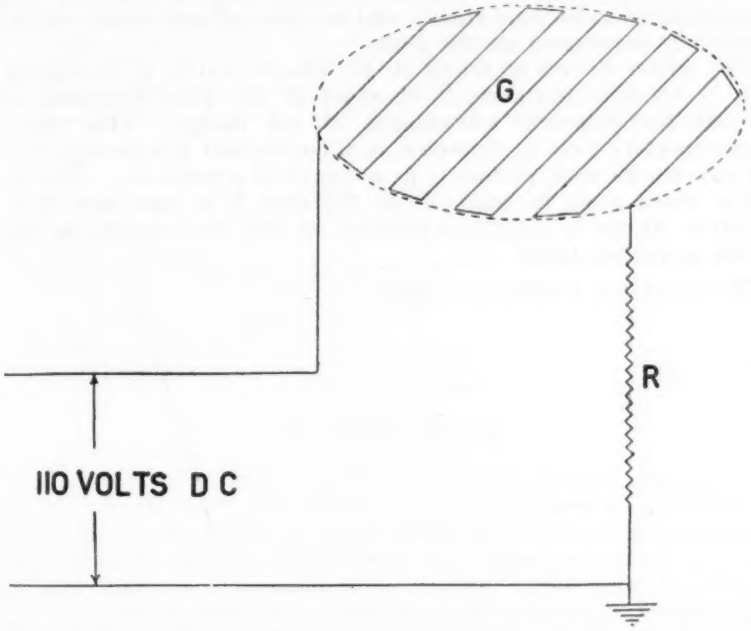

FIGURE 2.—*Diagram showing electrical connections of grid for removing water vapor from under side of glass cover*

behind the piston, B, building up a back pressure, which would cause the apparatus to fail to operate properly. To avoid this, a release valve, V, is provided to permit air to escape to the atmosphere on the return stroke of B. This valve is closed automatically by a spring on the working stroke as the piston, B, moves outward.

Some means of preventing the condensation of moisture on the underside of the glass disk, D, is required. This is ordinarily accomplished by water cooling the walls of the cylinder, A, so that the glass disk is at a slightly higher temperature than the piston, P. A more convenient method for a portable chamber is to mount a grid of fine wires spaced parallel to each other about 1 cm apart, connected in series. This grid, G, as shown in the diagram (fig. 2) is connected at one end with one side of the direct-current supply and at the other end through a high resistance to the opposite side of the direct-current

supply. The high resistance, R, is so chosen that the temperature of the grid wires rises only slightly above that of the room. This grid may simultaneously be made to provide the electric field in the cloud chamber to sweep out old ions so that the general fog of the chamber is reduced, thereby increasing the sharpness of the new tracks on each expansion. To do this it is only necessary to take care to connect the grounded side of the direct-current supply to the free end of the high resistance which is then also connected to the base plate of the apparatus. Since nearly the whole potential drop occurs in the high resistance, the grid will then be at a potential above that of the piston, P, which is approximately equal to that of the supply, say 110 volts, which is quite sufficient. In using this arrangement for freeing the under side of the glass from moisture, it is desirable to have the voltage applied some time before observing the tracks, to permit temperatures to become steady and to drive off any water which has previously condensed on the glass.

The writer desires to thank B. W. Brown and L. L. Stockman for help in constructing a small chamber of the kind described above to test the practical advantages of the design. This chamber, approximately 7 cm in diameter, is of convenient size for demonstrating ray tracks with polonium as a source of α-particles. The chamber is about 8 cm in height from the disk D to the base plate H, which is 50 cm in length, supported on legs, not shown, to raise it 30 cm above the table.

WASHINGTON, February 3, 1932.

ISOLATION OF NORMAL DECANE FROM PETROLEUM BY DISTILLATION AND EQUILIBRIUM MELTING [1, 2]

By Johannes H. Bruun [3] and Mildred M. Hicks-Bruun

ABSTRACT

A midcontinent petroleum was fractionated by distillation into cuts with boiling ranges of 0.5° C. From the cuts boiling in the neighborhood of 172° C. n-decane was isolated by systematic equilibrium melting in a low-temperature centrifuge. By this method *n*-decane with a purity above 99.999 mole per cent was obtained. The following physical constants were determined for the pure hydrocarbon: Freezing point, −29.68° C.; boiling point, +174.0° C.; specific gravity $d\ ^{20}_{4}$, 0.72994; refractive index $n\ ^{25}_{D}$, 1.4096; and aniline point, 77.6° C.

It was calculated that about 0.6 per cent of the crude petroleum consisted of n-decane.

CONTENTS

	Page
I. Introduction	583
II. Methods employed	584
III. Experimental procedure and results	584
1. Distillation	584
2. Equilibrium melting	585
IV. Discussion of the results	587
V. Acknowledgment	589
VI. Literature cited	589

I. INTRODUCTION

The presence of *n*-decane in different crude petroleums has been established by Mabery and Dunn (1) [4] and by others (2). However, the methods employed by previous investigators involved subjecting the distillates to vigorous treatments with strong chemical reagents. By such treatment it is possible to destroy completely the branch chain and cyclic hydrocarbons and leave the normal and quaternary paraffin hydrocarbons only partially attacked. Markownikoff (3) digested the fractions with strong nitric acid. Mabery and Hudson (4) used a mixture of nitric and sulphuric acids, while Aschan (5) found that chlorosulphonic acid would react less rapidly with normal and quaternary hydrocarbons than with other types of petroleum compoiunds. By means of chlorosulphonic acid Shepard, Henne, and Midgley (6) were able to isolate *n*-decane of high purity from petroleum.

[1] Financial assistance has been received from the research fund of the American Petroleum Institute. This work is part of project No. 6, The Separation, Identification, and Determination of the Constituents of Petroleum.

[2] Presented before the division of petroleum chemistry at the meeting of the American Chemical Society, New Orleans, La., Mar. 29, 1932.

[3] Research associate for the American Petroleum Institute at the Bureau of Standards.

[4] Figures in parentesis here and elsewhere in the text indicate reference given in the bibliography at the end of this paper.

II. METHODS EMPLOYED

Since the ultimate object of this research project is not only to isolate and determine the normal paraffin hydrocarbons, but also the other constituents of petroleum it is evident that the separation in every case should be conducted without the aid of destructive chemical reagents. In the present investigation, the isolation of the *n*-decane has, therefore, been accomplished by means of distillation and subsequent fractionation by equilibrium melting.

III. EXPERIMENTAL PROCEDURE AND RESULTS

1. DISTILLATION

The crude petroleum used for this investigation was obtained from No. 6 well of South Ponca City, Kay County, Okla.

The properties (7) of the material have been reported in previous papers, together with a description of the preliminary distillation (8)

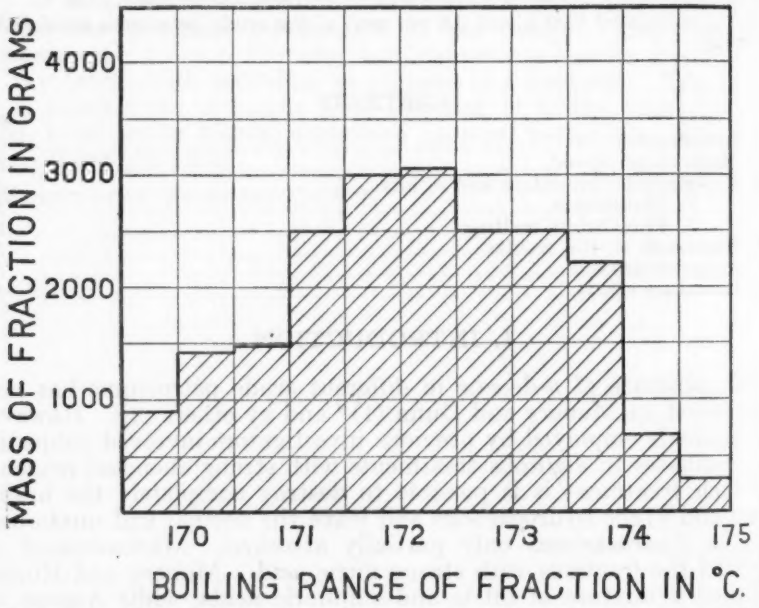

FIGURE 1.—*Distribution of the fractions over their boiling ranges after the completion of the distillation*

through a semicommercial column. Further distillations of the material were made by S. T. Schicktanz and a staff of assistants at this bureau by means of 30-plate bubbling-cap stills of glass (9), (10). These distillations were made under a pressure of 215 mm and with a reflux ratio of about 8:1. The distillates were collected at a rate of about 1 to 2 ml per minute. As a result of these distillations, a number of petroleum fractions were obtained, distributed according to boiling range in the manner shown in Figure 1. These boiling ranges have been corrected to 760 mm pressure. According to Figure 1 the largest volume of material is found between 171.5° and

172.5° C.; that is, about 2° below the boiling point (174° C.) of *n*-decane.

The refractive indices of the different cuts are shown by the graph of Figure 2. The minimum of this graph, exhibited by the two cuts boiling between 173° and 174° C., indicates that these fractions contain greater percentages of paraffin hydrocarbon than the others. The freezing points of the fractions were not accurately determined at this stage of the investigation. As should be expected, however, it was found that the fractions with boiling ranges between 173° and 174° C. could be solidified at considerably higher temperatures than the other fractions.

2. EQUILIBRIUM MELTING

During some of the preliminary experiments on the 173.0° to 173.5° C. fraction, it was discovered that the white crystalline material

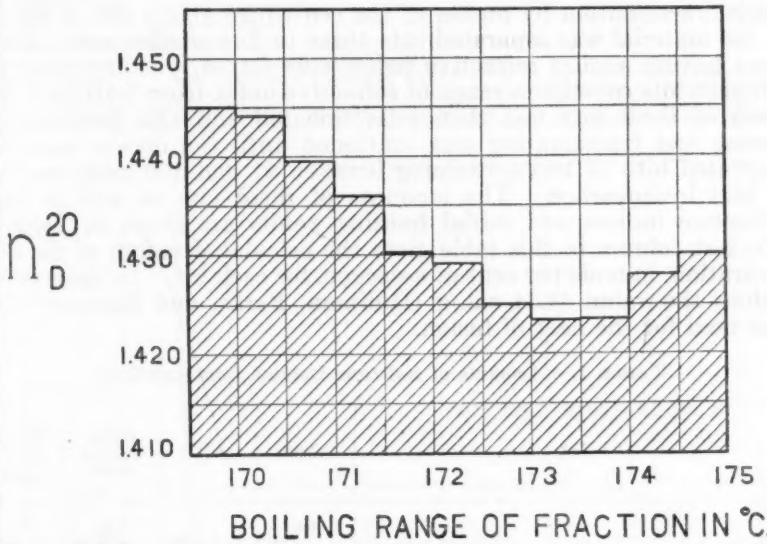

FIGURE 2.—*The refractive indices plotted against the boiling ranges of the final distillates*

which separated on cooling had physical constants which clearly indicated the presence of large quantities of *n*-decane. In order to isolate the *n*-decane from this as well as from the other cuts, a systematic fractionation by equilibrium melting was undertaken. The apparatus used for this work consisted of a freezing cylinder (with stirrer for impure and without stirrer for nearly pure decane) and a low-temperature centrifuge, and has been described in a previous paper (11). The technic employed was similar to that previously used for the purification of *n*-heptane and methylcyclohexane (11). The most satisfactory results were obtained when the temperature of the centrifuge was maintained about 2° to 5° C. above the initial freezing point of the material to be fractionated. In this way it was possible in a single fractionation to separate substantially pure *n*-decane from some of the cuts.

In some cases the following method, suggested by R. T. Leslie, was used for fractionation of nearly pure *n*-decane: The material was precooled to about −20° C. and mixed with about one-third of its volume of methyl ether. Under constant agitation in a freezing cylinder this mixture was then cooled to a soft crystalline slush. By subsequent centrifuging practically all of the impurities which were present in the *n*-decane, together with the methyl ether would separate in the "mother liquid." The removal of the last traces of impurities from the *n*-decane was further facilitated by washing the crystals on the rotating drum of the centrifuge with a small amount of methyl ether which previously had been cooled to about −35° C. Because of its low boiling point (−24.9° C.), the methyl ether could easily be removed from the hydrocarbon fractions by gentle heating under reduced pressure.

Each of the cuts shown in Figure 1 was fractionated by one of the above-described methods of equilibrium melting. As a result of a single fractionation by means of the centrifuge about 500 to 800 ml of the material was separated into three to five smaller cuts. Fractions having similar refractive index were mixed, yielding about 20 different lots covering a range of refractive index from 1.410 to 1.450. Each of these lots was then refractionated and this procedure of mixing and fractionating was continued until the decane was concentrated into 11 lots containing between 91 and 100 mole per cent of this hydrocarbon. The amounts of these lots as well as their refractive indices and initial freezing points are given in Table 1. The last column in this table gives the calculated values of the concentration, in mole per cent of *n*-decane, for each lot. In these calculations the value 48.34 cal./g (Huffman, Parks, and Barmore (12)) was used for the heat of fusion.

TABLE 1.—*Amounts of n-decane isolated from petroleum*

Lot	Volume	n_D^{25}	Initial freezing point	Purity in mole per cent *n*-decane
	ml		° *C.*	
1	200	1.4096	−29.68	100.0
2	150	1.4098	−29.70	99.8
3	200	1.4100	−29.78	99.4
4	800	1.4102	−29.80	99.3
5	1,100	1.4104	−29.98	98.2
6	1,600	1.4108	−30.20	97.0
7	2,400	1.4110	−30.32	96.2
8	400	1.4115	−30.58	94.6
9	2,100	1.4118	−30.68	94.0
10	900	1.4126	−31.17	91.0
11	2,100	1.4128	−31.25	91.1

Referring to Figure 1, it should be noted that by far the greatest quantities of *n*-decane were isolated from the cuts boiling between 171.5° and 174° C. The concentration of *n*-decane in the cuts boiling below 171.5° and above 174.0° C. diminished rapidly with the change in boiling temperature.

IV. DISCUSSION OF THE RESULTS

The identification of *n*-decane in the midcontinent petroleum was definitely established by comparing the physical properties of the purest sample of the isolated hydrocarbon (lot 1 in Table 1) with those of the purest samples of *n*-decane reported in the literature. The results of this comparison are shown in Table 2.

TABLE 2.—*Physical constants of n-decane*

n-decane ($C_{10}H_{22}$)	d_4^{20}	n_D^{25}	Boiling point corrected	Freezing point (in dry air)	Critical solution temperature in aniline
			°C.	°C.	°C.
Bruun and Hicks-Bruun	[1] 0.72994	[2] 1.40960	174.0	[3] −29.68	77.6
Shepard, Henne, and Midgley (6)	.73014	1.40986	174.06	−29.76	77.5
B. J. Mair (13)		[2] 1.40961	174.02	[4] −29.68	

[1] ±0.00002. Determined by the section of capacity and density of this bureau.
[2] Determined by L. W. Tilton, of the optical division of this bureau.
[3] Determined by B. J. Mair by means of a platinum resistance thermometer calibrated by this bureau.
[4] The freezing point of B. J. Mair's sample of synthetic *n*-decane was at first found to be −29.76° C. However, it was later submitted to fractionation by means of the centrifuge used in this work. Thus the freezing point was raised to the same final value (−29.68° C.) as that of the *n*-decane isolated from petroleum.

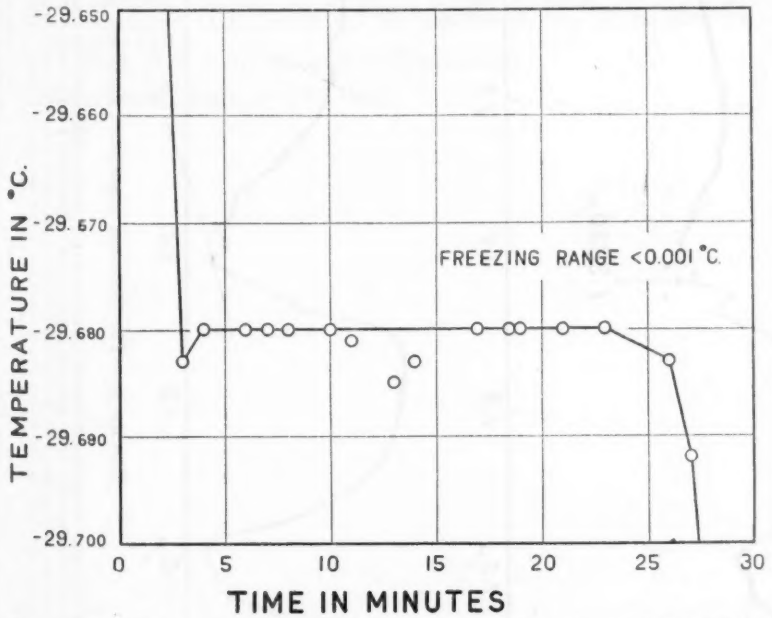

FIGURE 3.—*The time-temperature freezing curve of the n-decane isolated from petroleum*

The time-temperature cooling curve of the *n*-decane isolated from petroleum was obtained by B. J. Mair, of this bureau, using a platinum resistance thermometer and is shown in Figure 3. The whole sample froze solid within less than 0.001° C. (neglecting the irregularities in the middle portion of the curve, due to insufficient stirring) and is consequently of an exceptionally high degree of purity (above

99.999 mole per cent). The decane sample was subjected to further equilibrium melting by means of the centrifuge, but it was not possible to raise its freezing point above the determined value —29.68° C.

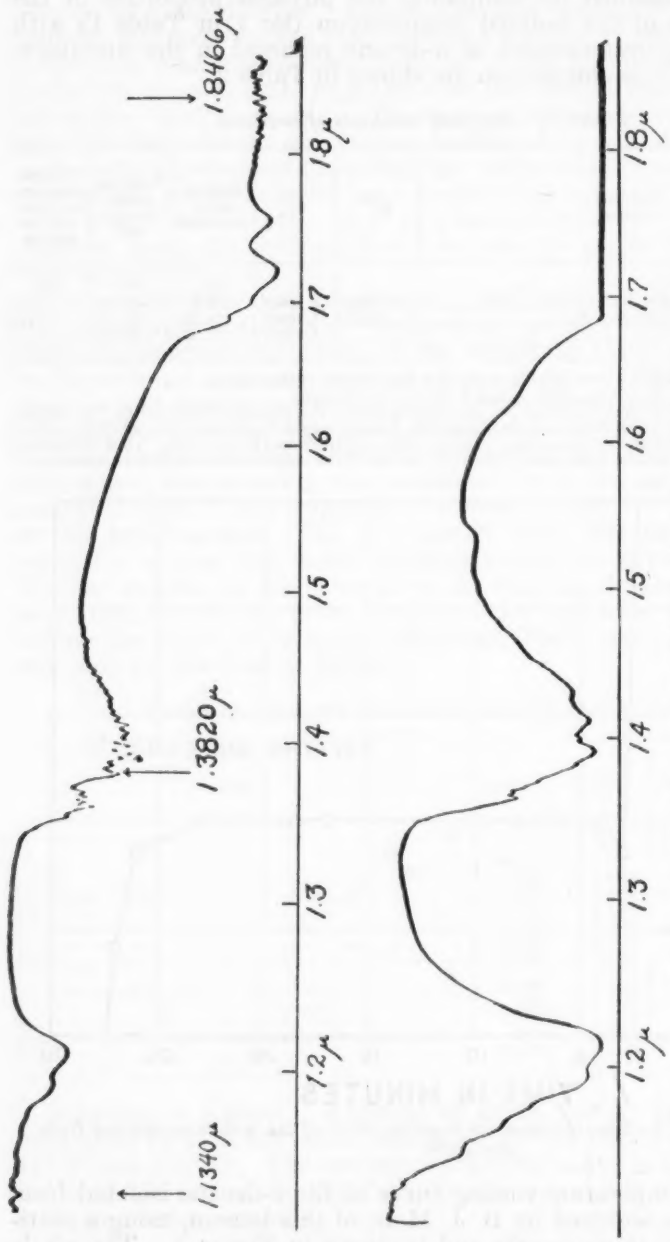

FIGURE 4.—*The infra-red absorption spectrum of the isolated n-decane*

These curves are the energy transmission lines of the emission of a tungsten filament lamp through 1 mm and 1 cm cell thicknesses, respectively, of normal decane, automatically recorded by an infra-red spectrograph in the region from 1μ to 2μ. These curves show the absorption of the compound at the first and second overtone frequencies of the 3.4 fundamental of hydrocarbon absorption at 1.73μ and 1.20μ and the combination band of this fundamental with another near 6μ at 1.42μ, besides the absorption of the water vapor necessarily present in the light path which is quite apparent as the fine band absorption and strong bands of which are indicated by the arrows. These spectra fit in nicely with the series of normal aliphatic hydrocarbon spectra studied by F. Hershel Allen and Ira Bell (Phil. Mag., vol. 4, p. 861, 1927). The records were taken with an effective slit-width of approximate 20 A. Measured by U. Liddel of the Fixed Nitrogen Research Laboratory, United States Department of Agriculture.

The infra-red absorption spectrum of the *n*-decane was measured by U. Liddel, of the fixed nitrogen research laboratory of the United States Department of Agriculture, and is shown in Figure 4.

Based upon the total amount of the crude petroleum used (600 gallons of specific gravity 0.9) and including fractionation losses, it is estimated that the percentage of *n*-decane in the crude petroleum is about 0.6.

V. ACKNOWLEDGMENT

The authors acknowledge the technical advice of E. W. Washburn, director of American Petroleum Institute project No. 6.

VI. LITERATURE CITED

1. C. F. Mabery and O. C. Dunn, Am. Chem. J., vol. 18, p. 230, 1896.
2. Engler-Höfer, Das Erdöl, vol. 1, p. 246, Hirzel, Leipzig, 1913.
3. W. Markownikoff, Ber., vol. 32, p. 1445, 1899.
4. C. F. Mabery and E. J. Hudson, Am. Chem. J., vol. 19, pp. 482–485, 1897.
5. O. Aschan, Ber., vol. 31, p. 1801, 1898.
6. O. E. Shepard, A. L. Henne, and T. Midgley, jr., J. Am. Chem. Soc., vol. 53, p. 1948, 1931.
7. E. W. Washburn, J. H. Bruun, and M. M. Hicks, B. S. Jour. Research, vol. 3, p. 469, 1929.
8. J. H. Bruun and M. M. Hicks-Bruun, B. S. Jour. Research. vol. 7, p. 608, 1931.
9. J. H. Bruun, Ind. Eng. Chem., anal. ed., vol. 1, p. 212, 1929.
10. J. H. Bruun and S. T. Schicktanz, B. S. Jour. Research, vol. 7, pp. 851–882, 1931.
11. M. M. Hicks-Bruun and J. H. Bruun, B. S. Jour. Research, vol. 8, p. 432, 1932.
12. H. M. Huffman, G. S. Parks, and M. Barmore, J. Am. Chem. Soc., vol. 53, p. 3882, 1931.
13. B. J. Mair, B. S. Jour. Research, (unpublished).

WASHINGTON, January 30, 1932.

A LABORATORY APPARATUS FOR THE CONTINUOUS EXTRACTION OF LIQUIDS BY LOW BOILING SOLVENTS [1]

By R. T. Leslie [2]

ABSTRACT

A laboratory apparatus for the extraction of liquids by low-boiling solvents is described. The apparatus is counter-current and continuous in operation. Important details of constructions are given and the method of operation is described. A brief discussion of the performance of the apparatus for the extraction of petroleum fractions with liquid sulphur dioxide is given.

CONTENTS

		Page
I.	Introduction	591
II.	Construction of glass apparatus	592
III.	Operation of the glass apparatus	593
IV.	Construction of metal apparatus	596
V.	Operation of the metal apparatus	597
VI.	Performance of the apparatus	599
VII.	Acknowledgment	599

I. INTRODUCTION

Differences in solubility in liquid sulphur dioxide have been used,[3] [4] as a means of separating aromatic and olefinic hydrocarbons from the paraffinic and naphthenic groups. In connection with the problem of determining the composition of petroleum it was deemed advisable to investigate the general method of fractionation by extraction with low-boiling solvents. It was found that extraction has the disadvantage that the distribution coefficients are seldom favorable for the complete separation of a distinct component from a mixture. Attempts have been made to estimate the composition of petroleum by applying correction factors to the sulphur dioxide soluble content of various distillation fractions, but the method is rendered somewhat uncertain by the effect of unknown constituents on the distribution coefficients.[5] [6] Extraction should be valuable, however, as a method of breaking up the constant boiling mixtures encountered in fractional distillation, and may be supplemented by subsequent further distillation or crystallization, or both, to obtain pure materials.

Sulphur dioxide is one of the best known extractants which has the property of selectively dissolving certain types of hydrocarbons, and considerable technic has been developed for its use both on a commercial and on a laboratory scale.[7] [8] [9] After some consideration, however,

[1] Financial assistance has been received from the research fund of the American Petroleum Institute. This work is part of project No. 6, The Separation, Identification, and Determination of the Constituents of Petroleum.

[2] American Petroleum Institute research associate.

[3] P. Walden, Ber., vol. 32, p. 2862, 1899.

[4] Edeleanu, Am. Inst. Mining Eng., vol. 93, p. 2313, 1914.

[5] S. E. Bowrey, Pet. Rev., vol. 36, pp. 352, 385, 401, 1917.

[6] See footnote 4.

[7] See footnote 4.

[8] Laboratory apparatus described in a circular published by Allgemeine Gesellschaft für Chemische Industrie, M. B. H., Berlin, W8.

[9] R. L. Brandt, Ind. Eng. Chem., vol. 22, p. 218, 1930.

it was decided that improvement could be made in the laboratory apparatus.

The apparatus which has been developed, although intended primarily for use with sulphur dioxide, can be used with any low-boiling solvent, the density of which is greater than that of the material to be extracted. For use with solvents of densities less than that of the hydrocarbon, some modification is necessary, but the same principles can be used.

Two forms of the apparatus will be described. The first type is entirely of glass and is the simpler to construct, but must be operated at temperatures below the boiling point of sulphur dioxide. The second type is of metal and may be operated at temperatures above the normal boiling point of sulphur dioxide. It also possesses the convenience that the sulphur dioxide need not be removed when the apparatus is not in use.

Both types operate on essentially the same principles, of which the salient features are (1) countercurrent flow of the liquids, (2) maintenance of a considerable excess of sulphur dioxide, (3) automatic control of the height of the column of sulphur dioxide by an overflow tube requiring no valve regulation, and (4) continuous operation in regard to circulation of both sulphur dioxide and hydrocarbon.

II. CONSTRUCTION OF GLASS APPARATUS

Figure 1 is nearly self-explanatory, but a few details of construction will be emphasized.

The extraction column, *G*, of the apparatus used in this laboratory is about 80 cm in height and 1.8 cm in diameter. It is difficult to maintain a smooth countercurrent flow in columns of smaller diameter. No packing is used because the hydrocarbon tends to cling to it and to displace the sulphur dioxide instead of rising through it. The tube, *O*, is made of 1 mm capillary to reduce the volume of sulphur dioxide outside the cooling bath and at the same time to afford mechanical support to the column. Smaller capillaries tend to clog. The upper section of the column, *F*, is made of smaller tubing to decrease the volume of immiscible hydrocarbon held up in this part of the apparatus.

The overflow tube, *H*, must be of such a height that the weight of extract in it will more than counterbalance the weight of extract plus the weight of the supernatant hydrocarbon in the column. For two liquids which differ as much in density as sulphur dioxide and petroleum hydrocarbon, it is necessary only to keep the height of the overflow a few centimeters (10 to 15 cm) below the outlet tube for the immiscible material. The vent tube E_2 prevents the overflow tube from acting as a siphon.

The jacket surrounding the column consists of a 5.5 cm glass tube in which the column is held in place by the split cork at the bottom. This cork is made liquid-tight by pouring a layer of collodion into the bottom of the jacket after it is assembled. Heavy felt packing may be used for heat insulation.

The two extract boilers, R_3 and R_4, are made from one-fourth-liter flasks. The reentrant tubes are bent so that they do not open directly over the drain tubes because the latter act as points of ebullition for the boiling sulphur dioxide and would interfere with the ready flow of

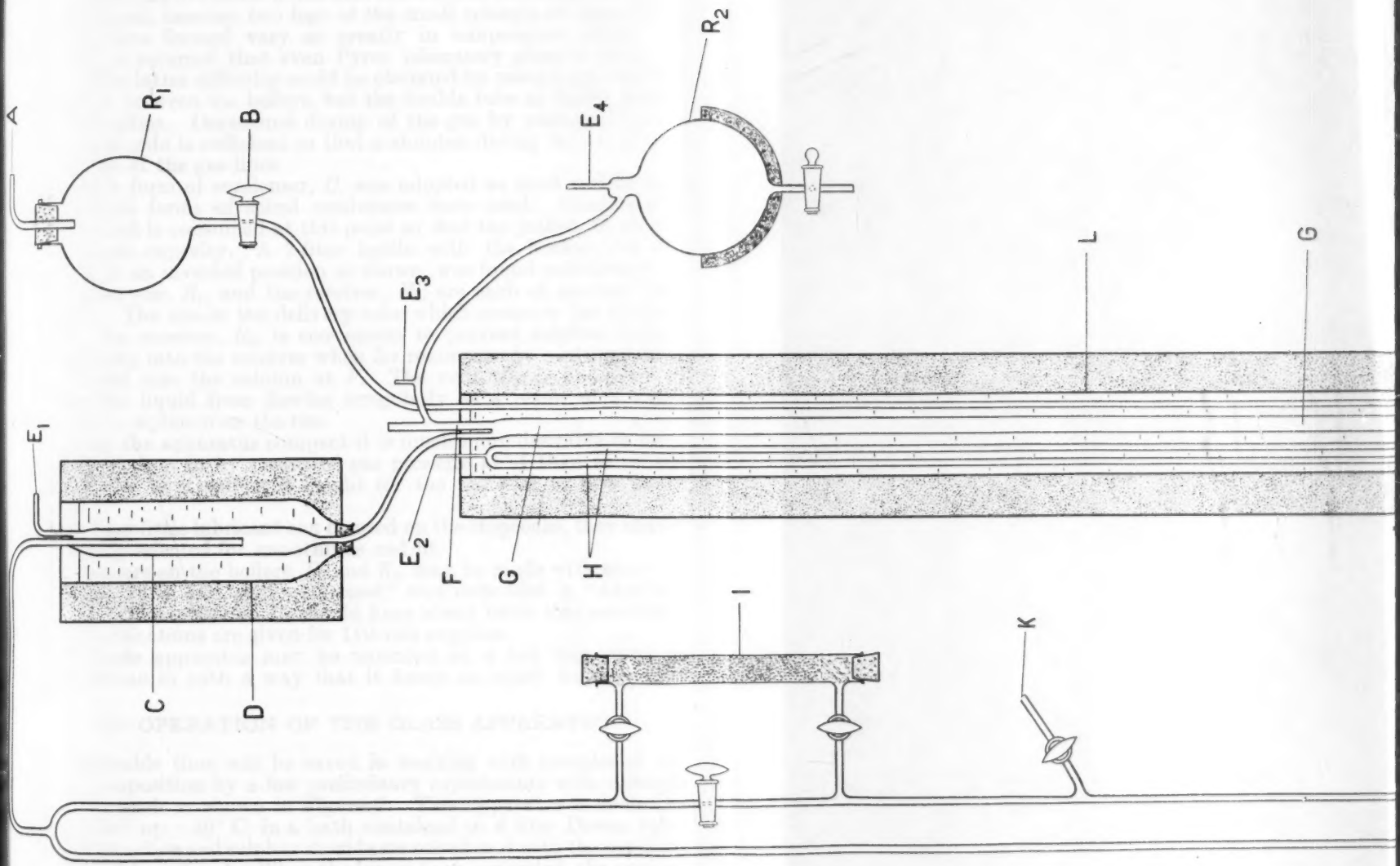
A
R1
B
E4
R2
E3
L
G
E1
E2
F
G
H
I
K
C
D

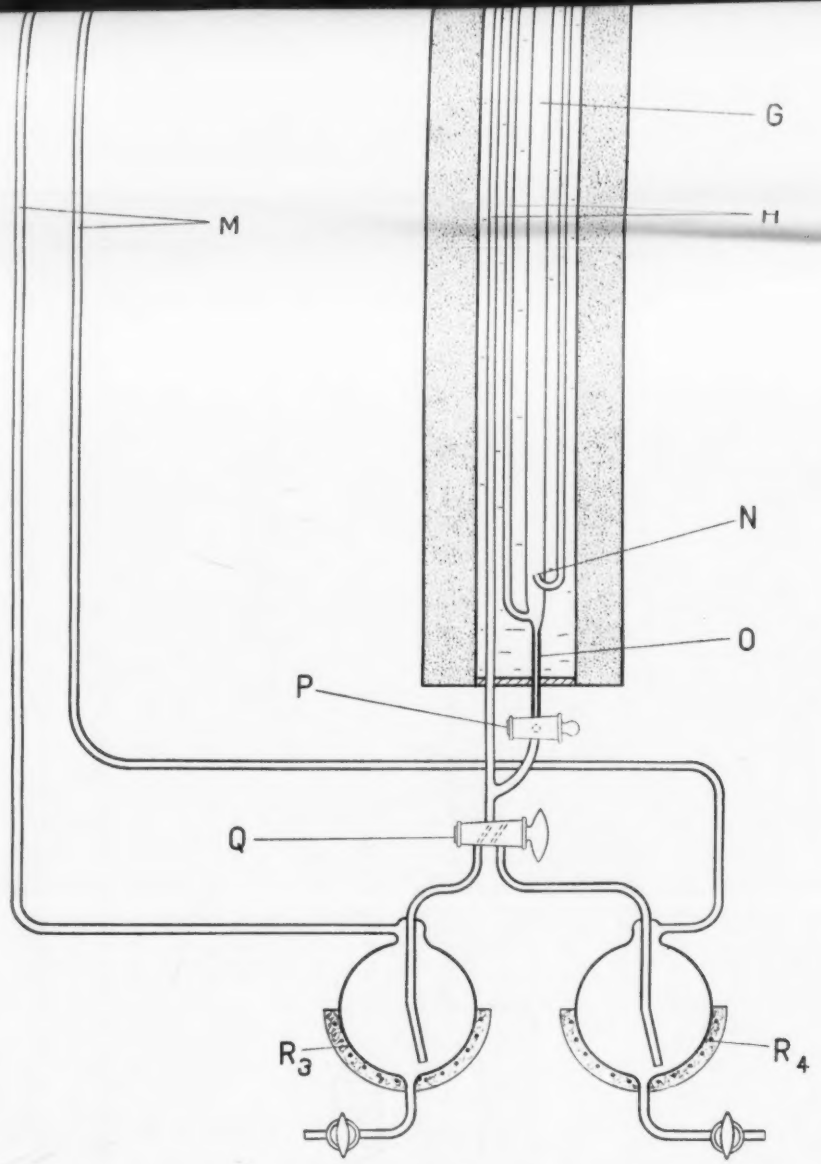

FIGURE 1.—*Continuous-flow extraction apparatus of glass construction*

A, gas pressure inlet; *B*, stopcock for regulation of hydrocarbon flow; *C*, SO_2 condenser; *D*, cooling path for condenser; E_1, E_2, E_3, E_4, vents to atmosphere; *F*, upper section of extraction column containing the immiscible hydrocarbon layer; *G*, extraction column; *H*, extract overflow; *I*, drying tube; *K*, SO_2 inlet; *L*, cooling bath for extraction column; *M*, SO_2 gas connections between boilers and condenser; *N*, hydrocarbon inlet; *O*, capillary tube; *P*, stopcock for draining the extraction column; *Q*, two-way stopcock for directing the flow of extract to the desired boiler; R_1, hydrocarbon reservoir; R_2, immiscible hydrocarbon receiver; R_3, R_4, extract boilers.

111260—32. (Face p. 592.)

liquid down the reentrant tubes. Individual gas tubes, M, should be run from the boilers to the condenser, C, for two reasons: First, because the short connecting tube, which results if the two boilers are connected to a single gas tube, allows the sulphur dioxide to distill directly from the hot boiler to the cold one without reaching condenser, C, and second, because two legs of the small triangle of glass tubes which is thus formed vary so greatly in temperature when the SO_2-cycle is reversed that even Pyrex laboratory glass is likely to crack. The latter difficulty could be obviated by using a spiraled gas connection between the boilers, but the double tube as shown avoids both difficulties. Occasional drying of the gas by passage through calcium chloride is sufficient so that a shunted drying tube is placed in only one of the gas lines.

The trap form of condenser, C, was adopted as most satisfactory after several forms of spiral condensers were tried. Considerable cooling agent is consumed at this point so that the jacket, D, should be of ample capacity. A 2-liter bottle with the bottom cut off, mounted in an inverted position as shown, was found satisfactory.

The reservoir, R_1, and the receiver, R_2, are each of one-half liter capacity. The rise in the delivery tube which connects the column, F, with the receiver, R_2, is convenient to prevent sulphur dioxide from running into the receiver when for reasons to be explained later it is poured into the column at F. The vent, E_3, is necessary to prevent the liquid from flowing irregularly as a result of a slight tendency to siphon over the rise.

To keep the apparatus compact it is much more desirable to force the hydrocarbon in by means of gas pressure at A than to mount the reservoir at a sufficient height for the material to flow in by gravity.

Since very little lubricant can be used on the stopcocks, they should be carefully selected for smoothness and fit.

The heaters on the boilers, R_3 and R_4, may be made with about 12 feet of No. 26 B. & S. gage "Chromel" wire imbedded in "Alundum cement." The heater on R_2 should have about twice this resistance. These specifications are given for 110-volt supplies.

The whole apparatus may be mounted on a tall ring stand or a rigid frame in such a way that it forms an easily transportable unit.

III. OPERATION OF THE GLASS APPARATUS

Considerable time will be saved in working with samples of unknown composition by a few preliminary experiments with a simple apparatus such as shown in Figure 2. This apparatus is cooled to about $-20°$ or $-30°$ C. in a bath contained in a liter Dewar tube. The hydrocarbon and sulphur dioxide are mixed in A with the capillary closed by the glass rod. When the layers have separated, the apparatus is lifted out of the bath long enough to permit the removal of the extract layer into E. After a precautionary cooling in the bath it is again lifted out and the extract forced out into a cold test tube through F by blowing into D. The sulphur dioxide can be boiled out of the extract, collected in a trap, and used for a second extraction. In this way the feasibility of extraction can be determined on a sample of a few milliliters.

If extraction is practicable it is necessary (1) that this test result in the formation of two layers, (2) that the hydrocarbon in the two layers differ in composition, (3) that no solid separate at the temperature of extraction. This third condition is necessary since the operation of the large apparatus depends on the flow of cold liquids through small tubes. If the mixture contains a constituent, such as benzene, in sufficient concentration to freeze out at a temperature approaching the boiling point of sulphur dioxide, it is best to use an apparatus of the type to be described later or to remove the excess of the interfering constituent by precooling and filtering the mixture to be extracted.

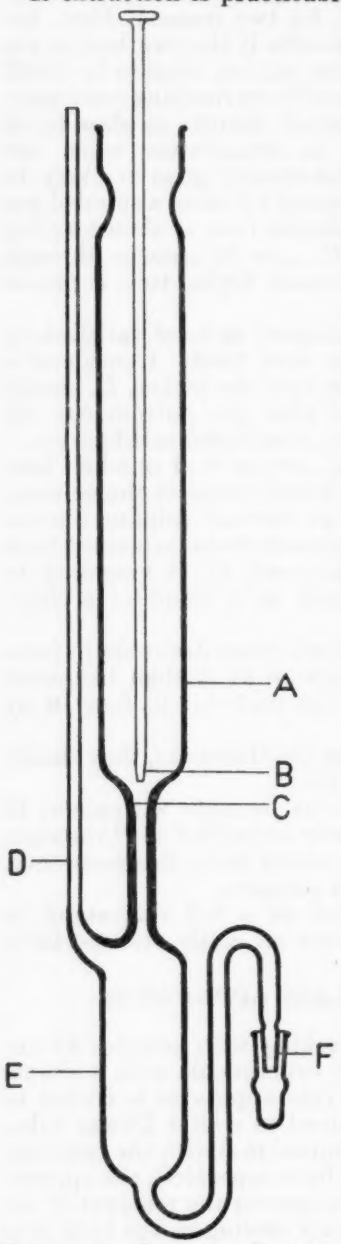

FIGURE 2.—*Apparatus for test extractions*

A, chamber in which SO_2 and hydrocarbon are mixed; *B*, glass rod with end tapered to fit *C*; *C*, capillary tube; *D*, vent tube; *E*, chamber into which lower immiscible layer is drained; *F*, exit tube for liquid (closed with ground stopper).

The larger apparatus must be thoroughly dry before beginning operations in order to avoid the formation of ice in the system. It is best to make a practice of washing the condenser and column with acetone and drying with dry air before cooling the apparatus.

The cooling jacket, *D*, is now filled with a thick slush of solid carbon dioxide in a mixture of chloroform and carbon tetrachloride and the jacket, *L*, is cooled to $-40°$ or $-50°$ C. by gradual addition of solid carbon dioxide to the cryostat liquid. The jacket, *L*, is maintained at the higher temperature because the sulphur dioxide which collects in the column would freeze at the sublimation temperature of carbon dioxide. The lower temperature can be used in *D*, since the sulphur dioxide drains from the condenser before it reaches the freezing temperature. It is well also, as a precaution, to connect all vents, such as E_1, E_2, E_3, E_4, and *F*, to a cold trap by rubber tubes to prevent the escape of sulphur dioxide into the room.

The stopcocks are greased lightly with an ordinary stopcock grease and the keys inserted firmly after the apparatus has cooled. To fill the apparatus, stopcock *P* is closed, *Q* is opened to R_3 or R_4, and the sulphur dioxide distilled in through *K* until about 100 ml runs down into the boiler, or chilled liquid sulphur dioxide may be poured in through *F*. Should the sulphur dioxide be a residue from a previous operation, it may be conveniently separated at this stage of the process from

any immiscible hydrocarbon by liquefying and pouring it into a cold separatory funnel from which the lower layer can be drained into the column. In this case stopcock P is left open long enough to allow all the sulphur dioxide which may be contaminated with hydrocarbon to run down into the boiler. The sulphur dioxide can be purified then by distillation through the apparatus, and the nonvolatile residue drained from the boiler.

The hydrocarbon is placed in R_1, with stopcock B closed and about a 3 or 4 pound pressure (air, CO_2, N_2) impressed on it through A. The circulation of sulphur dioxide is begun by starting the heater under the boiler which contains the sulphur dioxide and bringing the bath surrounding the column to the desired temperature.

The hydrocarbon is admitted slowly by opening stopcock, B. It has been found much easier to regulate the flow by this stopcock than by the gas pressure. If the hydrocarbon refuses to flow in, it is probable that the ice has formed in the inlet tube because the apparatus was not completely dried. In such event the apparatus must be emptied and brought up to room temperature again. In any case a short time is required to build up an immiscible layer above the sulphur dioxide in the column before liquid begins to run into receiver R_2. As long as the operation of extraction is continued it is only necessary to change the stopcock, Q, and the heater, and to drain out the degassed extract when the sulphur dioxide is driven out of a boiler. A small quantity of sulphur dioxide is unavoidably carried along with the product, so that it may be necessary to introduce fresh sulphur dioxide occasionally. Experience has shown that the operating capacity of the apparatus described is about one-half liter of hydrocarbon per hour.

As soon as the last of the hydrocarbon has run in, the gas pressure at A must be cut off to prevent sulphur dioxide from being blown out of the column.

The procedure to be employed in emptying the apparatus will depend on whether the operation of extraction is finished or merely temporarily suspended. If it is finished, the hydrocarbon in the column should be separated from the sulphur dioxide. This may be done by performing one or two cycles of sulphur dioxide circulation after the flow of hydrocarbon has been stopped. In this way most of the sulphur dioxide which contains hydrocarbon is washed from the column. Then stopcock P is opened to empty the column into one of the boilers and the sulphur dioxide is distilled off into the other boiler. The residue will contain the floating immiscible layer and some extracted material.

To store the sulphur dioxide it can be run directly from the boiler into a chilled "1-pound sulphur dioxide sample bottle" from which the valve has been temporarily removed. When the apparatus is to be filled again this cylinder can be cooled and the contents poured directly into the column through F or it may be distilled from the warm cylinder as described above.

If the extraction is merely suspended or if it is desired to stop the operation quickly, the column may be drained into one of the boilers

and the mixture run into a chilled cylinder and sealed. The sulphur dioxide and hydrocarbon may then be separated at leisure by distillation, or the cylinder may be again cooled and the immiscible material separated in a cold separatory funnel as mentioned above. Sulphur dioxide which has been used in the extraction of even moderately high boiling hydrocarbons (150° C.) will contain a considerable amount of the hydrocarbon after one distillation without rectification, so that care must be taken if it is to be used subsequently where contamination is undesirable.

IV. CONSTRUCTION OF METAL APPARATUS

By using metal is it possible to construct an apparatus which will function at pressures of several atmospheres and will therefore permit the use of solvents considerably above their boiling points. This makes it possible to extract materials which will congeal or become very viscous at the temperatures at which the open type must be operated. The change in the relative miscibility of the constituents with the temperature may also be investigated over a much wider range than with the glass apparatus. [10]

The chief difference in the construction of the two types lies in the use of pressure equalizing connections between various parts of the apparatus instead of vents to the atmosphere.

Figure 3 is a diagram of an apparatus which has been operated at +13° C. The barrel of the column, G_3, is made of three-fourths inch iron pipe about 30 inches long with sections of one-fourth inch pipe, G_1, placed at either end. The enlargements, G_2, are formed by inserting pipe couplings at these points. This decreases the velocity of counterflow at the points where liquid enters the column, thus preventing a dragging of the liquid in the wrong direction.

All connecting tubes in which liquid flows by gravity are made of three-sixteenths inch (outside diameter) copper tubing. Smaller tubes have too great a resistance to flow. All valves, except B_2, are of one-fourth inch bore for the same reason. The tubes M_1 and M_2 through which the gas distills are three-eighths inch (outside diameter) to allow rapid flow of gas. The pressure-equalizing tubes, E, are of small diameter. The needle valve, B_2, permits close regulation of flow in the inlet tube.

The sight glasses, of which a detail is given in Figure 4, are of soldered pyrex-to-copper construction, which requires no packing. Packed sight glasses obtainable on the market may be satisfactory, however. Glasses F_1, F_2, and F_4 are about 4 mm in bore to allow easy flow of liquid. Glass F_3 is of smaller bore (about 1 mm) to make the slow flow of liquid in the inlet line easily visible.

The reservoirs, R_1, R_2, R_3, and R_4 may be made from the iron cylinders in which sulphur dioxide is marketed in 6-pound quantities. If the heaters are to be operated at 110 volts and are to be used for sulphur dioxide, R_3 and R_4 should be wound with about 18 feet and R_2 with 24 feet of No. 24 B. & S. gage Chromel wire. The coils may be insulated from the cylinders with sheet mica and covered with asbestos. Valves B_7 and B_8 should be situated as far as possible from the boilers to keep the packing from melting.

[10] It has been found by Moore, Morrell, and Egloff (Ind. Eng. Chem., vol. 18, p. 396, 1918) that the miscibility of cyclic hydrocarbons in sulphur dioxide increases much more rapidly with a rise in temperature than that of the straight-chain hydrocarbons.

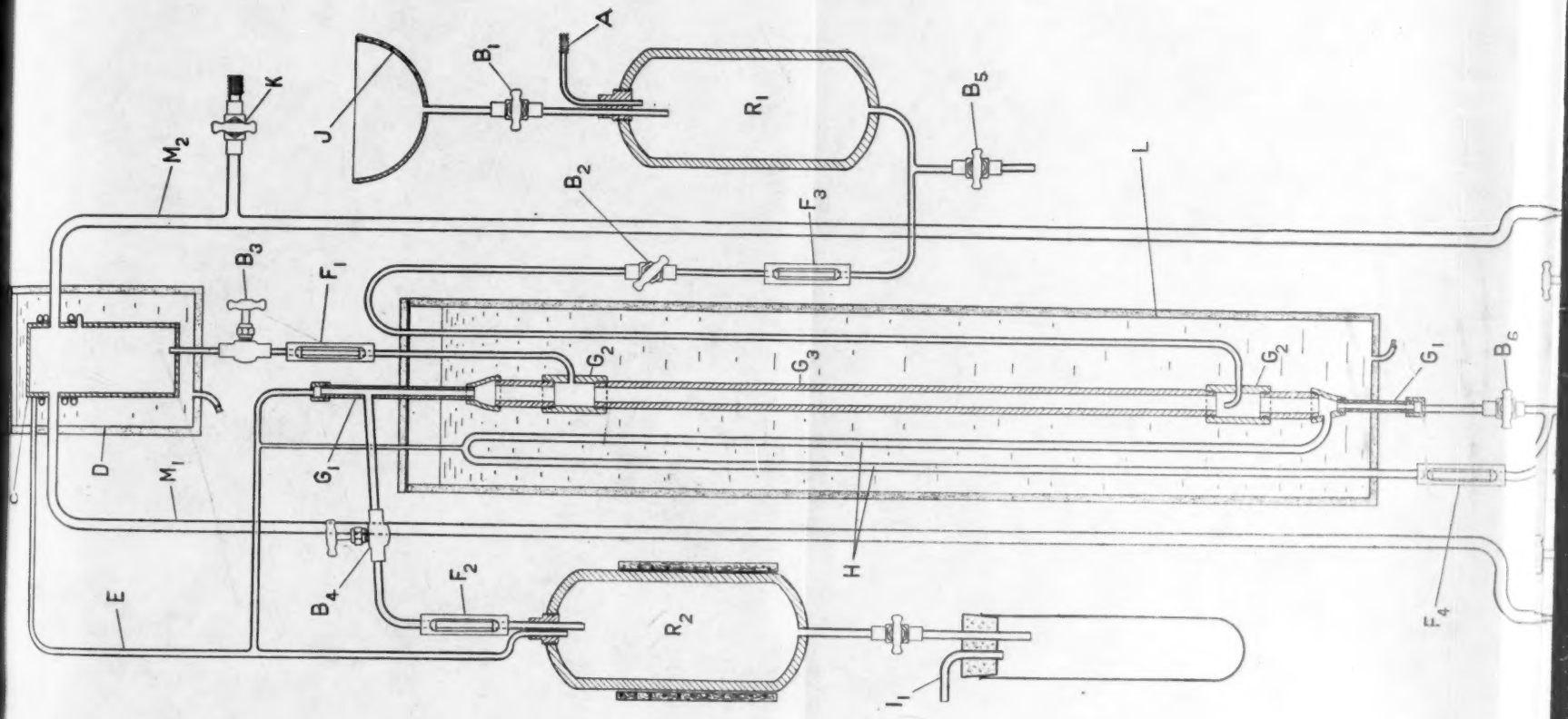
A
B1
B2
B3
B4
B5
B6
C
D
E
F1
F2
F3
F4
G1
G2
G3
H
I1
J
K
L
M1
M2
R1
R2

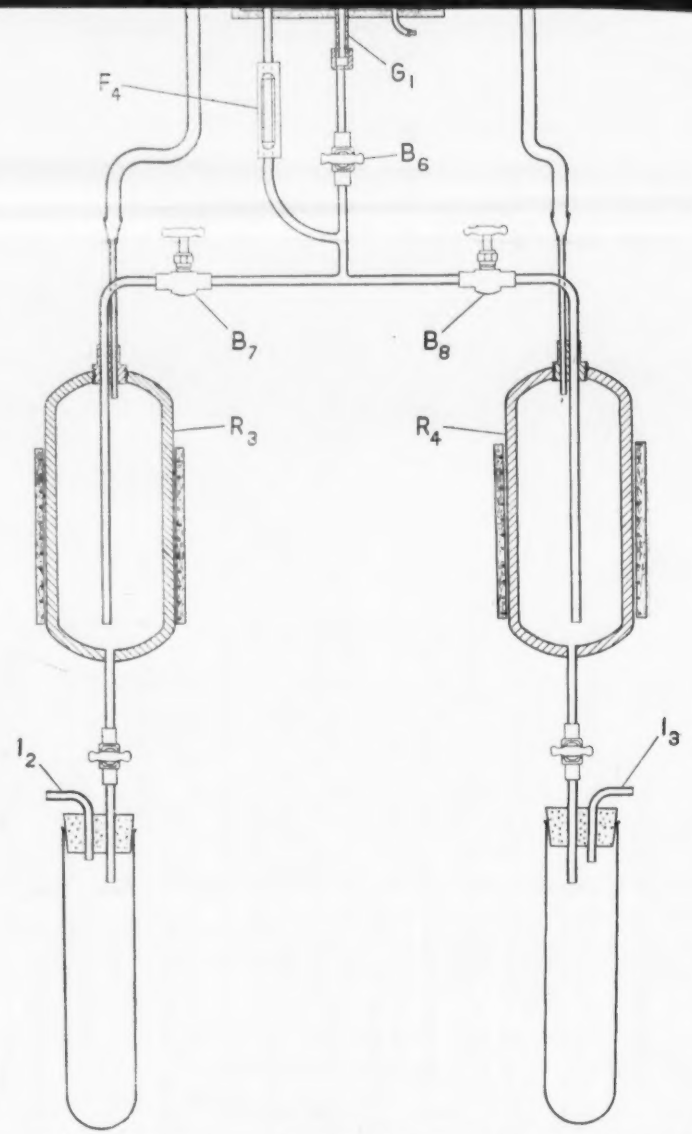

FIGURE 3.—*Continuous-flow extraction apparatus of metal construction*

A, gas-pressure inlet; B_1, B_3, B_4, B_5, B_6, B_7, and B_8, large-bore valves; B_2, needle valve; *C*, SO_2 condenser; *D*, cooling bath for condenser; *E*, pressure-equalizing tubes; F_1, F_2, F_4, large-bore sight glasses; G_1, one-fourth inch iron pipe; G_2, pipe coupling; G_3, extraction column, three-fourths inch diameter); *H*, extract overflow; *I*, vent to CO_2 ice trap; *J*, funnel for introducing hydrocarbon; *K*, SO_2 inlet; *L*, cooling bath for extract column; M_1, M_2, SO_2 gas tubes from boilers to condenser; R_1, hydrocarbon reservoir; R_2, receiver for immiscible material; R_3, R_4, extract boilers.

111280—32. (Face p. 596.)

The apparatus is mounted compactly in a frame consisting of four three-eighths inch iron pipes in 6-inch square formation.

V. OPERATION OF THE METAL APPARATUS

Precaution in the matter of drying this apparatus is unnecessary because of its closed construction. Before filling with sulphur dioxide all valves to the atmosphere should be closed, as well as B_2, B_4, B_6, and either B_7 or B_8. The condenser, C, and the column are then surrounded by a cooling agent, such as ice, ice salt, or carbon dioxide slush, depending on the temperature of extraction desired. If a thick slush of carbon dioxide ice is used on the condenser, valve B_3 must be opened wide and care should be exercised not to surround the column with a bath which will freeze the sulphur dioxide.

The sulphur dioxide container is connected to K by means of a copper tube and small union. The sulphur dioxide may then be distilled in, or if the container is a small tank it may be mounted in an inverted position and the sulphur dioxide forced in as a liquid by slightly warming the tank.

After filling, it is unnecessary to remove the sulphur dioxide, except for repairing or cleaning the apparatus. The operation of removal can be most easily performed by cooling the condenser, C, with carbon dioxide slush leaving valves B_3, B_6, and either B_7 or B_8 open. (It is unnecessary to cool the column for the operation.) This will cause the sulphur dioxide in the extract boiler to be cooled below its atmospheric boiling point by evaporation. It can then be run directly into a cooled metal cylinder as described above. All such operations are much more pleasant if precautions are taken to connect the exits to the atmosphere to carbon dioxide-slush traps or absorbers. A piece of cotton soaked in ammonia water can be used to detect small leaks in the apparatus.

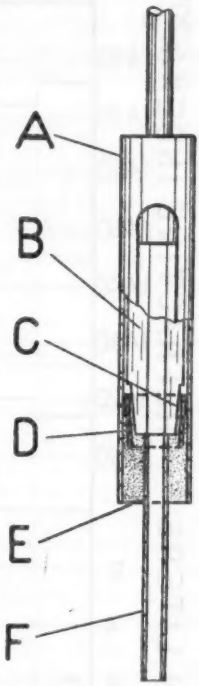

FIGURE 4.—*Sight glass detail*

A, copper or brass protecting sheath; *B*, heavy wall Pyrex laboratory glass tube tapered and ground into a copper ring *D* at each end; *C*, soldered joint between glass taper and copper ring; *D*, copper ring tinned with solder inside and out; *E*, solder cast into sheath, *A*, holding *D* and *F* in position; *F*, copper tube.

Before introducing the hydrocarbon into R_1, it is well to open B_5 momentarily to be sure that the reservoir is empty. The introduction of the hydrocarbon can be accelerated by applying a slight suction at A. B_1 is then closed and A is connected to a source of gas pressure through a reducing valve. The pressure required will depend on the vapor pressure of sulphur dioxide at the temperatureof extraction.

The bath surrounding the column is next brought to the desired extraction temperature and the condenser bath is cooled to a somewhat lower temperature to increase the rate of condensation. If the condenser temperature is more than 20° or 30° lower than the column, however, there will be a tendency for sulphur dioxide to distil

from the column and interfere with the flow of liquids. There will also be a large temperature difference between the contents of the column and the bath.

The circulation of sulphur dioxide is started by turning on the heater of the boiler in which the sulphur dioxide has collected. If the temperature of C is above the freezing point of sulphur dioxide,

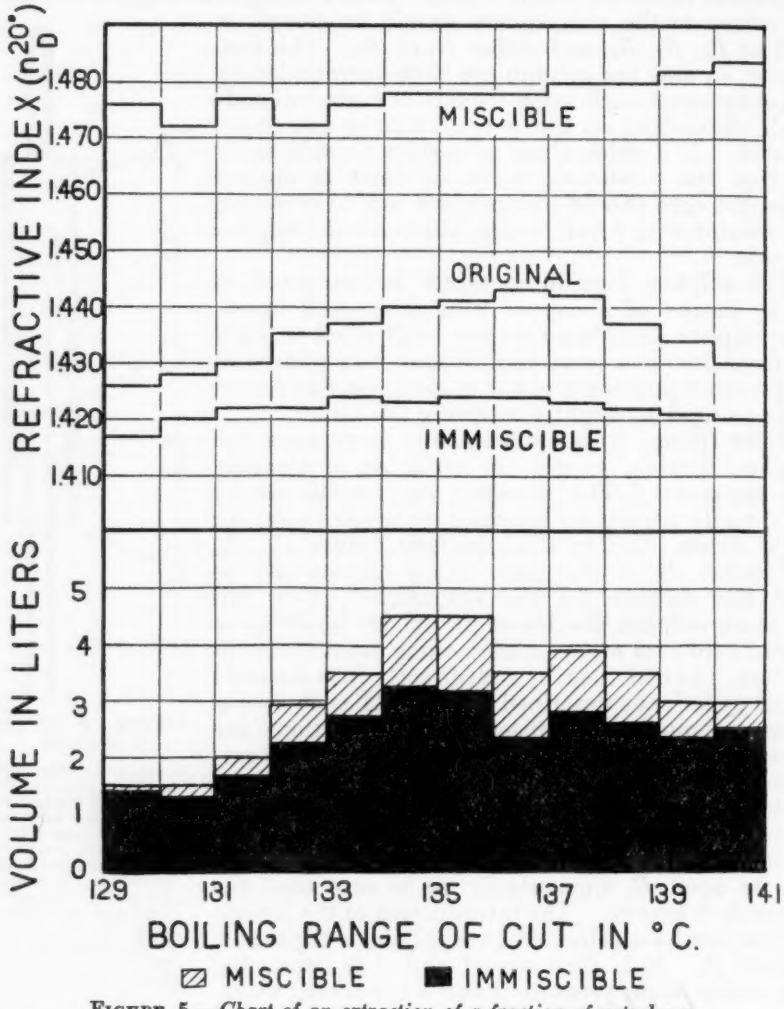

FIGURE 5.—*Chart of an extraction of a fraction of petroleum*

the flow may be regulated by B_3, otherwise it must be regulated by the heater.

Valve B_4 is then opened wide and B_2 opened slowly. An increased rate of flow of sulphur dioxide displaced by hydrocarbon will first appear in glass F_4 and in a short time a stream should appear in F_2. Observation is facilitated by placing a light behind the sight glasses.

It is possible to determine when all of the sulphur dioxide has been driven from a boiler by occasionally feeling the bottom. A sudden

increase of temperature occurs when the sulphur dioxide has been driven out. When this rise is observed the extracted hydrocarbon is blown out into a flask or test tube as shown in Figure 3, and the cycle reversed. The ejected hydrocarbon will contain some sulphur dioxide especially if the extraction is done at higher temperatures. Therefore it is necessary to introduce fresh sulphur dioxide into the apparatus occasionally. In order to prevent the escape of sulphur dioxide into the room, the receivers should be connected to solid carbon dioxide traps through I_1, I_2, and I_3. The heater on R_2 aids in degassing the immiscible material before it is expelled, but low boiling liquids should be kept at a low temperature or fractional distillation will occur.

B_2 should be closed as soon as the last of the hydrocarbon has run in, otherwise a pressure of inert gas, which will interfere with distillation, may be built up in the apparatus. The contents of the column are then drained into one of the boilers by opening B_6, and the sulphur dioxide distilled off into the other boiler. Several distillations made in this way also serve to purify the sulphur dioxide for subsequent use.

The apparatus as described has been found to operate satisfactorily at a rate of 2 liters of hydrocarbon per hour.

VI. PERFORMANCE OF THE APPARATUS

The glass apparatus has been used in the extraction of about 40 liters of petroleum fraction boiling in the range of temperature which includes the xylenes and other aromatic hydrocarbons in addition to a large proportion of paraffinic material.[11] Figure 5 is a graphical presentation of results obtainable with the apparatus when operated as described. Since the refractive indices of the aromatic compounds are much higher than those of the paraffins, the difference in refractive index of the miscible and immiscible fractions is indicative of the efficiency of extractions.[12] Further extraction of the immiscible material was found to change the refractive index very little.

The metal apparatus has been thoroughly tested with a sample of high-test gasoline containing considerable aromatic material and found to work smoothly. An attempt was also made to remove cyclic hydrocarbons from a petroleum fraction boiling in the neighborhood of 100° C. Extraction was tried at temperatures ranging from -10 to $+13°$ with little evidence of separation, however.

VII. ACKNOWLEDGMENT

The author acknowledges the technical advice of E. W. Washburn director of the American Petroleum Institute project No. 6, and also that of J. D. White and F. W. Rose.

WASHINGTON, February 13, 1932.

[11] Used by J. D. White and F. W. Rose, jr., as a step in a process for separating xylenes from petroleum.
[12] Unpublished data of J. D. White and F. W. Rose, jr.

VOLUME CHANGES OF CAST IRONS DURING CASTING

By E. J. Ash [1] and C. M. Saeger, jr.

ABSTRACT

The volume changes occurring in eight types of cast irons during cooling from the liquid state to room temperature are given in this paper. The irons varied in composition from gray iron to white iron.

The coefficient of volume shrinkage in the liquid state for the irons over the range of temperature studied was 0.011 per cent per °C. The volume change during solidification varied from an expansion of 1.65 per cent in a gray iron to a contraction of 5.85 per cent in a low-carbon low-silicon type of iron. The linear contraction of the sand-cast bars varied inversely with the silicon and carbon content and also with the cross-sectional area. The lowest linear shrinkage value measured was 0.67 per cent (1½ inch square bar) and the highest was 2.08 per cent (three-fourths inch square bar).

In both heating and cooling curves and in the sand-cast contraction bars, a pronounced effect was observed at about 1,070° C. possibly indicative of some transformation. An expansion was observed at this temperature during the freezing of all melts of cast iron. This expansion, however, was not due to decomposition of cementite alone, for white iron bars having no free graphite present showed this same phenomenon. This expansion may have been caused by the separation of dissolved gases during solidification as has been pointed out by previous investigators.

CONTENTS

	Page
I. Introduction	601
II. Materials	602
III. Apparatus and procedure	602
IV. Results	603
1. Specific volume-temperature curves	606
(*a*) Liquid	606
(*b*) Solid	607
2. Solidification range	609
V. Summary	614
VI. Acknowledgments	614

I. INTRODUCTION

The changes taking place in the linear dimensions of cast iron during cooling from the freezing range to room temperature have been the subject of many investigations. Few studies, however, have been made to determine the volume changes during cooling in the liquid state and during subsequent solidification. This latter information is of fundamental importance to foundrymen in the design and production of sound castings. Its application to the determination of the size and position of gates and risers is essential for the production of castings free from shrink holes and porosity. That soundness of the cast metal is essential in the production of high strength cast irons has been emphasized by Piwowarsky [2] and many others.

In 1929, the Bureau of Standards, cooperating with the American Foundrymen's Association, undertook the development of a method

[1] Research associate representing the American Foundrymen's Association.
[2] E. Piwowarsky, Production of High Test Cast Iron, Trans. Am. Fdymen's Assoc., vol. 34, p. 914, 1926.

for determining the volume changes occurring in cast irons during cooling from some temperature in the liquid state to room temperature.

At the time this work was initiated there were available reports on the determination of the specific volume of liquid cast iron by Benedicks and coworkers,[3] Desch and Smith,[4] and Honda and Endo.[5] Only Honda and Endo gave values for the volume change during solidification.

Recently, three additional papers dealing with the specific volume of liquid cast irons have been published. Both Benedicks[6] and Honda,[7] with their coworkers, have extended their results over a wide range of irons. Widawski and Sauerwald[8] determined the specific volume of a series of molten cast irons, making measurements up to 1,600° C. Again, only Honda and his collaborators gave values for the volume change during solidification.

A preliminary report covering the early stages of the work at the Bureau of Standards on the volume changes of cast irons was published in 1930.[9] A detailed account of the method finally developed for determining the volume changes occurring during the casting of metals and alloys has recently appeared in the Bureau of Standards Journal of Research.[10] The present paper gives the specific volume-temperature relations of a number of cast irons of varying composition on cooling from some temperature in the liquid state to room temperature.

II. MATERIALS

Pig iron from three sources was used in the preparation of the cast-iron melts. Pig iron B, a soft gray iron, was taken from stock at the Bureau of Standards; pig iron C, an iron of exceptionally uniform composition, all cast from a single ladle, was supplied through the courtesy of the Republic Iron & Steel Co., Birmingham, Ala.; pig iron D, a white iron, was made available through the kindness of H. A. Schwartz, of the National Malleable and Steel Castings Co., Cleveland, Ohio. The chemical composition of these pig irons is given in Table 2. Additions of commercial open-hearth ingot iron were made to the furnace charges when it was necessary to dilute the carbon, silicon, and other constituents of the above irons.

III. APPARATUS AND PROCEDURE

The apparatus and methods used for determining the specific volume-temperature relations of metals have been described in detail in previous publications.[11] The specific volume-temperature curves

[3] C. Benedicks, D. W. Berlin, and G. Phragmen, A Method for the Determination of the Specific Gravity of Liquid Iron and Other Metals of High Melting Point, J. Iron & Steel Inst., Carnegie Schol. Mem., vol. 13, p. 129, 1924.

[4] C. H. Desch and B. S. Smith, Interim Report on the Density of Molten Steel, J. Iron & Steel Inst., vol. 119, p. 538, 1929.

[5] K. Honda and H. Endo, On the Volume Change in Cast Iron during Solidification, Sci. Rpts., Tohoku Imp. Univ., vol. 16, p. 19, 1927.

[6] C. Benedicks, N. Ericsson, and G. Ericson, Bestimmung des Spezifischen Volumes von Eisen, Nickel und Eisenlegierungen im Geschmolzenen Zustand, Archiv für das Eisenhüttenwesen, vol. 3, p. 473, 1930.

[7] K. Honda, T. Kase, and Y. Matuyama, On the Change of Volume of Cast Iron during Solidification, Sci. Repts., Tohoku Imp. Univ., vol. 18, p. 699, 1929.

[8] E. Widawski and F. Sauerwalk, Über die Direckte Auftriebsmethode und die Dichte Schmelzflüssiger Metalle, Insbesondere von Eisenlegierungen bei Temperaturen bis 1,600° C., Zeitschrift für Anorganische und Allgemeine Chemie, vol. 192, p. 145, 1930.

[9] C. M. Saeger, jr., and E. J. Ash, Methods for Determining the Volume Changes Undergone by Metals and Alloys during Casting, Trans. Am. Foundreymen's Assoc., vol. 38, p. 107, 1930.

[10] C. M. Saeger, jr., and E. J. Ash, A Method for Determining the Volume Changes Occurring in Metals during Casting, B. S. Jour. Research, vol. 8, p. 37, 1932.

[11] See footnotes 9 and 10.

of liquid cast iron were constructed from data obtained by application of the crucible immersion method. In this method a graphite crucible of known volume is filled with liquid metal at a known temperature. The mass of this sample of metal is the same in the liquid phase as in the solid phase at room temperature. The specific volume of the liquid, therefore, can readily be calculated from the known volume of the crucible at the elevated temperature [12] and the weight of the solid metal sample. Data on the contraction of the solid metal, obtained by direct observations of the change in length with change in temperature of a sand-cast bar of metal permitted calculation of the specific volume-temperature relation of the solid metal. The difference between the specific volume of the liquid metal and of the solid metal at the temperatures corresponding to the liquidus and the solidus, respectively, represents the volume change during solidification. The liquidus and solidus temperatures for each composition were determined by thermal analysis.

The observations on each heat of cast iron were made as follows:

The charge of iron was melted in a high frequency induction furnace and heated to a maximum temperature of 1,500° C. for gray iron and 1,600° C. for white iron. Temperatures were measured by means of a platinum-rhodium thermocouple. When the melt had reached the desired maximum temperature, the power input was reduced sufficiently to permit cooling of the melt, but at a retarded rate, and also to continue a slow stirring action of the bath. The first liquid sample was then taken. Sufficient metal was then transferred to a preheated crucible for casting the solid contraction bars and a small ingot for subsequent determination of the freezing range. Additional liquid samples were taken as the metal cooled in the furnace.

After the samples of liquid metal had cooled to room temperature, the ingots were removed from the crucibles and weighed and the specific volume of the liquid metal was calculated for each sampling temperature. The specific volume-temperature curve of the liquid metal was constructed from these data.

In order to study the effect of cross-sectional area on the volume changes of cast iron two sizes of bars, one ¾-inch square and the other 1½-inch square, both 12 inches long, were poured from each melt.

The temperature range of solidification was determined by thermal analyses of the small ingot cast for this purpose.

IV. RESULTS

The shrinkage characteristics were determined for 14 melts of cast iron, representing eight different compositions. The material making up each charge is given in Table 1. The results of chemical analyses of each of the 14 melts and of the 3 pig irons used in making up the charges are given in Table 2. A summary of the shrinkage data obtained is given in Table 3.

[12] The calculation of the volume of the crucible at the elevated temperature depends upon the coefficient of thermal expansion of graphite. The value of this coefficient used in this report was obtained by extrapolation of experimental data from 600° C. to the temperatures of molten cast iron. Recently, however, this coefficient up to 1,000° C. has been determined at this bureau. The use of these later data considerably shortens the necessary extrapolation for obtaining the thermal expansion of graphite at the higher temperatures. Specific volumes calculated on the basis of the recent data confirm the validity of the earlier calculations.

TABLE 1.—*Materials constituting charges*

Melt No.	Pig iron			Open-hearth iron		Other additions
	Lot	Weight	Proportion of charge	Weight	Proportion of charge	
		Pounds	*Per cent*	*Pounds*	*Per cent*	
I	B	97	100			
II	B	105	100			
III	B	120	80	30	20	
IV	B	96	80	24	20	
V	B	72	60	48	40	
VI	B	78	60	52	40	
VII	B	125	100			
VIII	C	125	100			
IX	C	125	100			
X	D	115	100			
XI	D	140	100			
XII	D	140	100			1.4 pounds FeSi; [1] 0.5 pound FeMn.[2]
XIII	C	130	90	13	10	2.0 pounds FeSi; 0.2 pound FeMn; 0.8 pound FeP.[3]
XIV	C	127	80	32	20	0.75 pound FeSi; 0.1 pound FeMn; 0.4 pound FeP.

[1] FeSi, ferro silicon containing 50 per cent silicon.
[2] FeMn, ferro manganese containing 80 per cent manganese.
[3] FeP, ferro phosphorus containing 25 per cent phosphorus.

TABLE 2.—*Composition of cast-iron melts* [1]

Melt No.	Si	Mn	P	S	¾-inch square bar		1¼-inch square bar	
					Total carbon	Graphitic carbon	Total carbon	Graphitic carbon
	Per cent	*Per cent*	*Per cent*	*Per cent*	*Per cent*	*Per cent*	*Per cent*	*Per cent*
I	2.08	0.50	0.44	0.05	3.63	2.99	3.63	2.97
II	2.11	.50	.46	.05	2.71	2.96	3.71	2.99
III	1.68	.44	.35	.04	3.08	2.23	3.08	2.18
IV	1.69	.48	.35	.04	3.10	2.27	3.10	2.31
VI	1.24	.35	.27	.04	2.29	.42	2.18	.56
VII	2.10	.54	.46	.05	3.76	3.35	3.67	3.26
VIII	2.87	.59	.68	.03	3.63	3.42	3.69	3.53
IX	2.86	.58	.67	.03	3.60	3.40	3.39	3.20
X	.84	.24	.15	.06	2.00	.00	2.08	.00
XI	.85	.25	.14	.06	1.96	.00	1.98	.00
XII	1.50	.27	.14	.06	1.97	.00	1.87	.01
XIII	2.87	.52	.59	.03	3.27	2.90	3.27	2.88
XIV	2.88	.44	.66	.03	2.89	2.65	2.90	2.68

Pig iron	Si	Mn	P	S	Total carbon	Graphitic carbon	Combined carbon
B	2.31	0.67	0.46	0.045	3.81	3.15	0.66
C	2.90	.56	.67	.02	3.68		
D	1.00	.29	.15	.06	2.07		

[1] Analyses made by R. H. Elders, American Cast Iron Pipe Co., Birmingham, Ala.

TABLE 3.—*Shrinkage data on 14 cast-iron melts*

	Melt Nos.													
	I	II	III	IV	V	VI	VII	VIII	IX	X	XI	XII	XIII	XIV
Maximum heating temperature ° C	1,600	1,400	1,500	1,500	1,500	1,500	1,500	1,500	1,500	1,500	1,600	1,600	1,500	1,500
Temperature of liquidus do	------	------	1,250	1,250	1,350	1,350	1,150	1,150	1,150	1,380	1,380	1,365	1,155	1,195
Specific volume at liquidus cm^3/g	------	------	0.1445	0.1445	0.1442	0.1442	0.1441	0.1452	0.1452	0.1440	0.1440	0.1438	0.1448	0.1449
Specific volume at 1,150 ° C., ¾-inch bar do	0.1452	0.1453	0.1417	0.1420	------	0.1372	0.1457	0.1476	0.1468	0.1381	0.1380	0.1381	0.1467	0.1450
Specific volume at 1,150 ° C., 1½-inch bar do	0.1448	0.1451	0.1422	0.1417	0.1372	0.1358	0.1450	0.1453	0.1464	0.1360	0.1373	0.1374	0.1447	0.1449
Density at room temperature, ¾-inch bar g/cm^3	7.128	7.116	7.307	7.285	------	7.699	7.0952	7.005	7.039	7.720	7.716	7.692	7.082	7.148
Density at room temperature, 1½-inch bar do	7.103	7.115	7.266	7.261	7.571	7.662	7.092	7.022	7.031	7.732	7.734	7.698	7.082	7.143
Specific volume at room temperature, ¾-inch bar cm^3/g	0.1403	0.1405	0.1369	0.1373	------	0.1299	0.1410	0.1428	0.1420	0.1295	0.1296	0.1300	0.1412	0.1399
Specific volume at room temperature, 1½-inch bar do	0.1408	0.1405	0.1376	0.1377	0.1321	0.1305	0.1410	0.1424	0.1422	0.1285	0.1293	0.1299	0.1412	0.1400
Average contraction of liquid per 100 ° C per cent	------	------	1.1	1.1	1.1	1.1	1.1	1.1	1.1	1.1	1.1	1.1	1.1	1.1
Shrinkage during solidification (liquid to 1,150 ° C):														
¾-inch bar do	------	------	1.94	1.73	------	4.85	−1.11	−1.65	−1.10	4.10	4.17	3.96	−1.31	−0.07
1½-inch bar do	------	------	1.59	1.94	4.85	5.82	−0.62	−0.07	−0.82	5.55	4.65	4.45	0.07	0.00
Linear contraction from 1,150 ° C., ¾-inch bar do	1.13	1.11	1.12	1.11	------	1.77	1.08	1.08	1.08	2.08	20.3	1.97	1.09	1.17
Linear contraction from 1,150 ° C., 1½-inch bar do	0.93	1.06	1.08	0.95	1.23	1.31	0.83	0.67	0.97	1.83	1.95	1.81	0.98	1.12
Linear contraction from 1,070 ° C., ¾-inch bar do	------	1.25	------	1.22	------	------	1.14	1.17	1.19	2.08	2.00	------	1.13	1.21
Linear contraction from 1,070 ° C., 1½-inch bar do	1.13	1.24	1.19	------	------	------	1.04	0.90	1.12	1.75	1.91	------	1.03	1.17

1. SPECIFIC VOLUME-TEMPERATURE CURVES

(a) LIQUID

Figure 1 shows the relation between specific volume and temperature of the liquid metal for 12 melts of cast iron. Cast irons having relatively high carbon and silicon contents (melts VII, VIII, IX,

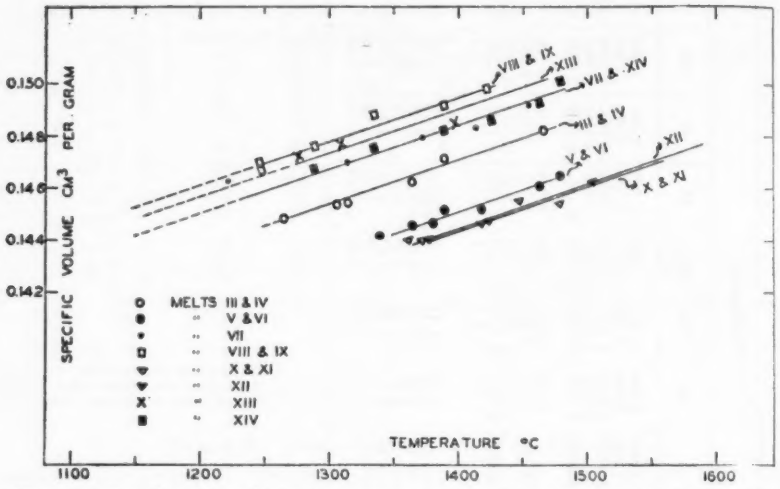

FIGURE 1.—*Specific volume-temperature curves of cast irons in the liquid state*

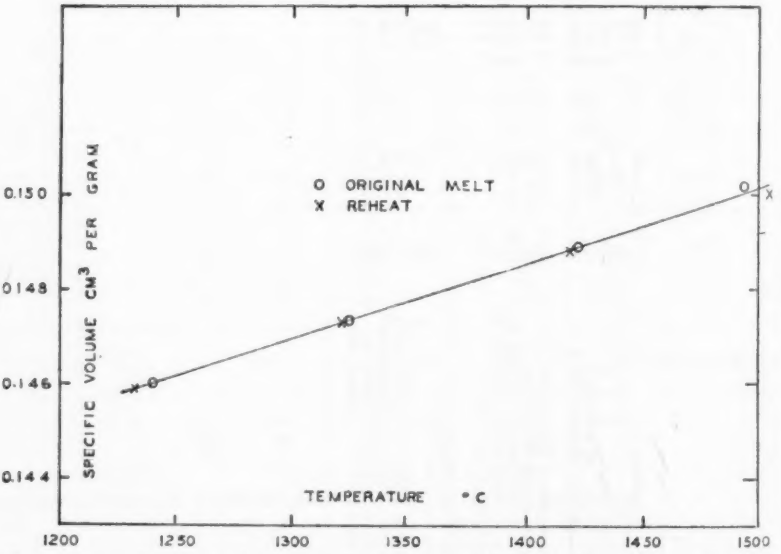

FIGURE 2.—*Specific volume-temperature curve of a liquid cast iron after repeated heating and cooling*

XIII, and XIV) have greater specific volumes at a given temperature than the cast irons with lower carbon and silicon contents.

Repeated heating and cooling of liquid cast iron indicated no measurable change in the specific volume of the metal. The results

of a study of this nature are shown in Figure 2. This metal was heated to a maximum temperature in the furnace, poured into a crucible and four liquid samples were taken as the metal cooled. The remaining metal in the crucible was returned to the furnace, reheated to a maximum temperature, again poured into the crucible and four additional liquid samples were obtained as the metal cooled.

(b) SOLID

The linear contraction-temperature curve of each composition of cast iron in the solid state was obtained by plotting observed changes in length with change in temperature of the cast bars referred to previously. Figure 3 shows a contraction curve for a typical gray

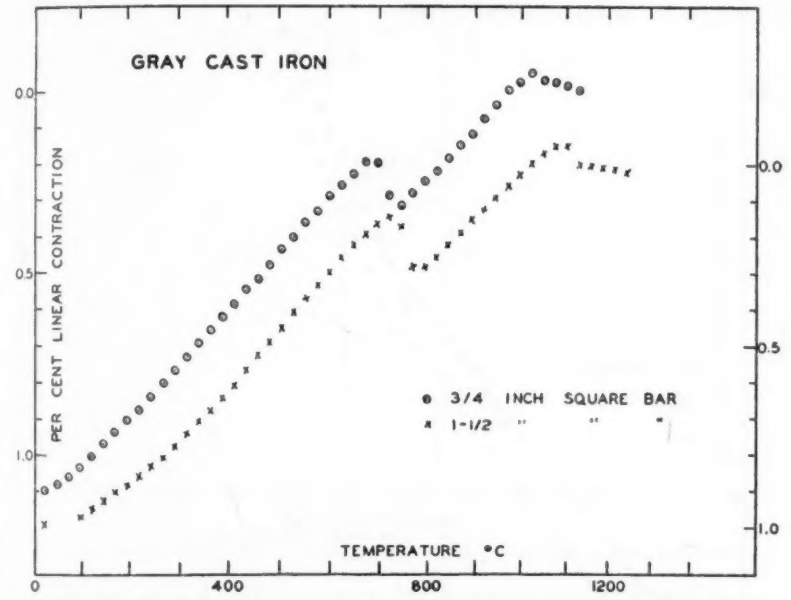

FIGURE 3.—*Linear contraction-temperature curve of a gray cast iron*

cast iron. In general, all gray cast irons undergo an expansion during or immediately after solidification. The initial expansion indicated by the bar begins at a temperature above 1,130° C., and reaches a maximum at approximately 1,070° C. This expansion is also characteristic of white cast iron (fig. 4) and hence, should not be attributed to the decomposition of the cementite because no primary graphite is formed in white iron.

A comparison between the linear shrinkage values from 1,150° and 1,070° C., respectively, to room temperature is given in Table 3.

As the specific volume (or density) of cast iron at room temperature varies with composition and with rate of cooling, the density was determined on each bar. Specimens, one-half inch thick, cut from the free end of the contraction bar were considered to be representative of the metal in that bar. This experimental value for the density of the metal of a given contraction bar at room temperature, together with the observed changes in linear dimensions, of the bar during cooling from the freezing range, permitted the calculation of the

specific volume of the solid metal throughout the range from the temperature of complete solidification to room temperature.

The expansion phenomenon associated with freezing of cast irons has been observed by a number of investigators. Bardenheuer and Ebbefeld[13] have attributed this expansion to the release of gases during the transition from fluid to the solid state. This view is in

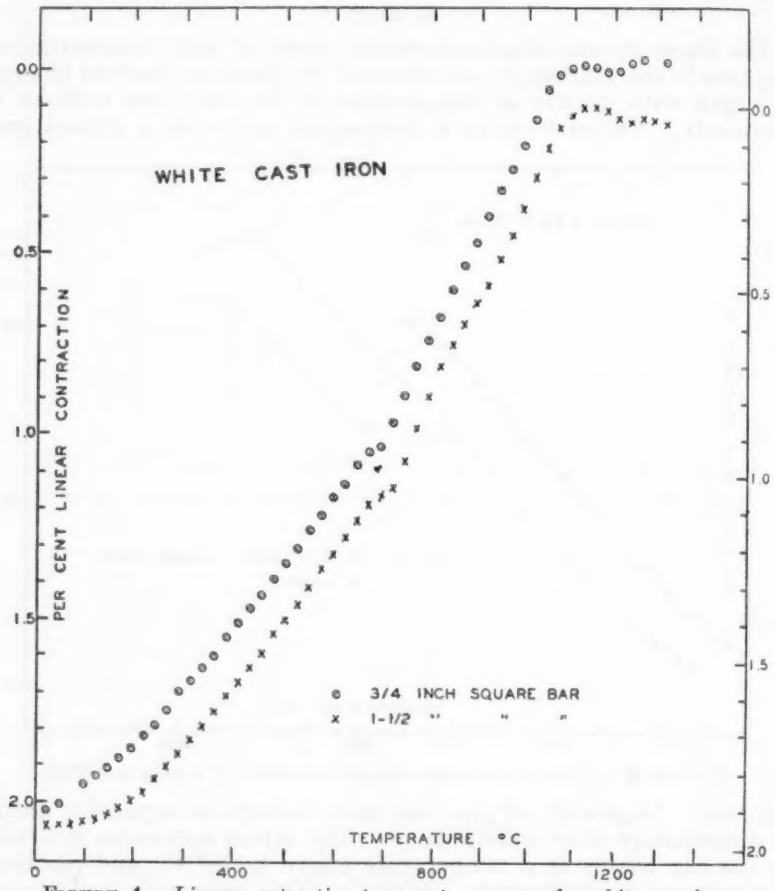

FIGURE 4.—*Linear contraction-temperature curve of a white cast iron*

agreement with Boehm,[14] who observed a similar phenomenon for copper-tin alloys.

Piwowarsky[15] reported a relation between the amount of gas released during solidification and the temperature to which the cast iron had been superheated. He reported the amount of gas given off by a series of cast-iron melts as varying from 1.12 to 2.74 cubic inches per pound of metal. The gas liberated was composed of CO, CO_2, H_2, N_2, and CH_4. He concluded that this observed expansion at the end of the freezing range was detrimental to the metal inasmuch as it decreased its density.

[13] P. Bardenheuer and C. Ebbefeld, Beitrag zur Analyse des Schwindungsvorganges von weissem und grauem Gusseisen, Stahl u. Eisen, vol. 45, pp. 825 and 1022, 1925.
[14] F. Boehm, Über die Schwindung von Legierungen. Dissertation, Technischen Hochschule zu Breslau, 1930.
[15] See footnote 2 p. 601.

2. SOLIDIFICATION RANGE

For the present investigation, because the evaluation of the volume change during solidification depended on the specific volume change between the liquidus and solidus, the extent of the freezing range was determined for each cast iron studied. Typical inverse rate heating and cooling curves for a gray cast iron are shown in Figure 5. There was a break in the time-temperature curve on cooling at about 1,147° C. which was taken as an indication of the liquidus. On heating, the break in the time-temperature curve was consistently found at about 1,070° C., the temperature of the solidus.

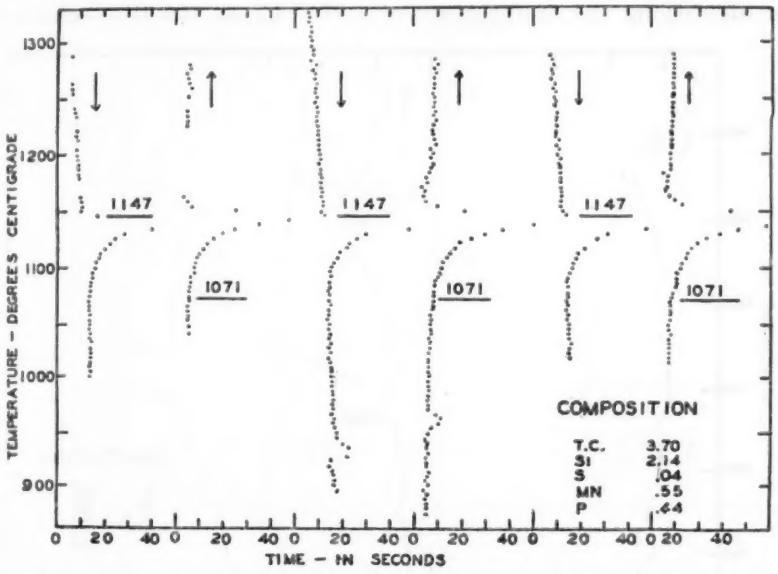

FIGURE 5.—*Inverse rate heating and cooling curves of a gray cast iron*

A heating and a cooling curve for a white cast iron are given in Figure 6. The liquidus is indicated at 1,380° C. and the solidus at 1,063° C.

The occurrence of an apparent solidus at about 1,070° C. was typical of every cast-iron composition studied. Thermal analyses of specimens of different sizes also indicated this thermal change at approximately 1,070° C. both on heating and cooling.

This deviation of the cooling curve at about 1,070° C, appears to be more pronounced in those cast irons containing higher amounts of combined carbon. Thus, in Figure 7, the cooling curve of melt No. VI shows a very distinct halt at approximately this temperature. This is also observed in white cast iron. (See fig. 6.)

The temperature of the occurrence of the maximum expansion of the solid contraction bars coincides with the observed temperature of the apparent solidus for these irons. Because of the complex nature of cast iron, this temperature may represent the change of state of a low melting material (eutectic) formed from the various constituents in the material. The change of structure occurring at 1,070° C. is not very great because the amount of heat evolved or

absorbed at this temperature appears to be small. If this expansion phenomenon is due to the separation of occluded gases, the material could not possibly be completely solid until after the maximum expansion had taken place.

Hanson states[16] "that portion (of the iron-carbon diagram) down to and including the eutectic represents an iron-graphite system, but at some temperature below the eutectic line the alloys undergo transformations according to the system iron-cementite." In the diagrams referred to in his statement, the Acm line was not connected with the eutectic horizontal.

The data of the present investigation are considered insufficient for identifying the temperature of 1,070° C., as the true solidus of

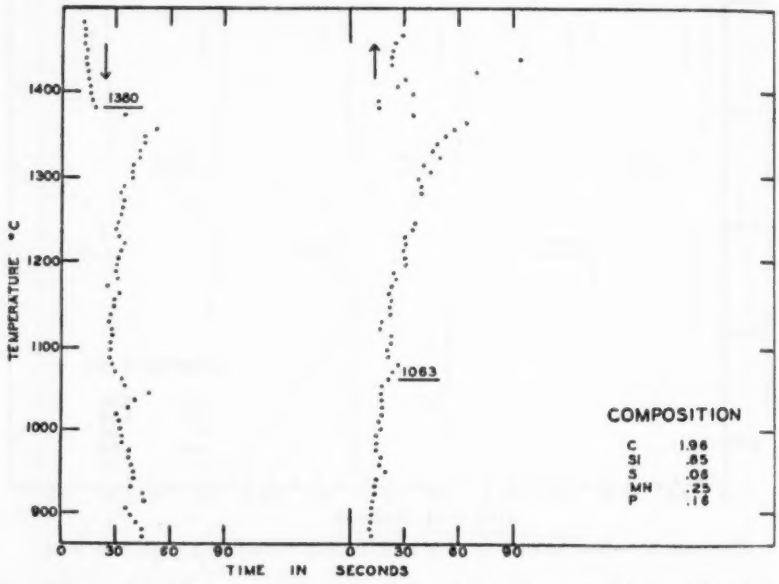

FIGURE 6.—*Inverse rate heating and cooling curves of white cast iron*

these cast irons. The solidus of cast iron is usually considered to occur between 1,130° and 1,150° C., depending upon the composition. Temperature-contraction data of the present investigation indicated that at 1,150° C. the bars had not, in general, moved appreciably. However, at 1,130° C., the temperature at which the next observation was made, the free ends of the bars were in motion. Since it was desired to select the solidus at or just above the temperature representing initial movement in the solid bar, the temperature, 1,150° C., was chosen as the solidus point for all irons.

The specific volume-temperature relations for a cast iron from some temperature in the liquid state to room temperature can be plotted on a single curve. Such curves for three cast irons are shown in Figure 8. These melts (see Table 1) were made from the same lot of pig iron, but two contained different proportions of open-hearth iron. Melt VII was all pig iron B; melt IV was 80 per cent pig iron B and 20 per cent open-hearth iron; melt VI was composed of 60 per

[16] D. Hanson, The Constitution of Silicon-Carbon-Iron Alloys and a New Theory of the Cast Irons, J. Iron & Steel Inst., vol. 114, p. 129, 1927.

cent pig iron B and 40 per cent open-hearth iron. The effect of decreasing amounts of carbon, silicon, and other constituents on the shrinkage characteristics of cast iron is shown in this figure.

The complete shrinkage data for a typical white cast iron (melt XI) are represented in Figure 9.

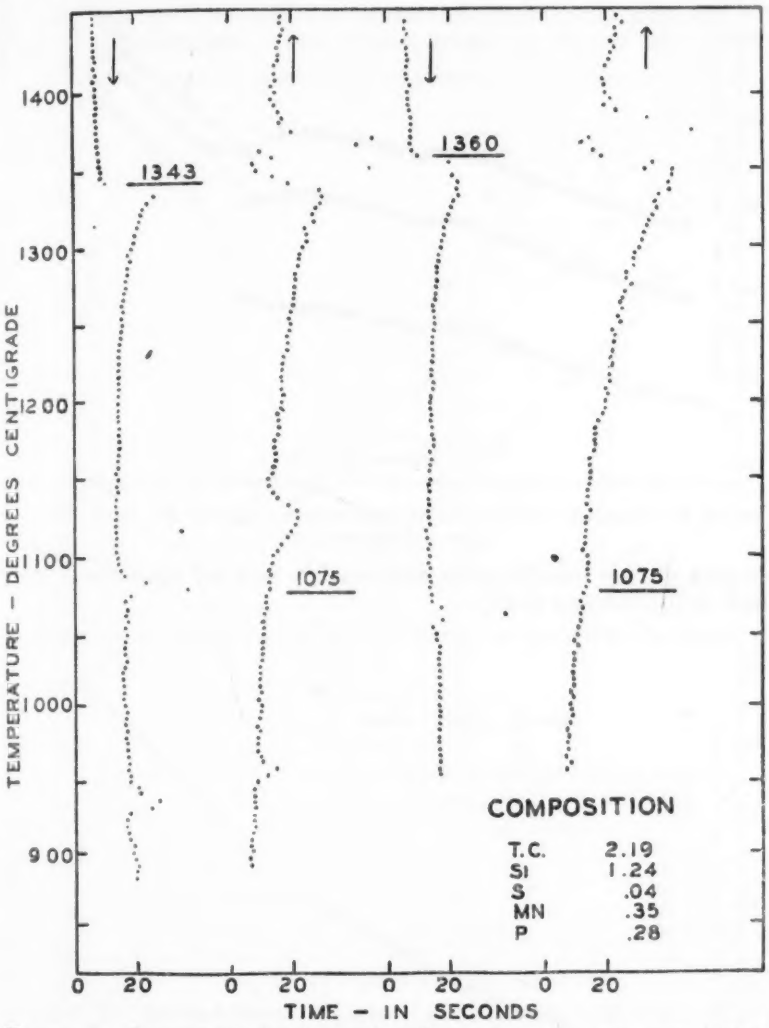

FIGURE 7.—*Inverse rate heating and cooling curves of a cast iron diluted with 40 per cent commercial open-hearth ingot iron*

In Figure 10, the volume change during solidification of the cast irons studied in this investigation is plotted against the amount of graphitic carbon contained in the solid contraction bars. For purposes of comparison, there are plotted in the same manner the values

obtained by Honda and his coworkers [17] on cast irons differing widely in composition from those used in this investigation. The values obtained by Honda, by means of the thermobalance, indicate volume

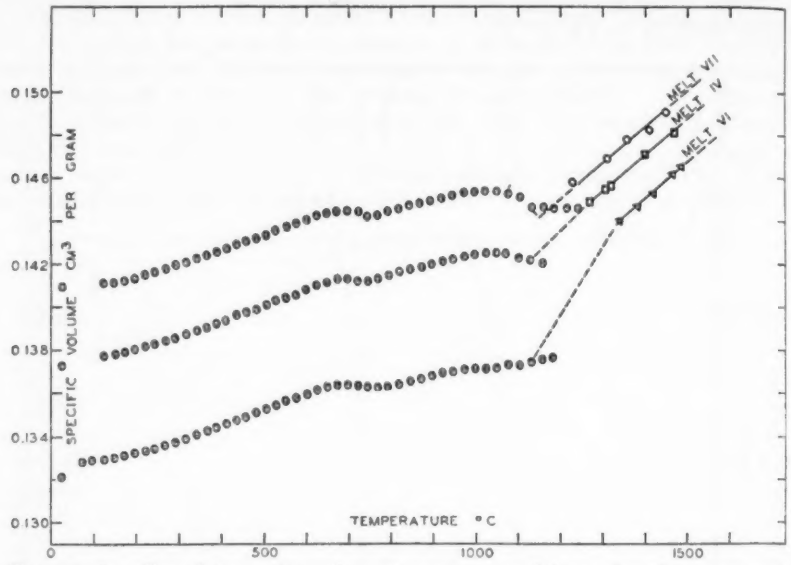

FIGURE 8.—*Complete specific volume-temperature relations for three compositions of gray cast iron*

decreases during solidification appreciably smaller than those determined in the present study.

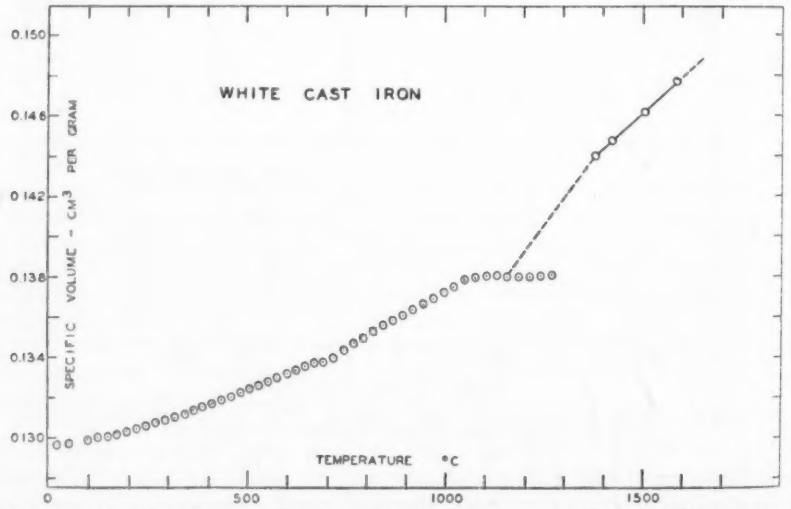

FIGURE 9.—*Complete specific volume-temperature curve typical of white cast iron*

Two factors may be suggested as quite probably contributing to the differences between Honda's data and the results of the present work.

[17] See footnotes 5 and 7 p. 602.

1. In the present study, the volume change during solidification has been defined [18] as the change in volume in passing from the liquid state at the beginning of the freezing range to the solid state at the end of the freezing range. In alloys having a freezing range, as in many cast irons, the shrinkage during solidification includes, therefore, not only shrinkage resulting from the change of state, but also the shrinkage of the liquid and of the solid metal occurring within the range of solidification. The values given by Honda for shrinkage

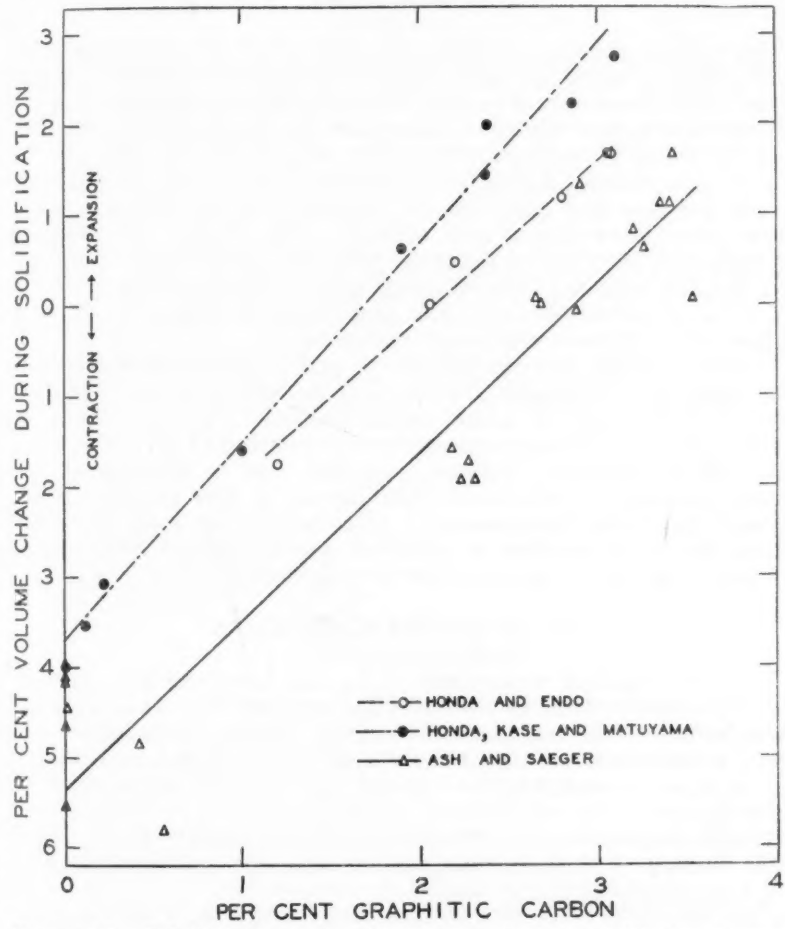

FIGURE 10.—*Relation between the volume change during solidification of some cast irons and the graphitic carbon content*

during solidification represent only the volume change resulting from the change of state and should be expected, therefore, to be less than the values obtained in the present work.

2. In a previous publication [18] it has been pointed out that volume changes during solidification may not be measured accurately by the thermobalance owing to the very great probability of the formation of internal shrinkage cavities in the specimen during the change of

[18] See footnotes 9 and 10, p. 602.

state. Internal voids, whether localized in a pipe or distributed throughout the metal result in values for the shrinkage during solidification which are less than the correct values.

Both of these factors, therefore, the difference in definition of solidification shrinkage, and the liability of the thermobalance method to errors caused by porosity—would tend to make Honda's shrinkage values less than those of the present work.

V. SUMMARY

The volume changes occurring in eight types of cast irons during cooling from the liquid state to room temperature are given in this paper. The irons varied in composition from gray iron to white iron.

The coefficient of volume shrinkage in the liquid state for the irons over the range of temperature studied was 0.011 per cent per ° C. The volume change during solidification varied from an expansion of 1.65 per cent in a gray iron to a contraction of 5.85 per cent in a low-carbon, low-silicon type of iron. The linear contraction of the sand-cast bars varied inversely with the silicon and carbon content and also with the cross-sectional area. The lowest linear shrinkage value measured was 0.67 per cent (1½-inch square bar) and the highest was 2.08 per cent ¾-inch square bar).

In both heating and cooling curves and in the sand-cast contraction bars, a pronounced effect was observed at about 1,070° C., possibly indicative of some transformation. An expansion was observed at this temperature during the freezing of all melts of cast iron. This expansion, however, was not due to decomposition of cementite alone, for white-iron bars, having no free graphite present showed this same phenomenon. This expansion may have been caused by the separation of dissolved gases during solidification as has been pointed out by previous investigators.

VI. ACKNOWLEDGMENTS

This investigation was sponsored by the American Foundrymen's Association from 1929 to 1931 and the authors wish to express their appreciation to the members of the gray cast-iron committee of the above association, and particularly to J. T. MacKenzie, chairman of the research committee, for his aid and counsel throughout this investigation.

Much credit is due L. D. Jones, A. I. Krynitsky, C. B. Riecks, C. E. Jackson, and H. B. Gardner, for valuable assistance rendered.

WASHINGTON, March 2, 1932.

A STUDY OF THE DELTA LACTONES FORMED BY THE OXIDATION OF ALDOSES WITH BROMINE WATER

By Horace S. Isbell

ABSTRACT

Inasmuch as the free sugar acids are converted to their barium salts by barium carbonate but their lactones are left unaltered, this substance may be used for determining whether the free acid is formed at any time during the course of the oxidation of the aldoses with bromine water. If the oxidation product were the free acid it would be neutralized by the barium carbonate, but if it were the lactone it would not be changed. It has been found in some cases that only 1 or 2 per cent of the oxidation product is neutralized, which proves that the sugar acids are not produced in the course of the oxidation of the aldose sugars by bromine water in the presence of barium carbonate. The products produced are neutral substances which on standing in aqueous solution develop acidity. Measurements of the optical rotations, as well as the changes in acidity, indicate that delta lactones are formed by the bromine oxidation of α- and β-*d*-mannose, α- and β-*l*-rhamnose, α- and β-lactose, β-cellobiose, and β-maltose.

The beta forms of the sugars are more easily oxidized than the alpha, but delta lactones are produced from both. The fact that delta lactones are obtained from α- and β-*d*-mannose (as well as from the other sugars) is at least circumstantial evidence supporting the 1, 5 ring structure for the substances investigated.

CONTENTS

	Page
I. Introduction	615
II. Experimental method	616
III. Discussion of results	618
IV. Experimental details	623
V. Acknowledgment	624

I. INTRODUCTION

In a previous publication C. S. Hudson and the writer [1] reported some observations which indicate that delta lactones are formed directly from certain aldose sugars by oxidation with bromine water. This experimental evidence requires the abandonment of the generally accepted concept that the aldehyde form of the sugar is oxidized to the monocarboxylic acid, in favor of a new hypothesis, which, stated briefly, is that the cyclic forms of the normal sugars give delta lactones by oxidation with bromine water. Since the evidence for this was derived solely from the optical rotations of the sugars during the oxidation, it is desirable to obtain more direct evidence in support of the new hypothesis.

The lactones of the sugar acids are neutral substances which, on standing in aqueous solution, are partially hydrolyzed to the corresponding acids. As a result of this hydrolysis the hydrogen-ion concentration of a freshly prepared solution of the lactone increases on standing; whereas the hydrogen-ion concentration of the corresponding acid decreases on standing because of lactone formation. Since

[1] Isbell and Hudson, B. S. Jour. Research, vol. 8 (RP418), p. 327, 1932.

the oxidation product reported in the previous paper was dissolved in a solution buffered with sodium acetate, it was not possible to follow its hydrolysis by means of hydrogen-ion determinations. This objectionable feature has been overcome by selecting an insoluble buffer (barium carbonate), the excess of which may be removed by filtration after the oxidation is complete. The experimental conditions are such that any acid which may be present is neutralized by the barium carbonate, but the lactone is not saponified. It will be shown in Section III that in some cases only 1 or 2 per cent of the oxidation product is neutralized by the barium carbonate. This is direct proof that the oxidation product is not the acid, as previously believed. The hydrogen-ion concentrations, as well as the specific rotations of the products obtained from α- and β-*d*-mannose, α- and β-*l*-rhamnose, α- and β-lactose, β-cellobiose, and β-maltose, indicate that these substances give delta lactones on bromine oxidation.

II. EXPERIMENTAL METHOD

In order to study the substance produced by the oxidation of a sugar with bromine water, it is highly desirable that the sugar be converted as completely as possible into the primary oxidation product. When the reaction is conducted according to the method previously used [2] a substantial portion of the sugar is not oxidized. The presence of the unoxidized sugar is particularly objectionable because it is not known whether this residual sugar is in equilibrium immediately after the oxidation. If it is not in equilibrium, the observed mutarotation is the resultant of the changes due to the unoxidized sugar and those due to the oxidation product. Obviously this complication would be eliminated if the sugar were converted completely into the oxidation product. The experimental conditions must be such that the delta lactones formed in the reaction may be identified. Previously Bunzel and Mathews [3] showed that the bromine oxidation of the aldoses is retarded by the presence of a small quantity of acid. Since the delta lactones are saponified very rapidly by dilute alkali, the reaction must be maintained on the acid side of neutrality. A suspension of calcium or barium carbonate in water, saturated with carbon dioxide, may be used as a means for maintaining the reaction of a solution nearly neutral, but on the acid side of neutrality. As first shown by Clowes and Tollens [4] the aldose sugars are oxidized rapidly by bromine water in the presence of calcium carbonate. Although they, and subsequent investigators using the same buffer, obtained the calcium salt rather than the unchanged oxidation product, their experimental conditions were such that, even though the lactone were formed, it would have been hydrolyzed and finally neutralized with calcium carbonate. The writer has found that delta lactones are formed by the oxidation of the aldoses by bromine water in the presence of calcium carbonate and carbon dioxide. When this buffer is employed the solution of the delta lactone contains considerable calcium bicarbonate, which is objectionable. The use of barium carbonate instead of calcium carbonate gives a product which contains less bicarbonate, and consequently this buffer was selected.

[2] See footnote 1, p. 615.
[3] Bunzel and Mathews, J. Am. Chem. Soc., vol. 31, p. 464, 1909.
[4] Clowes and Tollens, Ann., vol. 310, p. 166, 1900.

Barium carbonate in the presence of carbon dioxide maintains the reaction of the solution slightly acid, in which condition the interchange between the alpha and beta forms of the sugars is slow and the oxidation is relatively rapid. The preliminary results of an investigation [5] of the reaction rates of the alpha and beta forms of the principal sugars has shown that the beta forms are oxidized much more readily by bromine water than the corresponding alpha isomers. By taking advantage of this fact it is possible in some cases to convert over 95 per cent of the sugar to the lactone in five minutes.

The crystalline sugar is added to a suspension of barium carbonate in bromine water and the oxidation is allowed to continue in the presence of carbon dioxide for a predetermined time. The barium carbonate neutralizes the hydrobromic acid formed from the bromine and thus maintains a nearly neutral reaction. Since the barium carbonate in the presence of carbon dioxide is difficultly soluble and nearly neutral it does not appreciably decompose the lactone, which remains in solution as such.[6] When the oxidation is nearly complete the excess bromine is removed by shaking the solution with linseed oil, and the excess barium carbonate is separated by filtration. The solution thus obtained does not contain free bromine or a buffering agent. Therefore the hydrolysis of the lactone may be followed by hydrogen-ion determinations. The amount of the oxidation product neutralized by the barium carbonate may be estimated from the difference in the quantity of the oxidation product theoretically formed, as calculated from the weight of the sugar actually oxidized, and the quantity of lactone actually present in the solution, as determined by titration with standard alkali.

TABLE 1.—*Oxidation of aldoses by bromine water in the presence of barium carbonate*

Aldose used	Grams of sample in 200 ml [a]	Time (in minutes) allowed for oxidation	Per cent of sample not oxidized	Per cent of sample oxidized	Moles of product formed by oxidation [b]	Moles of unchanged lactone in oxidation product [c]	Per cent of oxidation product present as lactone	Per cent of oxidation product neutralized by $BaCO_3$
α-*d*-mannose	9	10	20.0	80.0	0.0400	0.0396	99.0	1.0
β-*d*-mannose	9	5	2.9	97.1	.0485	.0478	98.6	1.4
α-*l*-rhamnose (hydrate)	9.1	15	9.0	91.0	.0455	.0448	98.5	1.5
β-*l*-rhamnose	8.2	10	4.4	95.6	.0478	.0466	97.5	2.5
α-lactose (hydrate)	18	10	39.9	60.1	.0200	.0228	76.0	24.0
β-lactose	17.1	5	3.4	96.6	.0483	.0432	89.4	10.6
β-cellobiose	17.1	10	2.3	97.7	.0488	.0364	74.6	25.4
β-maltose	18	4	2.4	97.6	.0488	.0470	96.3	3.7

[a] The samples correspond to 0.05 mole.

[b] This value is based on the assumption that the sugar was converted quantitatively into the lactone, and consequently the numerical value is the same as the amount of sugar actually oxidized.

[c] This value was determined by the amount of alkali necessary to effect the saponification of the oxidation product.

[5] This investigation, which was outlined briefly in the Journal of the American Chemical Society, vol. 54, p. 1692, 1932, is being conducted with the assistance of W. W. Pigman.

[6] The solution resulting from the oxidation contains barium bromide and the delta lactone. The barium bromide may be removed with silver sulphate, leaving a solution of the nearly pure delta lactone. This new method for obtaining delta lactones is being applied to certain sugar acids which have not given crystalline delta lactones by other methods.

III. DISCUSSION OF RESULTS

The results given in Table 1 were obtained in the manner outlined in the previous paragraph. Since there is a considerable difference in the reaction rates of the sugars, a corresponding length of time was allowed for each oxidation, as shown in the third column of Table 1. As may be seen from the percentage of the sample oxidized, column 5, the beta forms of the sugars are attacked more rapidly than the corresponding alpha isomers. The amount of each oxidation product was calculated by multiplying the moles of the sugars used (0.05) by the percentage of the sugar oxidized. Before considering the amount of the unchanged lactone in the oxidation product, column 7, and the percentage of the oxidation product neutralized by barium carbonate, column 9, it should be recalled that the oxidation was conducted in the presence of barium carbonate and that the free sugar acids are quickly neutralized by shaking with this substance, but the delta lactones are not. The moles of unchanged lactone in the oxidation product, column 7, were determined by titration after the reaction was stopped and the barium carbonate removed. The difference between the total amount of the product formed by oxidation, column 6, and the amount of the unchanged lactone, column 7, gives the amount of the oxidation product neutralized by barium carbonate. This is expressed in per cent in column 9 of Table 1. The amount of the oxidation product neutralized varies with different sugars. The fact that in some cases only 1 or 2 per cent of the products was neutralized by barium carbonate is particularly significant because any free acid which might be formed, perhaps by the oxidation of the open-chain form of the sugar, would be neutralized by the barium carbonate. Surprisingly small amounts of the lactones derived from mannose and rhamnose were saponified, but more decomposition was found for the lactones derived from lactose, cellobiose, and maltose. Lactobionic, cellobionic, and maltobionic lactones are more readily hydrolyzed than the delta lactones of mannonic and rhamnonic acids. It should be recalled again that the oxidation product is exposed during the oxidation to barium carbonate which neutralizes any acid which may be formed directly from the sugar or by hydrolysis. The differences in the amounts of decomposition are probably due to differences in the rates of hydrolysis, together with the fact that when the oxidation was allowed to continue for longer periods, there was more opportunity for the hydrolysis of the lactone and the neutralization of the acid thus formed.

The oxidation of the alpha and beta forms of mannose is of interest because of the uncertainty regarding their structure.[7] [8] [9] If a sugar containing a 1, 5 ring is oxidized to give a delta lactone we would expect a sugar containing a 1, 4 ring to give a gamma lactone.[10] Hence if α-*d*-mannose contained a 1, 4 ring we would expect it to give a gamma lactone. The gamma lactones differ from the delta lactones in that they are more slowly hydrolyzed, requiring weeks to reach equilib-

[7] Hudson, J. Am. Chem. Soc., vol. 52, p. 1689, 1930.
[8] Haworth, Hirst, Streight, Thomas, and Webb, J. Chem. Soc., p. 2636, 1930.
[9] Isbell, B. S. Jour. Research, vol. 7 (RP392), p. 1115, 1931.
[10] Some 1, 4 methylated sugars are being made with the object of submitting them to bromide oxidation in order to determine whether they give gamma lactones or acids. The method is being applied also to the free aldehyde forms of certain acetylated sugars. By oxidation with bromine water the free aldehyde form should give the free acid, but its semiacetal form may give the ethyl esters.

rium. If a gamma lactone were formed from either α- or β-*d*-mannose the changes in acidity and optical rotation would be so gradual that they would not be apparent in the course of several hours.

The changes in the specific rotations of the oxidation products derived from α- and β-*d*-mannose are given in Curves I and II of Figure 1; and the corresponding increases in acidity are illustrated in Curves III and IV of the same figure. As illustrated in Curve II, the product derived from β-*d*-mannose gives an initial specific rotation of about +110 which decreases to about +30 in 24 hours and thereafter slowly increases. According to Nef [11] the delta mannonic lactone gives $[\alpha]_D^{20} = +111.1$ initially, which decreases to +28 in 24 hours, and thereafter slowly increases. The values for the specific rotations of the product derived from α-*d*-mannose (Curve I) are lower than

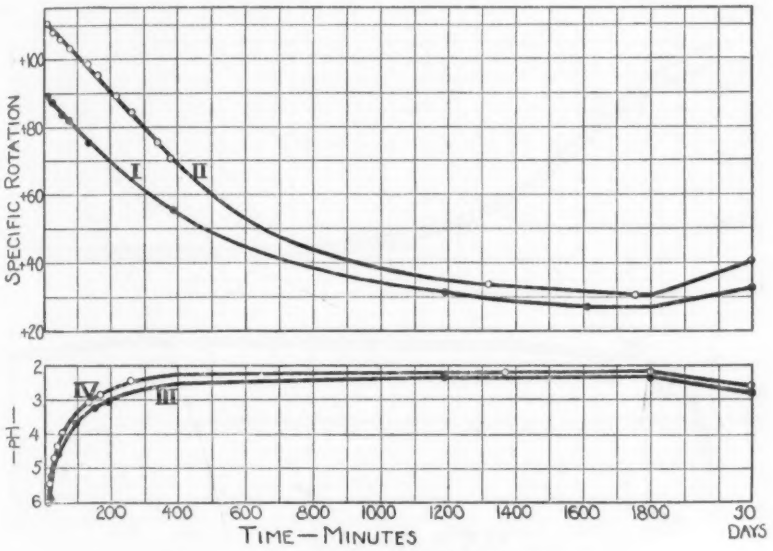

FIGURE 1.—*Bromine oxidation of mannose*

I, changes in the specific rotation of the product derived from α-*d*-mannose.
II, changes in the specific rotation of the product derived from β-*d*-mannose.
III, changes in acidity (pH) of the product derived from α-*d*-mannose.
IV, changes in acidity (pH) of the product derived from β-*d*-mannose.

those from β-*d*-mannose (Curve II) because the sample of α-*d*-mannose was oxidized less completely. The oxidation of the sample of β-*d*-mannose was 97 per cent complete, but the sample of α-*d*-mannose was oxidized only to the extent of 80 per cent. The rotation of the lactone formed from α-*d*-mannose may be calculated from the observed rotation by assuming that the solution contains only the lactone and the unoxidized sugar. The specific rotation of the unoxidized sugar, when the first reading was taken, was somewhere between the specific rotation of α-*d*-mannose and the equilibrium rotation. If we assume that the rotation of this unoxidized sugar is +30 (the rotation of α-*d*-mannose) the calculated specific rotation of the lactone formed is +104. Assuming that the specific rotation of the unoxidized sugar is +14.6 (the equilibrium rotation) then the calculated specific

[11] Nef, Ann., vol. 403, p. 312, 1914.

rotation of the lactone formed is +107. This value is near to the specific rotation of the delta lactone (+111) although somewhat lower. Hence it appears that the delta lactone is derived from both α- and β-*d*-mannose. This conclusion is further supported by the changes in pH shown in Curves III and IV. The changes are relatively rapid in both cases and show that the acidity increases on standing, reaching a maximum value in several hours. This increase in acidity indicates that the oxidation product is hydrolyzed to give an acid. A small decrease in acidity occurs on long standing. This is caused by the formation of the gamma lactone from the quasi equilibrium mixture of the free acid and the delta lactone, a reaction characteristic of acids which are capable of forming gamma and delta lactones.[12] The slightly lower acidities found for the product derived from α-*d*-man-

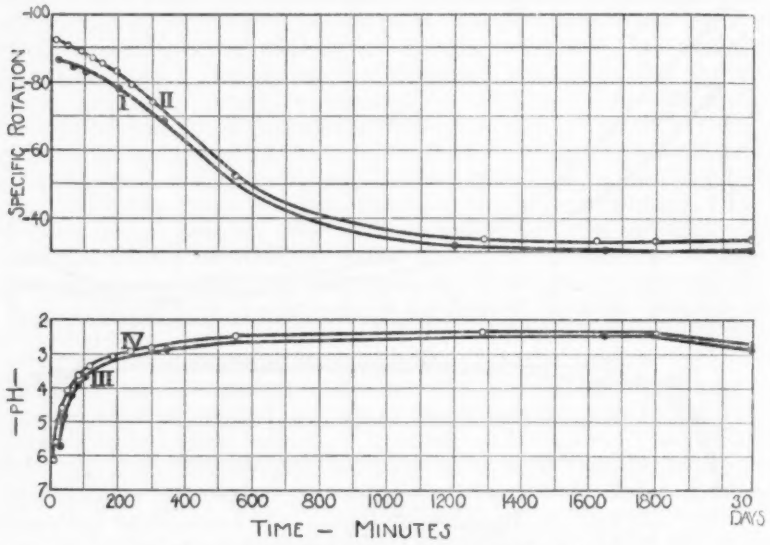

FIGURE 2.—*Bromine oxidation of rhamnose*

I, changes in the specific rotation of the product derived from α-*l*-rhamnose.
II, changes in the specific rotation of the product derived from β-*l*-rhamnose.
III, changes in acidity (pH) of the product derived from α-*l*-rhamnose.
IV, changes in acidity (pH) of the product derived from β-*l*-rhamnose.

nose (Curve III) are caused by the less complete oxidation of this sugar giving less lactone, which in turn gives less of the acid. The differences just mentioned are small and attention is directed again to the close similarity of the curves, which clearly indicate that the same substance is present in both cases.

Since the α- and β-forms of rhamnose react more slowly than the corresponding forms of mannose the oxidations of these sugars were allowed to continue 10 and 15 minutes, respectively. The results are shown in Figure 2. A comparison of the specific rotations of the product derived from α-*l*-rhamnose (Curve I), with the specific rotations of the product derived from β-*l*-rhamnose (Curve II), reveals a marked similarity between the two which indicates that the same product is obtained from α-*l*-rhamnose as from β-*l*-rhamnose. The

[12] Levene and Simms, J. Biol. Chem., vol. 65, p. 31, 1925.

oxidation product from β-*l*- rhamnose gave $[\alpha]_D^{20} = -92.5$, 15 minutes after the addition of the bromine, changing in 24 hours to −34. Jackson and Hudson[13] report that the delta rhamnonic lactone gives $[\alpha]_D^{23} = -98.4$ (7 minutes after solution), changing to −61 in 6 hours and thereafter to −30 in 11 weeks. Since the sample of β-*l*-rhamnose was oxidized only to the extent of 95.6 per cent, the observed rotation is sufficiently near to that reported by Jackson and Hudson to indicate that it is the delta lactone. Further evidence in support of this conclusion is given in Curves III and IV which show the changes in pH of the oxidation products obtained from α- and β-*l*-rhamnose. In each case the acidity increases on standing, which shows that an acid is formed from the oxidation product.

The specific rotations of solutions obtained after oxidations of α- and β-lactose are illustrated by Curves I and II in Figure 3. The

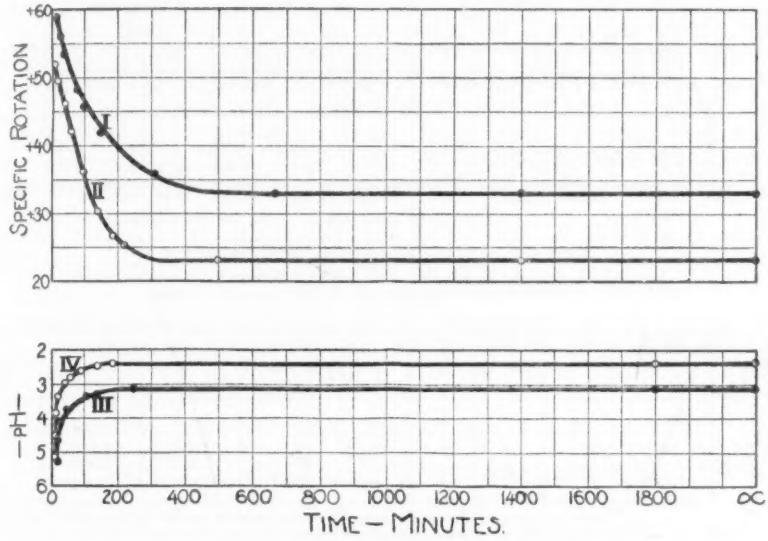

FIGURE 3.—*Bromine oxidation of lactose*

I, changes in the specific rotation of the product derived from α-lactose.
II, changes in the specific rotation of the product derived from β-lactose.
III, changes in acidity (pH) of the product derived from α-lactose.
IV, changes in acidity (pH) of the product derived from β-lactose.

oxidation of β-lactose was 96.6 per cent complete in 5 minutes, but the oxidation of α-lactose was only 60.1 per cent complete in 10 minutes. The values for the specific rotations of the oxidation product derived from α-lactose are larger than those obtained from β-lactose because the sample of α-lactose was not completely changed into the delta lactone. As may be seen from Curves III and IV of Figure 3 the oxidation product from both α- and β-lactose is hydrolyzed relatively fast. Since it is hydrolyzed so easily, there is some decomposition during the preparation of the sample and the acid formed thereby is neutralized with barium carbonate. Inasmuch as the oxidation of α-lactose was allowed to continue longer than the oxidation of β-lactose the amount of the oxidation product neutralized, as given in Table 1, is greater.

[13] Jackson and Hudson, J. Am. Chem. Soc., vol. 52, p. 1273, 1930.

The changes in the specific rotation of the oxidation product derived from β-cellobiose are illustrated in Curve I of Figure 4. The corresponding changes in pH are shown in Curve II of the same figure. The changes are rapid, indicating that the lactone is easily hydrolyzed. This accounts for the relatively large amount of cellobionic lactone

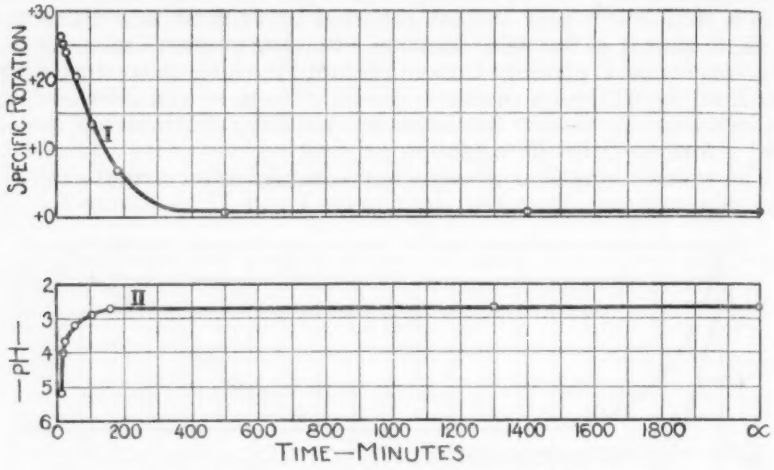

FIGURE 4.—*Bromine oxidation of cellobiose*

I, changes in the specific rotation of the product derived from β-cellobiose.
II, changes in acidity (pH) of the product derived from β-cellobiose.

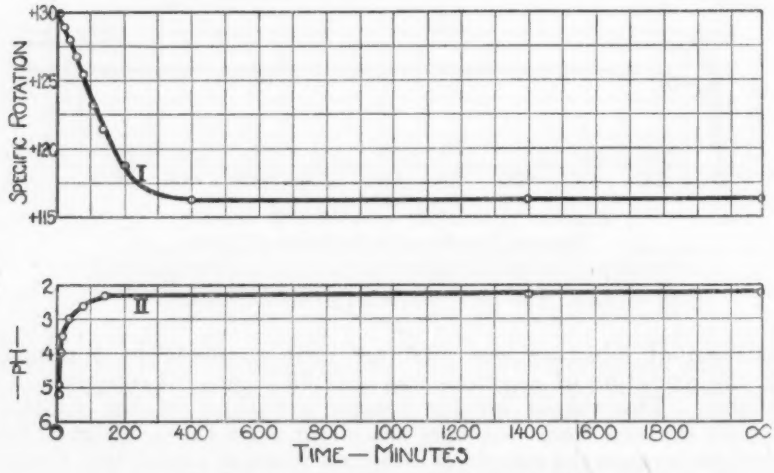

FIGURE 5.—*Bromine oxidation of maltose*

I, changes in the specific rotation of the product derived from β-maltose.
II, changes in acidity (pH) of the product derived from β-maltose.

which was hydrolyzed during the oxidation of the sugar and subsequently neutralized with barium carbonate, as given in the right-hand column of Table 1.

The changes in the specific rotation and pH of the oxidation product derived from β-maltose are shown in Curves I and II of Figure 5. Maltobionic lactone is easily hydrolyzed, but since the

oxidation of maltose was allowed to continue for only four minutes the hydrolysis of the lactone as indicated by the right-hand column of Table 1 was less than that found with cellobiose and lactose.

IV. EXPERIMENTAL DETAILS

The bromine oxidation of the sugar was conducted in the presence of 30 g of barium carbonate which was placed in a 1-liter flask and a predetermined quantity of water added. The amount of water used was such that the volume of the solution was 200 ml after the addition of 0.05 mole of the sugar and the subsequent oxidation thereof. The suspension of the barium carbonate in water was saturated with carbon dioxide at 20° C. and, after the addition of 10 ml of bromine, 0.05 mole of the finely powdered crystalline sugar was added. The flask was shaken and cooled in running water to maintain the temperature at 20° C. After 3, 4, 9, or 14 minutes, depending upon the sugar, the flask was cooled in ice water for 1 minute, during which the temperature decreased to about 12° C. The oxidation was then stopped by the addition of 50 ml of linseed oil dissolved in 50 ml of benzene, the flask being continuously cooled by ice water. The solution became colorless in about 15 seconds, showing that all the bromine was removed. The flask was shaken for one minute more, and then the cold solution was filtered. Sometimes a second filtration was necessary in order to remove any oil which passed through the first filter. A colorless filtrate was obtained which was used for following the optical rotations and hydrogen-ion concentrations.

After standing for several hours the solution of the oxidation products obtained as given above frequently developed a small amount of color, which appears to be due to free bromine. This was removed by shaking with a drop of linseed oil and filtration prior to all analytical work.

The optical rotations were read in a 2 dm water-jacketed tube on a Bates saccharimeter. The specific rotations were calculated for the anhydrous lactones, since it may be assumed that the sugar is converted into the lactone. The weights of the lactones are only slightly different from the weights of the corresponding sugars.

The hydrogen-ion determinations were made with a quinhydrone electrode in the usual manner. The samples of the oxidation products were carefully freed from all bromine and kept in a thermostat at 20° C. The results are expressed in the curves in terms of pH.

The amount of unoxidized sugar (reducing substance) remaining in the solution after the oxidation was determined by Scales's method[14] and, as given in Table 1, the percentage of the sample oxidized, as well as the equivalents of lactone formed by oxidation, were calculated from the amount of unoxidized sugar. The reagents used in determining the amount of unoxidized sugar were standardized by analyzing a solution containing a known amount of the sugar under investigation.

The equivalents of lactone present in the solution of the oxidation product were obtained by titration of the solution with standard alkali. A sample of the solution (10 ml) was heated to boiling to remove the carbon dioxide and 25 ml of *N*/10 barium hydroxide added. After a few minutes the excess alkali was titrated with

[14] Scales, J. Ind. Eng. Chem., vol. 11, p. 747, 1919.

$N/10$ sulphuric acid, using phenolphthalein as an indicator. The results were corrected for the small amount of barium bicarbonate or other basic constituents which remained in the solution. This was determined from a blank experiment which was conducted in manner analogous to the oxidation of the sugar, except that 9 g of barium bromide was substituted for the sugar. The barium carbonate, carbon dioxide, bromine, and linseed oil were added as before. A 10 ml sample of the final solution was heated to boiling with 5 ml of $N/10$ sulphuric acid and the excess acid was subsequently determined by titration with standard alkali. The 10 ml sample of the blank neutralized 0.4 ml of $N/10$ acid, and hence this correction was applied to the titrations of the oxidation products derived from the sugars.

A portion of the solution prepared for the blank run was used also for showing that in the absence of the product obtained by the oxidation of the sugars no changes in the hydrogen-ion concentration occurred on standing. The pH of the solution remained constant at 6.4

V. ACKNOWLEDGMENT

The writer expresses his appreciation to Miss Harriet Frush and W. W. Pigman, who assisted in the analytical work.

WASHINGTON, March 16, 1932.

EFFECT OF ANTIMONY ON THE MECHANICAL PROPERTIES OF A BEARING BRONZE (CU 80 : SN 10 : PB 10)

By C. E. Eggenschwiler [1]

ABSTRACT

A study of was made the effect of additions of antimony (from 0 to 0.58 per cent)upon the Brinell hardness, the structure, the Izod impact value, the deformation under pounding, and the broaching properties of a bearing bronze containing 80 per cent copper, 10 per cent tin, and 10 per cent lead.

In general, increasing the antimony content from 0 to 0.58 per cent had no effect upon the broaching properties nor upon the distribution of the lead particles throughout the copper-tin matrix. There was a slight tendency toward an increased size of the areas of the hard delta constituent with the higher antimony content. Additions of antimony lowered the Izod impact value. The deformation under pounding was markedly lowered with the first addition of antimony, reaching a minimum at 0.2 per cent antimony. Higher antimony additions tended to increase the deformation. The addition of antimony up to about 0.2 per cent slightly increased the Brinell hardness of the alloy, but further additions of antimony, up to 0.58 per cent, caused little or no further change in hardness.

CONTENTS

	Page
I. Introduction	625
II. Preparation of the castings	626
III. Methods of testing	627
IV. Effects of antimony	628
1. Microstructure	628
2. Resistance to pounding	629
3. Impact value	630
4. Broaching properties	630
5. Hardness	633
V. Summary and conclusions	634
VI. Acknowledgments	634

I. INTRODUCTION

Previous studies of bearing bronzes reported from the Bureau of Standards have described the effect of variations in composition and in casting temperatures upon the properties of bronze bearing metals.[2] [3] [4] [5] As a continuation of this work, the present paper reports a study of the effect of small additions of antimony upon some properties of a leaded bronze containing 80 per cent copper, 10 per cent tin, and 10 per cent lead.

The main object of the present investigation was to determine the effect of small additions of antimony (below 0.5 per cent) upon the machinability of this alloy when broached. This method of machining the cylindrical bearing surfaces is widely used in finishing the bore of bearings because it is less expensive than other methods. It was pointed out by manufacturers of bearing bronzes that many of

[1] Research associate representing the Bunting Brass & Bronze Co., Toledo, Ohio.

[2] H. J. French, S. J. Rosenberg, W. LeC. Harbaugh, and H. C. Cross, Wear and Mechanical Properties of Railroad Bearing Bronzes at Different Temperatures, B. S. Jour. Research, vol. 1 (RP13), September, 1928.

[3] H. J. French and E. M. Staples, Bearing Bronzes With and Without Additions of Zinc, B. S. Jour. Research, vol. 2, (RP68), June, 1929.

[4] E. M. Staples, R. L. Dowdell, and C. E. Eggenschwiler, Bearing Bronzes With Additions of Zinc, Phosphorus, Nickel, and Antimony, B. S. Jour. Research, vol. 5 (RP205), August, 1930.

[5] C. E. Eggenschwiler, Effect of Casting Temperatures and of Additions of Iron on Bearing Bronze (Cu 80 : Sn 10 : Pb 10), B. S. Jour. Research, vol. 8 (RP401), January, 1932.

the failures observed during the broaching of bushing bearings, failures from fracture, or from scoring, checking, tearing, or other roughening of the bore often appeared to be attributable to an undesirable antimony content.

Varied opinions have been expressed as to the effect of antimony upon copper, brass, and bronze. The consensus of opinion seems to be that antimony causes brittleness of copper alloys. St. John has described several effects of antimony on copper and copper alloys [6] and Dews has given the results of some investigations on the effect of antimony on admiralty gun metal (88–10–2).[7] The latter author pointed out that antimony present in amounts over 0.5 per cent decreases both the tensile strength and the elongation of bronzes. A recent publication of the Bureau of Standards also shows that the addition of 1 per cent antimony to bronzes reduced the Izod value considerably.[8]

Although antimony is rarely added to bronzes intentionally, it is usually present to a small extent. It probably makes its way into bronze largely through the use of secondary lead and tin which contain antimony. Zinc and copper may also contain small amounts of antimony. The antimony content of bronze obviously may be increased considerably if unserviceable and "worn out" bronze bearings carrying either lead-base or tin-base babbitt metal are used as a portion of the furnace charge.

This investigation is a continuation of the study of bearing bronzes which has been in progress for the last four years in cooperation with the Bunting Brass & Bronze Co. under the research-associate plan.[9]

II. PREPARATION OF THE CASTINGS

Cylindrical castings for the broaching test specimens and plate castings for the impact, pounding, and hardness specimens were cast, with the dimensions and with the method of gating illustrated in Figure 1. In the present work on the effect of antimony only four cylinders were cast in a flask, instead of six as has been done in previous work on bearing bronzes and as illustrated in Figure 1. These castings were of relatively thin section and approximated the average thickness of castings used for bushing bearings in the automotive industry.

The following procedure was followed in the founding of the specimens: A stock alloy of copper and tin was first prepared and poured into small ingots. The furnace charge in making this stock alloy consisted of 96 pounds of electrolytic copper and 12 pounds of refined Straits tin. The copper was melted under a slag of glass, and tin was then added. Two such heats were prepared. The chemical composition of each is given in Table 1.

TABLE 1.—*Chemical composition of the stock copper-tin alloy*

Heat No.	Copper	Tin
	Per cent	*Per cent*
1	88.90	11.15
2	88.97	11.11

[6] H. M. St. John, The Influence of Impurities in Foundry Brasses and Bronzes, Metals & Alloys, vol. 2, p. 243, 1931.
[7] H. C. Dews, Metallurgy of Bronze, Sir Isaac Pitman & Sons, N. Y., pp. 86-91, 1930.
[8] See footnote 4, p. 363 of reference.
[9] B. S. Circular No. 296.

In the preparation of the castings, between 20 and 24 pounds of the stock alloy, together with the desired amounts of copper were melted under a slag of glass. After the charge had become molten, tin and refined lead were added in calculated amounts to bring the composition to 80 per cent copper, 10 per cent tin, and 10 per cent lead. The antimony was melted with a small amount of tin and was added prior to pouring the alloy. Metallic antimony could not be added directly to the molten metal without considerable spattering. The bearing bronze alloys were prepared in a graphite crucible heated in a gas-fired furnace and were poured into sand molds. No defects were noted in any of the castings.

Copper and lead in the castings were determined by the electrolytic method, tin gravimetrically and antimony volumetrically. All chemical analyses were carried out in accordance with American Society for Testing Materials standard methods for the analysis of bearing metals.[10] The chemical compositions of the alloys are given in Table 2.

TABLE 2.—*Chemical compositions and pouring temperatures of the bronzes*

Alloy No.	Casting temperature	Chemical composition			
		Copper	Tin [1]	Lead	Antimony [1]
	°F.	*Per cent*	*Per cent*	*Per cent*	*Per cent*
27-A-10	2,085	80.10	9.80	9.90	0.12
27-A-1	2,100	80.00	9.90	10.10	.19
27-A-25	2,100	79.74	10.00	10.00	.26
27-A-3	2,085	79.95	9.90	9.55	.33
27-A-45	2,090	79.50	9.90	10.00	.48
27-A-5	2,100	79.25	10.30	9.88	.58

[1] Since antimony and tin were both present in the bronze samples, a deduction was made in the gravimetric determination of tin for the antimony remaining with the ignited tin oxide.

Temperature measurements were made with a chromel-alumel thermocouple and a portable potentiometer. The thermocouple was incased in a glazed porcelain tube which, in turn, was inclosed in a graphite tube. This assembly was preheated before immersing in the molten metal. Casting temperatures were determined from readings taken in the crucible immediately before pouring.

III. METHODS OF TESTING

The tests applied to the bearing bronze alloys consisted of microscopic examination, resistance to deformation under pounding, resistance of notched specimens to single-blow impact, Brinell hardness, and machinability in broaching. As the effect of antimony upon the resistance to wear[11] and upon tensile properties[12] has been previously investigated, it was unnecessary to make wear resistance and tensile tests in the present work.

The procedure used in all of the above tests, except that of machinability in broaching, has been fully described in previously published work.[13]

[10] A. S. T. M. standards, 1930, Pt. I, Metals, pp. 852-863. Standard Methods of Chemical Analysis of Bronze Bearing Metals, B46-27.
[11] See footnote 4, p. 625.
[12] See footnote 7, p. 626.
[13] See footnote 4, p. 625.

The broaching tests were included for the purpose of correlating a practical machining test with the results of the laboratory tests. The broaching tests were made in the plant machine shop by the Bunting Brass & Bronze Co.

Three of the cast cylinders (fig. 1) from each heat were used for broaching tests. The three specimens from any one heat, representing a given content of antimony, were bored before broaching in order to eliminate variations in the inside surface of the cylinder and in order to prepare specimens of three different wall thicknesses. This latter object was accomplished by boring the No. 1 specimen of each heat to an inside diameter of 1.375 inches, the No. 2 specimen to 1.625 inches, and the No. 3 specimen to 1.750 inches. The original cast outside surface remained on all specimens and the outside diameter of all cylinders for broaching was, therefore, the original cast diameter of 2.167 inches.

The broaching tools used each had four cutting edges spaced one-half inch apart along the axis of the broach. These cutting edges made an angle of 90° with the axis of the broach. The four edges of each broach cut to a total depth of 0.045 inch. All broaching was at a tool speed of 70 feet per minute.

Broaching and Brinell hardness tests were conducted at room temperature. Impact and pounding tests were conducted at both room and elevated temperatures.

IV. EFFECTS OF ANTIMONY

1. MICROSTRUCTURE

A small section was cut from each of the plate castings, polished, etched, and examined visually for any differences in grain size that might indicate differences in casting temperatures. The grain size was similar in all the alloys and no serious defects were observed in any of the castings.

Microscopic examination of the bronzes containing antimony from 0.12 to 0.58 per cent disclosed no significant differences in either the structure or the distribution and size of the lead particles. The black areas in Figure 2 (*a*) and (*b*) which shows the bronzes containing 0.12 and 0.58 per cent antimony, the extremes of the range of antimony content used, are representative of the lead distribution in all the alloys prepared.

The structures revealed by etching these same specimens are shown in Figure 2 (*c*) and (*d*). Again these micrographs are typical of all the bronze specimens of the series. The hard delta constituent is shown in relief in the copper-tin solid solution. The delta constituent particles appeared slightly larger in the alloys of higher antimony content.

No separate constituent characteristic of the presence of antimony could be detected in the microstructure of the bronzes studied. Since antimony may be in solid solution in lead to the extent of 0.25 per cent,[14] in copper to about 7 per cent,[15] and in tin to about 9 per cent,[16] it is not surprising that, within the range of antimony content studied (0.12 to 0.58 per cent) this impurity should be in solid solution in the ternary alloy of copper-tin-lead.

[14] National Metals Handbook, 1930 ed., American Society for Steel Treating, Cleveland, Ohio, p. 716.
[15] International Critical Tables, McGraw-Hill Book Co., New York, vol. 2, p. 434, 1927.
[16] National Metals Handbook, 1930 ed., American Society for Steel Treating, Cleveland, Ohio, p. 764.

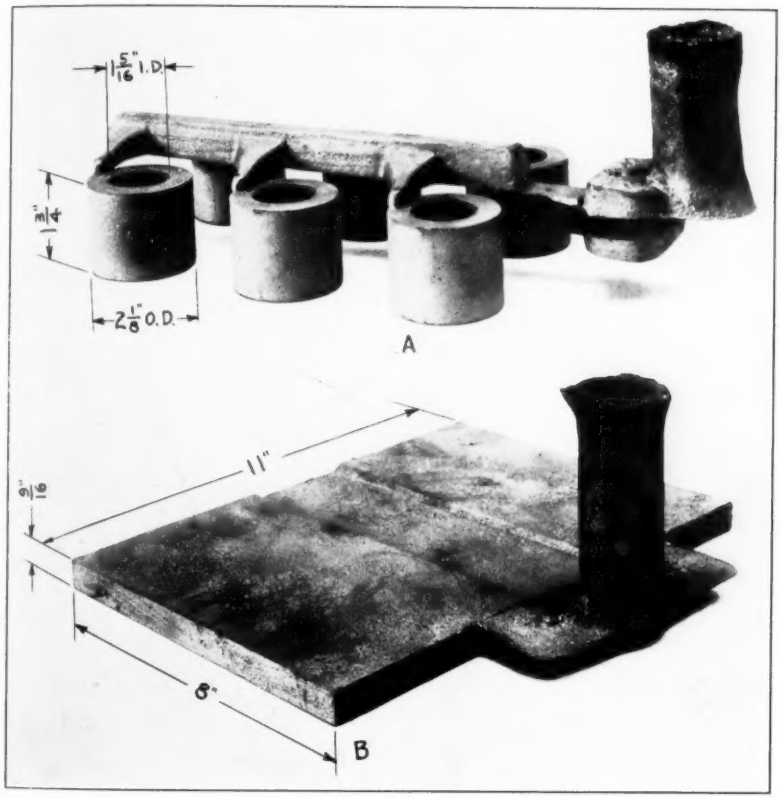

FIGURE 1.—*Test castings*

A, For broaching test specimens; *B*, for pounding, impact, and hardness tests.

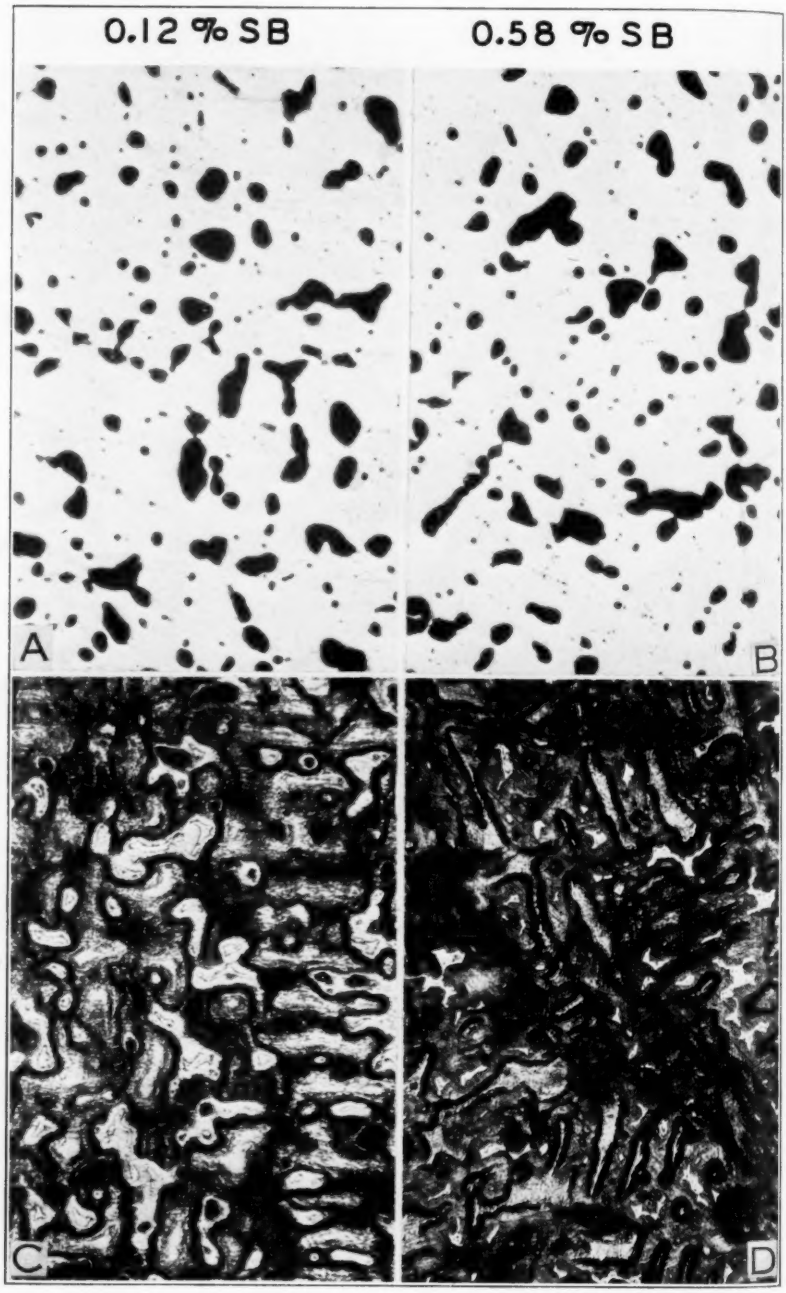

FIGURE 2.—*Distribution of the lead (A and B) and microstructure (C and D) of 80–10–10 bronze containing additions of antimony.* × *100*

C and *D*, etched with a solution of 3 parts of NH_4OH plus 1 part H_2O_2 followed by a solution of $FeCl_3$ (10 g $FeCl_3$ plus 30 ml concentrated HCl plus 120 ml H_2O).

2. RESISTANCE TO POUNDING

The results of the pounding tests at room temperature, 350° F., and 600° F. are shown in Figures 3, 4, 5, and 6. Since pounding produces work hardening of the bronze, the first application of blows resulted in a relatively higher rate of deformation, but as the number of blows increased the rate of deformation decreased rapidly.

In previous investigations of bearing bronzes either the number of blows necessary to produce 5 per cent deformation or curves similar to those of Figure 6 showing the number or the per cent deformation produced by a definite number of blows, have been used as the basis for comparison of the test results.[17] While these methods are quite adequate for comparative results, there are also given in the present

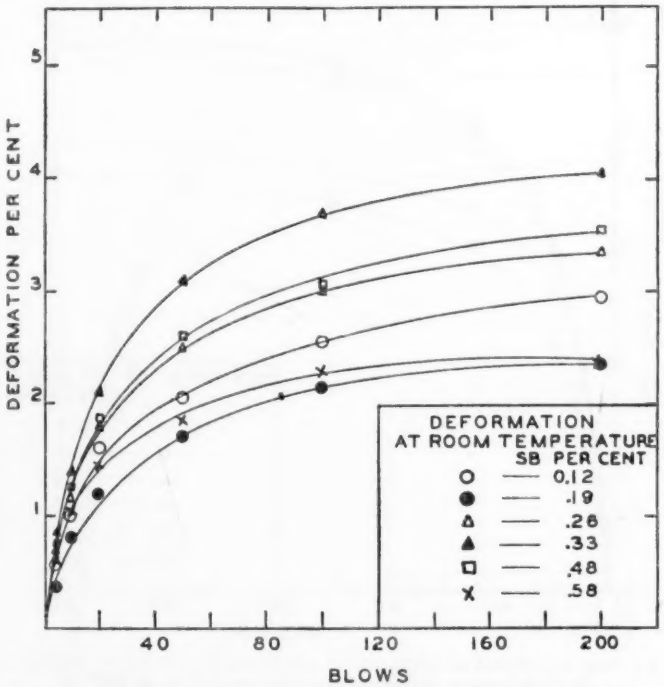

FIGURE 3.—*Effect of additions of antimony to 80–10–10 bronze on the resistance to deformation under pounding at room temperature*

report the rates of deformation of the various alloys studied. (Figs. 3, 4, and 5.) These latter figures give an approximate idea of the amount of deformation these alloys may undergo in service unless, as a part of the manufacturing process, they have been work hardened by plastic deformation. It will be observed that increasing the temperature of the specimen very noticeably increased the rate of deformation in the beginning of the test.

The data given in Figures 3, 4, and 5 are summarized in Figure 6. The alloys containing 0.2 and 0.6 per cent antimony deformed the least. There was a marked tendency for the alloys to show increased deformation when the antimony content increased from about 0.20

[17] See footnotes 2, 3, and 4, p. 625.

to about 0.40 per cent. It is noteworthy that the alloys containing no additions of antimony suffered a greater deformation at a given temperature than any of the bronzes containing antimony.

3. IMPACT VALUE

Previous work [18] has shown that additions of 1 per cent antimony to a number of bearing bronzes produced a quite noticeable decrease in the resistance to impact.

Figure 7 shows the effects of antimony upon the resistance to impact. Tests at room temperature and 350° F. indicated that antimony additions up to 0.25 per cent caused a marked decrease in the

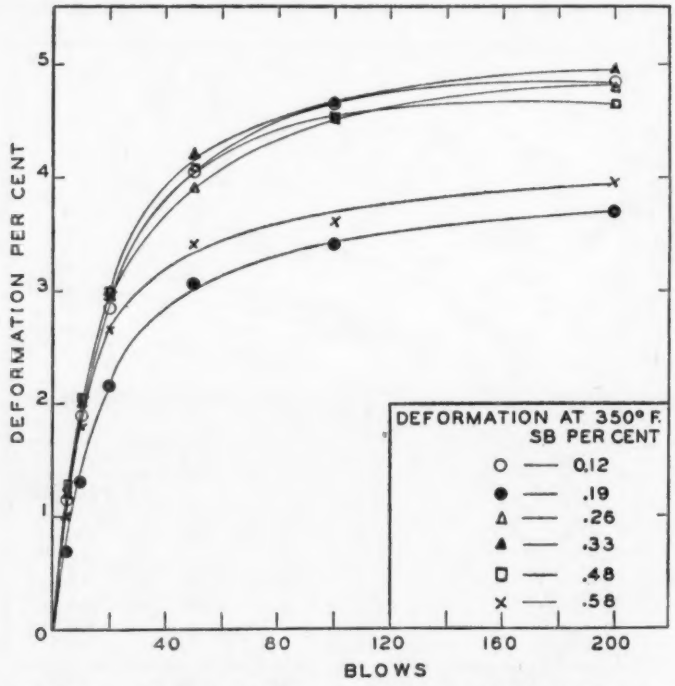

FIGURE 4.—*Effect of additions of antimony to 80–10–10 bronze on the resistance to deformation under pounding at 350° F.*

resistance to impact. The impact value decreased less rapidly with larger proportions of antimony in the alloy. At 600° F. very little effect on the impact resistance was observed as the antimony content was increased.

The effect of increasing the temperature from room temperature to 350° F. was a relatively small decrease in the resistance to impact, but increasing the temperature to 600° F., resulted in a very marked lowering of the impact resistance.

4. BROACHING PROPERTIES

The results obtained in the broaching tests, given in Table 3, indicated that all the specimens behaved satisfactorily in the broaching tests described in a preceding section of this report.

[18] See footnote 4, p. 363 of reference.

As a more searching test of the possible effect of the antimony present, an additional broaching operation was conducted. Specimens previously broached in test No. 1, that is, having the original "as cast" outside diameter of 2.167 inches and an inside diameter of 1.465 inches, were machined to an outside diameter of 1.875 inches and an inside diameter of 1.625 inches, thus leaving a wall thickness

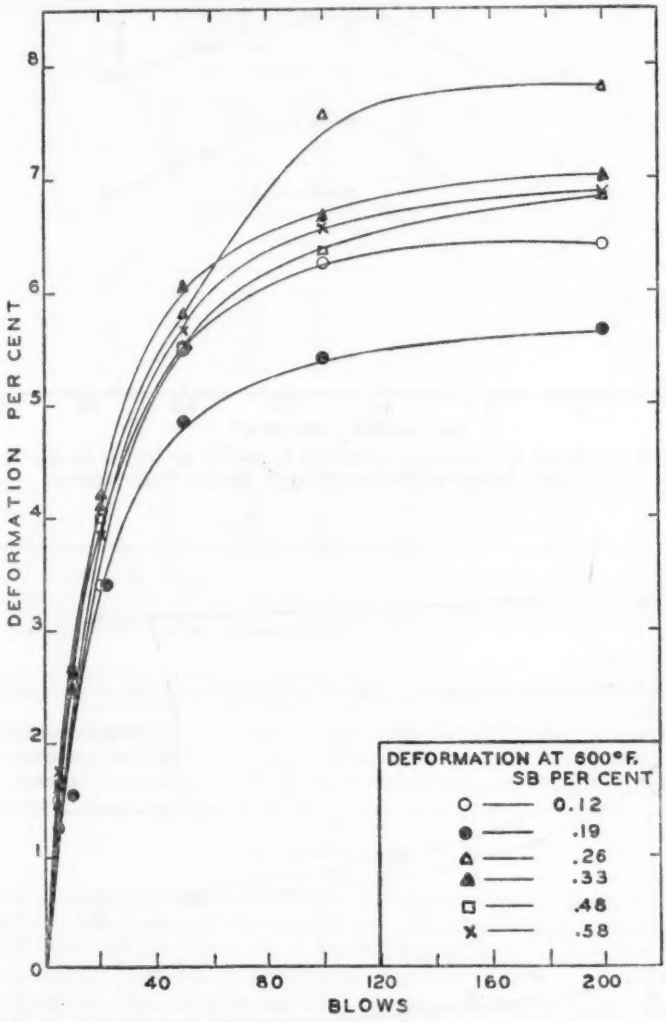

FIGURE 5.—*Effect of additions of antimony to 80–10–10 bronze on the resistance to deformation under pounding at 600° F.*

of 0.125 inch. They were then broached in the manner previously described. After this operation the outside surfaces of all specimens showed marked fracturing at the grain boundaries and the broached cylinders emitted a dull sound when tapped with a metal rod. There was no apparent difference in behavior under this test between the low antimony and the high antimony alloys.

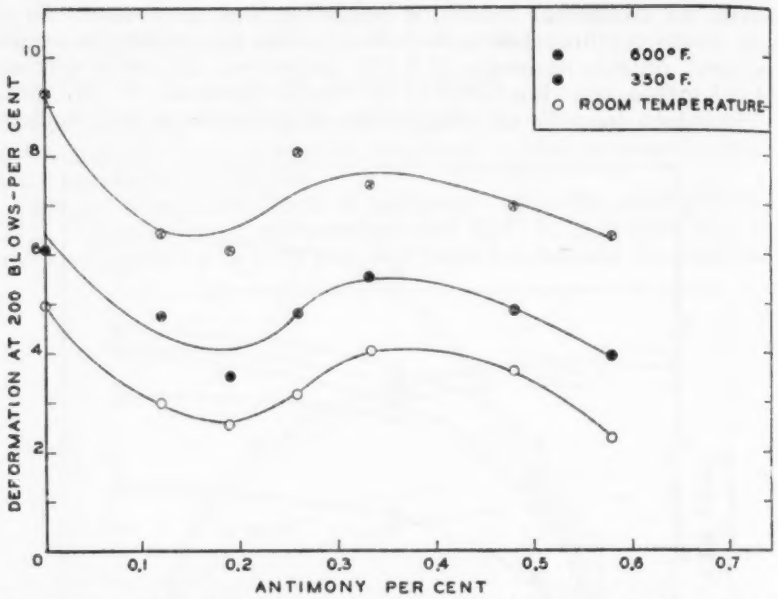

FIGURE 6.—*Effect of antimony additions to 80–10–10 bronze on the resistance to deformation under pounding at various temperatures*

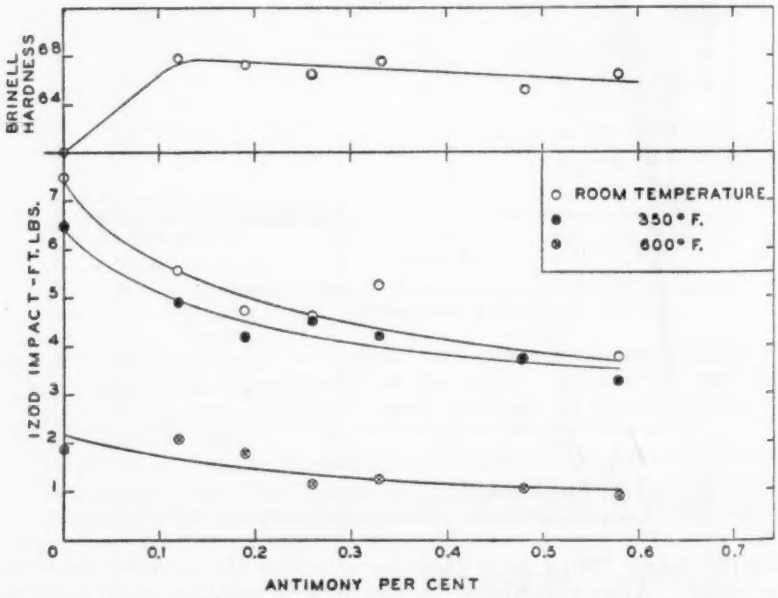

FIGURE 7.—*Brinell hardness and Izod impact tests at various temperatures on 80–10–10 bronze containing additions of antimony*

TABLE 3.—*Broaching tests of cylindrical bronze castings containing antimony*

[Depth of broaching throughout, 0.045 inch. Rough outside (as cast) diameter of all specimens, 2.167 inches]

TEST NO. 1

Alloy No.	Specimen No.	Antimony [1]	Inside diameter as machined preliminary to broaching	Wall thickness	Inside diameter after broaching	Remarks
		Per cent	*Inches*	*Inch*	*Inches*	
27-A-10	1	0.13	1.375	0.396	1.465	Fractures, none; scoring, none; checking, none; tearing, none; bore, smooth.
27-A-1	1	.18	1.375	.396	1.465	
27-A-25	1	.23	1.375	.396	1.465	
27-A-3	1	.28	1.375	.396	1.465	
27-A-45	1	.40	1.375	.396	1.465	
27-A-5	1	.53	1.375	.396	1.465	

TEST NO. 2

27-A-10	2	0.13	1.625	0.271	1.715	Fractures, none; scoring, none; checking, none; tearing, none; bore, smooth.
27-A-1	2	.18	1.625	.271	1.715	
27-A-25	2	.23	1.625	.271	1.715	
27-A-3	2	.28	1.625	.271	1.715	
27-A-45	2	.40	1.625	.271	1.715	
27-A-5	2	.53	1.625	.271	1.715	

TEST NO. 3

27-A-10	3	0.13	1.750	0.2085	1.840	Fractures, none; scoring, none; checking, none; tearing, none; bore, smooth.
27-A-1	3	.18	1.750	.2085	1.840	
27-A-25	3	.23	1.750	.2085	1.840	
27-A-3	3	.28	1.750	.2085	1.840	
27-A-45	3	.40	1.750	.2085	1.840	
27-A-5	3	.53	1.750	.2085	1.840	

[1] Analyses made by L. M. Long, of the Bunting Brass & Bronze Co. The antimony contents of these specimens differ slightly from those given in Table 2 due to the fact that the cylinders for broaching tests were from different castings than the specimens used for all other tests.

The broaching qualities of the bronzes, therefore, were not adversely affected by additions of antimony up to 0.53 per cent. It should be pointed out, however, that antimony was the only minor element or impurity added to these bronzes. If antimony does affect the broaching qualities of commercial bronzes it would appear that this influence may be dependent on the simultaneous presence of other impurities.

5. HARDNESS

It was found in some previous investigations [19] that antimony increased the hardness of bronze alloys. Most of these investigations indicated that while there is a hardening effect, this effect is not progressive with increasing additions of antimony.[20]

According to the results of the present investigation, given in Figure 7, the presence of 0.1 per cent antimony was sufficient to cause a perceptible increase in the Brinell hardness. However, larger amounts of antimony, up to 0.58 per cent, had slight effect upon the hardness at room temperature.

[19] See footnote 4, p. 363 of reference.
[20] See footnote 7, p. 89 of reference.

V. SUMMARY AND CONCLUSIONS

A study has been made of the effect of antimony (up to 0.58 per cent) on the deformation under pounding, the Izod impact value, microstructure, hardness, and broaching properties of a bearing bronze containing 80 per cent copper, 10 per cent tin, and 10 per cent lead. In addition to the tests made at room temperature, many tests were made at 350° and 600° F.

Increasing the antimony content decreased the Izod impact value; had no effect upon the size or distribution of lead particles in the structure of the bronze; produced a slight increase in the size of the hard (delta) constituent; had no effect upon the machinability under broaching; and decreased the deformation under pounding when the antimony content was present to the extent of 0.2 or 0.58 per cent. The Brinell hardness of the alloys was slightly increased by the addition of 0.2 per cent antimony; further additions of antimony produced no signficant change in hardness.

It may be concluded that the effect of additions of small amounts of antimony was seriously detrimental only to the notch toughness of the bronzes studied. It is to be kept in mind, however, that the above conclusions are applicable only to the type of test specimens and test castings employed, and to bronzes which do not contain, in addition to antimony, the other impurities usually present in similar commercial bronzes.

VI. ACKNOWLEDGMENTS

The author expresses his appreciation to L. M. Long and other members of the Bunting Brass & Bronze Co., for their cooperation in conducting the broaching tests and for their helpful comments and suggestions.

Acknowledgment is also made to Louis Jordan, for his supervision.

WASHINGTON, March 5, 1932.

INVESTIGATION OF THE METHOD OF DETERMINING THE RELATION OF STATICAL HYSTERESIS AND FLEXURAL STRESS BY MEASUREMENT OF THE DECREMENT OF A FREELY VIBRATING U BAR

By G. H. Keulegan

ABSTRACT

This investigation was undertaken to determine whether measurements of the decrement of a vibrating U bar could be used to measure with sufficient accuracy the statical hysteresis of the material. The statical hysteresis of a U bar of Armco iron was first measured under cyclic static loading, and then the decrement of the vibrations of the same bar were measured. The results of the experiments showed that within the limits of accuracy of the approximate theory used, both methods gave equivalent results. For stresses above a certain small threshold value, it was found that in Armco iron the energy lost by statical hysteresis varied approximately as the cube of the amplitude of the maximum stress.

CONTENTS

	Page
I. Introduction	635
II. Theory of the energy loss in a straight bar due to statical hysteresis	637
1. During alternating flexure produced by a load cycle	637
2. During alternating flexure produced by lateral vibrations	642
III. Application of the theory to a U bar	643
IV. Apparatus and experimental procedure	644
1. Statical measurement during a load cycle	644
2. Dynamical measurement during lateral vibrations	644
3. Description of the U bar	645
V. Experimental results on an Armco iron U bar	646
1. Statical alternate cycles of flexure	646
(*a*) Energy loss as a function of the length of the U bar	646
(*b*) Energy loss as a function of the maximum deflection	648
2. Energy loss during vibration	651
(*a*) Effect of method of supporting of the U bar	651
(*b*) Energy loss per cycle	653
VI. Comparison of the experimental results	654
VII. Law of statical hysteresis in Armco iron	656

I. INTRODUCTION

This investigation is part of a general investigation of statical hysteresis in metals. Three reports have been previously published,[1] [2] [3] in the first and second of which it is shown, in common with the results of other workers in this field, that the statical hysteresis in flexure is, to the first order, a function of the stress alone. This report is a continuation of the first report,[4] extending the experimental data and involving the investigation of a different and more convenient method of experimentation.

[1] G. H. Keulegan, Statical Hysteresis in the Flexure of Bars, B. S. Tech. Paper No. 332, 1926.
[2] G. H. Keulegan, Statical Hysteresis in Cycles of Equal Load Range, B. S. Tech. Paper No. 365, 1928.
[3] G. H. Keulegan, On the Vibration of U Bars, B. S. Jour. Research, vol. 6, pp. 553-592, 1931.
[4] See footnote 1.

Methods used by other investigators of hysteresis phenomena include measurement of (*a*) static deformation of rods in uniform flexure,[5] (*b*) static deformation of strips in elongation[6]; (*c*) the rise of temperature of rods in alternate, axial stress cycles[7]; (*d*) the amplitude at resonance during the forced oscillations of tubes in flexure[8]; (*e*) the distortion of loaded rotating rods[9]; (*f*) the decrement of the longitudinal vibrations of a rod[10]; and (*g*) the torque of a Rayleigh disk in the proximity of a longitudinally vibrating rod[11]; the decay of the lateral oscillations of clamped and loaded strips.[12] It is planned to consider the results obtained by these methods in a future paper.

The term statical hysteresis refers, as in the earlier reports,[13] to the component of elastic lag which is independent of rate of loading of the elastic body during the load cycle. The elastic lag is the difference in deflection of an elastic body at any load in a load cycle in which the load is first increased to higher values and then decreased to the original value again. The component of the elastic lag dependent on the rate of loading is due to elastic after working and is called hereditary hysteresis.

The direct method of measuring elastic lag involves applying a series of loads at a given rate to the body under investigation and measuring the corresponding deflections. This method is difficult to use in an extensive investigation owing to the small values of the elastic lag and the large number of independent readings which must be taken. For this reason the present investigation was undertaken to determine if measurements of the decrements of the amplitude of a freely vibrating U bar would give comparable results for materials subjected to flexural stresses. As the loss in energy is all that can be determined from the decrement, the elastic hysteresis must be expressed in terms of the loss in energy per cycle, but this is no disadvantage since the relation of elastic hysteresis to load (or deflection) is well known and its magnitude can be calculated if the energy loss per cycle is known.

In general, the damping of a vibrating body is brought about by the combined effects of elastic afterworking and statical hysteresis. If the effect of elastic afterworking is negligible in comparison with that of statical hysteresis, the vexing question of the time element is eliminated from consideration, and the hysteresis calculated from the decrement of a vibrating body should be directly comparable with that calculated from slowly alternating static deformations. Armco iron appears to be a material in which the elastic afterworking is negligible. Consequently, the experimental data were obtained on a U bar of this material.

---

[5] Sayre, M. F., and Hoadley, A. Stress Distribution and Hysteresis Losses in Springs, Applied Mechanics (A. S. M. E. Trans.), vol. 51, pp. 287-303, 1929.
[6] Sayre, M. F. Elastic and Inelastic Behaviour in Spring Materials, Applied Mechanics (A. S. M. E. Trans.), vol. 52, pp. 105-111, 1930.
[7] B. Hopkinson and G. T. Williams, London, Proc. R. Soc., vol. 87, p. 502; 1912.
[8] R. H. Canfield, Internal Friction in Metals, Phys. Rev., vol. 32, pp. 521-530, 1928.
[9] A. L. Kimball and D. E. Lovell, Internal Friction in Solids, Phys. Rev., vol. 30, pp. 948-959, 1927.
[10] E. Voigt. Eine neue Methode zur Bestimmung der inneren Arbeitsaufnahmefähigkeit von Werkstoffen bei dynamischer Beanspruchung, Zeit. f. Tech. Phys., vol. 9, pp. 321-337, 1928.
[11] S. L. Quimby, On the Experimental Determination of the Viscosity of Vibrating Solids, Phys. Rev., vol. 25, pp. 558-569, 1925.
[12] K. Honda and S. Konno, On the Determination of the Coefficients of Normal Viscosity of Metals. Phil. Mag., vol. 42, pp. 115-123, 1921.
[13] See footnotes 1 and 2, p. 635.

Two sets of independent data were obtained on the U bar, (*a*) when stressed flexurally by means of a series of static loads and (*b*) when vibrating freely. The results, in the light of the theory adopted, are shown to be equivalent, thus indicating that the decrement of the amplitude of vibration is sufficient to determine the hysteresis of materials of the type where elastic afterworking is negligible in comparison with statical hysteresis.

II. THEORY OF THE ENERGY LOSS IN A STRAIGHT BAR DUE TO STATICAL HYSTERESIS

1. DURING ALTERNATING FLEXURE PRODUCED BY A LOAD CYCLE

Consider a straight rectangular bar of uniform thickness $2a$, width b, and length s_1 (see fig. 1) clamped at one end and a load L

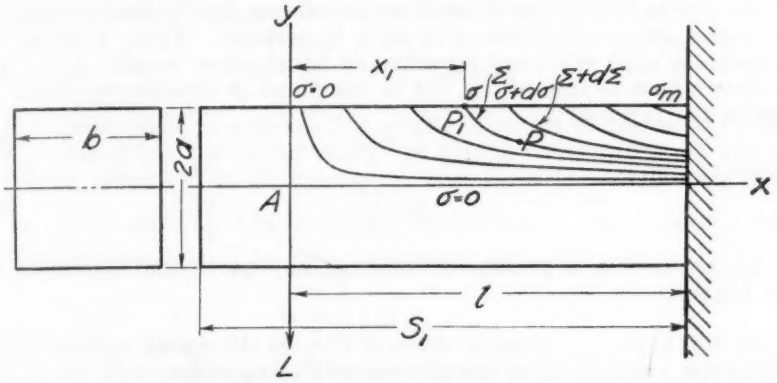

FIGURE 1.—*Lines of equal stress amplitude σ in the upper section of the clamped-free bar in the plane of bending*

applied at some point A. Let l denote the distance of this point from the fixed end. (Hereafter, l will be called the effective length of the bar in flexure.) The alternating flexure of the bar is produced by varying the load L between the limits $+L_m$ and $-L_m$ in a cyclic manner. (Hereafter L_m will be called the amplitude of the alternating load in the cycle.) Construct a set of coordinate axis with the origin at A, the x axis in the neutral plane of the bar and the y axis in the plane of bending. During a cycle of alternating flexure the material at a point P (x, y) (see fig. 1) undergoes a cycle of alternating stress of amplitude σ, which, in terms of the amplitude of the alternating load, is

$$\sigma = xy\frac{L_m}{I} \tag{1}$$

where I is the moment of inertia of the section of the bar at P. For a rectangular bar

$$I = \frac{2}{3}ba^3 \tag{2}$$

During each cycle of alternating stress statical hysteresis causes a loss of a certain amount of elastic energy. This loss in elastic energy

in a differential of volume, dv, represented by dH, is assumed to be proportional to the volume and a function of the stress amplitude σ at any point P in the bar; that is

$$dH=f(\sigma)\,dv \tag{3}$$

The form of this function is to be determined by experiment.

The total loss of energy, H, in the whole bar during a cycle of alternating flexure is

$$H=2\int f(\sigma)\,dv \tag{4}$$

where the integration is made through the upper half of the bar. The next step in the calculation of H is to determine dv as a function of σ and the constants of the bar.

Equation (1) states that during a cycle of alternating flexure, points of the bar in the plane of bending (xy plane, fig. 1) and possessing the same stress amplitude σ lie on a hyperbola. Thus, a family of hyperbolae each representing a line of equal stress amplitude σ may be drawn in a section of the bar in the plane of bending as shown in Figure 1. If we write

$$\Sigma=xy \tag{5}$$

where

$$\Sigma=\frac{\sigma I}{L_m} \tag{6}$$

Σ can be used as a parameter defining any particular hyperbola of the family.

Let the hyperbola passing through P meet the upper surface of the bar at the point P_1. Let the abscissa of P_1 be x_1, then

$$\Sigma=ax_1 \tag{7}$$

Now the area F of the bar below the hyperbola with parameter Σ is

$$F=ax_1+\int_{x_1}^{l}y\,dx=\Sigma+\int_{\frac{\Sigma}{a}}^{l}\frac{\Sigma}{x}\,dx=\Sigma+\Sigma\log\frac{al}{\Sigma} \tag{8}$$

Hence, if we differentiate F, with respect to Σ, we obtain the expression

$$dF=\left(\log\frac{al}{\Sigma}\right)d\Sigma \tag{9}$$

which is the elementary area lying between the two consecutive hyperbolae with parameters Σ and $\Sigma+d\Sigma$. All of the points in this elementary area have the same stress amplitude σ. Since the bar is of uniform width b, the volume of the elementary portion of the bar, having the same value of σ, is

$$dv=b\left(\log\frac{al}{\Sigma}\right)d\Sigma \tag{10}$$

Next, let σ_m be the maximum stress amplitude σ in the bar during a cycle of alternating flexure in which the load amplitude is L_m. This maximum stress amplitude occurs at the point $x=l$, $y=a$; that is,

at the upper and the lower surfaces of the bar in the neighborhood of the clamp. Then equation (1) becomes

$$\sigma_m = \frac{alL_m}{I} \tag{11}$$

Substituting from equations (6), (7), and (11), equation (10) becomes

$$dv = \frac{alb}{\sigma_m} \log \frac{\sigma_m}{\sigma} d\sigma \tag{12}$$

Letting V be one-half of the volume of the bar, or alb,

$$dv = \frac{V}{\sigma_m} \log \frac{\sigma_m}{\sigma} d\sigma \tag{13}$$

Substituting the value of dv from equation (13) in equation (4) we obtain the loss in energy in terms of the stress amplitude

$$H = \frac{2V}{\sigma_m} \int_0^{\sigma_m} \log \frac{\sigma_m}{\sigma} f(\sigma)\, d\sigma \tag{14}$$

It is convenient to express the results in terms of the ratio of the energy loss H to the entire energy of elastic deformation W of the bar when subjected to the maximum load L_m of the alternating load cycle. This ratio, $\frac{H}{W}$ will be called the fractional loss of energy due to statical hysteresis. In terms of the stress amplitude

$$W = \frac{1}{E} \int \sigma^2\, dv$$

where the integration is taken over the upper half of the bar. E is Young's modulus of elasticity of the bar material. Introducing the value of dv from equation (13),

$$W = \frac{V}{E\sigma_m} \int_0^{\sigma_m} \left(\log \frac{\sigma_m}{\sigma} \right) \sigma^2 d\sigma$$

and, after integration,

$$W = \frac{V}{9} \frac{{\sigma_m}^2}{E} \tag{15}$$

The fractional loss of energy is then:

$$\frac{H}{W} = \frac{18E}{{\sigma_m}^3} \int_0^{\sigma_m} \log \frac{\sigma_m}{\sigma} f(\sigma)\, d\sigma \tag{16}$$

This is the basic equation for the study of statical hysteresis in the alternating flexure of rectangular bars having one end clamped. Here, as previously stated, σ_m is the maximum stress amplitude in the bar corresponding to the load L_m.

It has been found by preliminary experiments that $f(\sigma)$ is given with sufficient approximation by the relations

$$f(\sigma) = 0 \quad \sigma \leqq \sigma_0$$

$$f(\sigma) = \left(1 - \frac{\sigma_0}{\sigma}\right) \sum_{r=2}^{r=n} \beta_r \sigma^r, \quad \sigma \geqq \sigma_0 \tag{17}$$

where the quantities β_r are undetermined constant coefficients and σ_0 is a small stress, which in a particular case may be zero. This gives

$$\frac{H}{W}=\frac{18E}{{\sigma_m}^3}\sum_{r=2}^{r=n}\beta_r\left[-\left(\log\frac{\sigma_0}{\sigma_m}\right)\frac{{\sigma_0}^{r+1}}{r\,(r=1)}\right.$$
$$\left.+\frac{{\sigma_m}^{r+1}}{(r+1)^2}-\frac{\sigma_0\,{\sigma_m}^r}{r^2}+\frac{(2\,r+1)\,{\sigma_0}^{r+1}}{r^2(r+1)^2}\right] \tag{18}$$

When σ_m is large in comparison with σ_0, we can neglect small quantities and (18) becomes

$$\frac{H}{W}=\frac{18E}{{\sigma_m}^3}\sum_{r=2}^{r=n}\beta_r\left[\frac{{\sigma_m}^{r+1}}{(r+1)^2}-\frac{\sigma_0\,{\sigma_m}^r}{r^2}\right] \tag{19}$$

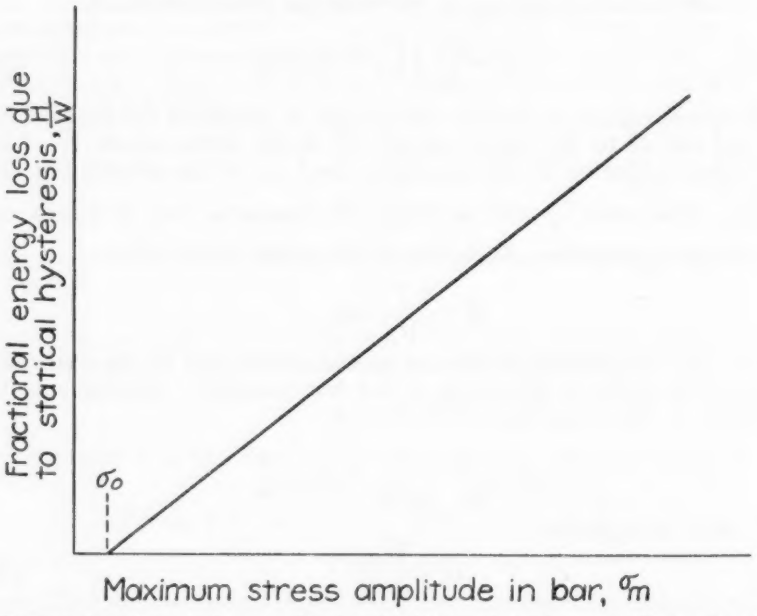

FIGURE 2.—*A typical curve showing the linear dependence of the fractional energy loss due to statistical hysteresis on the difference in the stress amplitudes* $\sigma-\sigma_0$

In practice, equation (19) is sufficiently accurate since $\frac{H}{W}$ can be accurately determined only for large values of σ_m (that is, of L_m). To determine the constants β_r in equation (17), express the experimentally determined values of $\frac{H}{W}$ as a power series in σ_m, and substitute in equation (19). Then equate the coefficients of like powers of σ_m, after experimentally obtaining the value of σ_0 as the maximum value of σ_m for which $\frac{H}{W}$ is practically zero. There will be some indefiniteness in the determination of σ_0, but the errors arising from this source are not serious.

Plotting the experimental results shows that the relation between $\frac{H}{W}$ and σ_m is very closely linear as illustrated in Figure 2. This gives

$$\frac{H}{W}=0,\ \sigma_m \leqq \sigma_0$$
$$\frac{H}{W}=A\ (\sigma_m-\sigma_0),\ \sigma_m \geqq \sigma_0 \tag{20}$$

Substituting in equation (19)

$$\beta_2=\tfrac{7}{16}\beta_3\sigma_0$$
$$\beta_4=\beta_5=0$$

we find

$$\frac{H}{W}=\frac{18}{16}\beta_3\left[\sigma_m-\sigma_0-\frac{7}{4}\frac{\sigma_0^2}{\sigma_m}\right]E \tag{21}$$

The third term in the parenthesis can be neglected so that equations (20) and (21) are of the same form. Inserting the value of β_2 and β_3 in equation (17) we obtain

$$f\ (\sigma)=0\ \sigma \leqq \sigma_0$$
$$f\ (\sigma)=\beta_3\sigma^3\left[1-\frac{9}{16}\frac{\sigma_0}{\sigma}-\frac{7}{16}\left(\frac{\sigma_0}{\sigma}\right)^2\right] \tag{22}$$

where

$$\frac{9}{8}\beta_3=\frac{A}{E}$$

Introducing the value of σ_m from equation (11) equation (20) may be written

$$\frac{H}{W}=\frac{AalL_m}{I}-B \tag{23}$$
$$B=A\sigma_0$$

Thus, when the load amplitude L_m of the alternating flexure cycles is kept contant, the fractional loss of energy is a linear function of the effective length l of the bar.

The deflections d_m and d_0 of the bar at the point of application of the corresponding loads L_m and L_0 are given by the following equations.

$$d_m=\frac{1}{3}\frac{L_m l^3}{IE}=\frac{1}{3}\frac{\sigma_m l^2}{aE}$$
$$d_0=\frac{1}{3}\frac{L_0 l^3}{IE}=\frac{1}{3}\frac{\sigma_0 l^2}{aE} \tag{24}$$

L_0 is the upper limit of the amplitudes of the load cycles for which no appreciable loss of energy is observed. Substituting the value of $\sigma_m-\sigma_0$ obtained from these equations in equation (20), another expression for the energy loss is obtained.

$$\frac{H}{W}=A^3\frac{3Ea}{l^2}\ (d_m-d_0) \tag{25}$$

If D_m and D_0 are the deflections at the end of the bar corresponding to d_m and d_0 (see fig. 3) and if the ratio of the effective length l to the length s_1 of the bar is q, it can be shown that

$$\begin{aligned} l &= q\, s_1 \\ d_m &= \frac{2q}{3-q} D_m \\ d_0 &= \frac{2q}{3-q} D_0 \end{aligned} \tag{26}$$

And by substituting for $d_0 - d_m$ from equation (26) in equation (25) that

$$\frac{H}{W} = \frac{6EaA}{(3q-q^2)s_1^2}(D_m - D_0) \tag{27}$$

If q is equal to unity

$$\frac{H}{W} = \frac{3EaA}{s_1^2}(D_m - D_0) \tag{28}$$

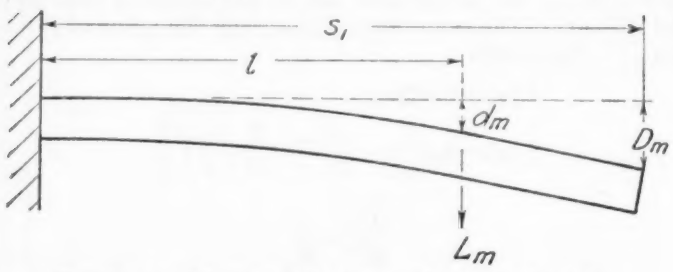

FIGURE 3.—*Diagram of the flexure of a clamped-free bar*

l is the effective length of the bar in flexure under the load L_m.

That is, when the load is applied at the end of the bar the fractional energy loss due to statical hysteresis in the cycles of alternating flexure varies linearly with the maximum deflection D_m. D_0 is the upper limit of the deflection amplitudes of the cycle at which practically no hysteresis is observed. The following relation between σ_0 and D_0, when q is unity, is obtained from equation (24) after obvious substitutions are made

$$\sigma_0 = \frac{3aE}{s_1^2} D_0 \tag{29}$$

2. DURING ALTERNATING FLEXURE PRODUCED BY LATERAL VIBRATION

The expressions for the energy loss due to statical hysteresis in cycles of alternating statical flexure derived above are readily applicable to the loss of energy per cycle in the lateral vibrations of the bar, provided the vibrations are of the fundamental mode. The transfer of expressions from the one case to the other is made possible by the fact that the configuration of a vibrating bar can be approximated with sufficient closeness by a statical deformation of the same bar.[14] It is sufficient for this purpose to deflect the bar by applying

[14] Rayleigh, The Theory of Sound, vol. 1, 2d ed., p. 284.

a single load at a distance from the free end equal to one-fourth of the length of the bar; that is, if the length of the bar is s_1, the effective length l to be chosen is

$$l = \tfrac{3}{4} s_1$$

Let α be the amplitude of the excursions of the end of the bar, W be the energy of deformation of the bar at this amplitude, and H be the loss of energy due to statical hysteresis. The fractional loss of energy per cycle due to statical hysteresis, $\frac{H}{W}$, can then be evaluated by substituting the following quantities into equation (27)

$$q = \tfrac{3}{4}$$
$$\alpha = D_m$$
$$\alpha_0 = D_e$$

This gives

$$\frac{H}{W} = \frac{32}{9} \frac{EaA}{{s_1}^2} [\alpha - \alpha_0] \tag{30}$$

Here α_0 represents the upper limit of the amplitudes of the vibrations which gives practically no damping. But the fractional loss of energy $\frac{H}{W}$ is

$$\frac{H}{W} = \frac{2d\alpha}{\alpha dn}$$

where $\frac{d\alpha}{dn}$ is the decrement of the amplitude per vibration. Hence

$$\frac{2}{\alpha} \frac{d\alpha}{dn} = \frac{32}{9} \frac{Ea}{{s_1}^2} (\alpha - \alpha_0) A \tag{31}$$

Thus, in the lateral vibration of the bar the fractional loss of energy per cycle, due to statical hysteresis, is a linear function of the amplitude of vibration. The relation of α_0 to σ_0 is derived from equations (24) and (26).

$$\sigma_0 = \frac{32}{9} a \frac{E}{{s_1}^2} \alpha_0 \tag{32}$$

III. APPLICATION OF THE THEORY TO A U BAR

In a previous paper,[18] it is shown that the states of deformation of an elongated U bar in vibration and of a vibrating straight clamped-free bar are practically alike. Consider, for example, the frequency of vibration. If the ratio of the median length of the yoke to the total median length of the U bar equals one-tenth, the frequency of vibration of the U bar will be only 0.5 per cent higher than that of a straight clamped-free bar with a length the same as the median length of each arm of the U bar. Thus, all the equations for the statical hysteresis of a clamped-free bar can be applied to an elongated U bar, with only a small error caused by the yoke configuration, provided that the axial or median length of the straight clamped-free bar, measured from the fixed end, is the same as the median length of the arms of the U bar, measured from the mid-point of the yoke. (See fig. 4.)

[18] See footnote 3, p. 635.

IV. APPARATUS AND EXPERIMENTAL PROCEDURE

1. FOR MEASUREMENTS DURING A LOAD CYCLE

The essential features of the apparatus used to measure the statical hysteresis in the alternating flexure of U bars produced by a load cycle are shown in Figure 5. The fork of the U bar A is gripped by the two clamps B and C. A transmitting rod R is attached to clamp B in a direction normal to the axis of the U bar. Forces L act normally at the ends of the transmitting rod R and are of two kinds; first, the weights on the panel P pull the rod downwards and second, the buoyant force of mercury in the basins acting on the floats attached to the end of rod R push it upward. Actually four mercury basins were used although only two are shown in Figure 5. The value of L is varied by varying the load on the panel P.

The lower clamp C is free to rotate about axis ff in the cradle D, which is attached firmly to a heavy base plate E. The arms F extend

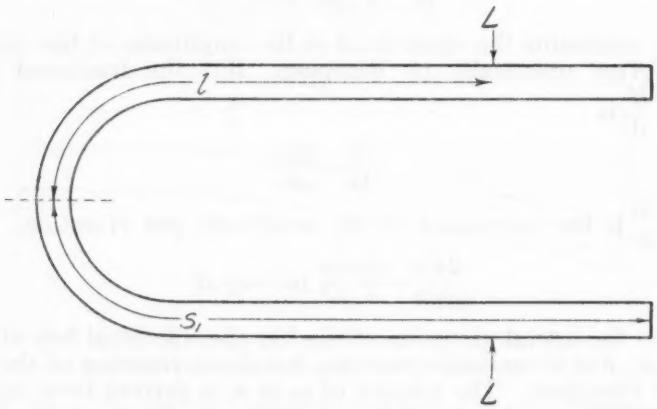

FIGURE 4.—*Diagram of the* U *bar*

out from the lower portion of clamp C and is used to control the direction of the axis of the U bar in space. Before each measurement of the deflection of the U bar is made, F is adjusted by the screw support until the principal axis of the U bar is horizontal. The sensitive spirit level h serves to determine this position. The micrometer M measures the displacement of the upper prong relative to the lower prong, at the points where the load L is applied. The contact between the micrometer and the upper prong is determined electrically. In most of the experiments the error caused by uncertainty of the contact was not greater than 0.0002 mm.

2. DYNAMICAL MEASUREMENT DURING LATERAL VIBRATIONS

For the study of the damping of the vibrations of the U bar, photographic records of the amplitudes of the end excursions were obtained by permitting a beam of light to traverse first a slit in a vane mounted on one of the prongs, then a spherical lens, and finally a cylindrical lens before reaching the photographic paper. This paper was mounted on a rotating wheel whose axis was parallel to the direction of the lateral vibrations of the prongs. Since the beam

of light emerging from the slit was in the form of a ribbon, the cylindrical lens was used to focus the line section of the ribbon to a sharp point. The magnification employed was in the neighborhood of 10.

For these experiments the U bar was clamped at the yoke, in the manner described later in the section on experimental results.

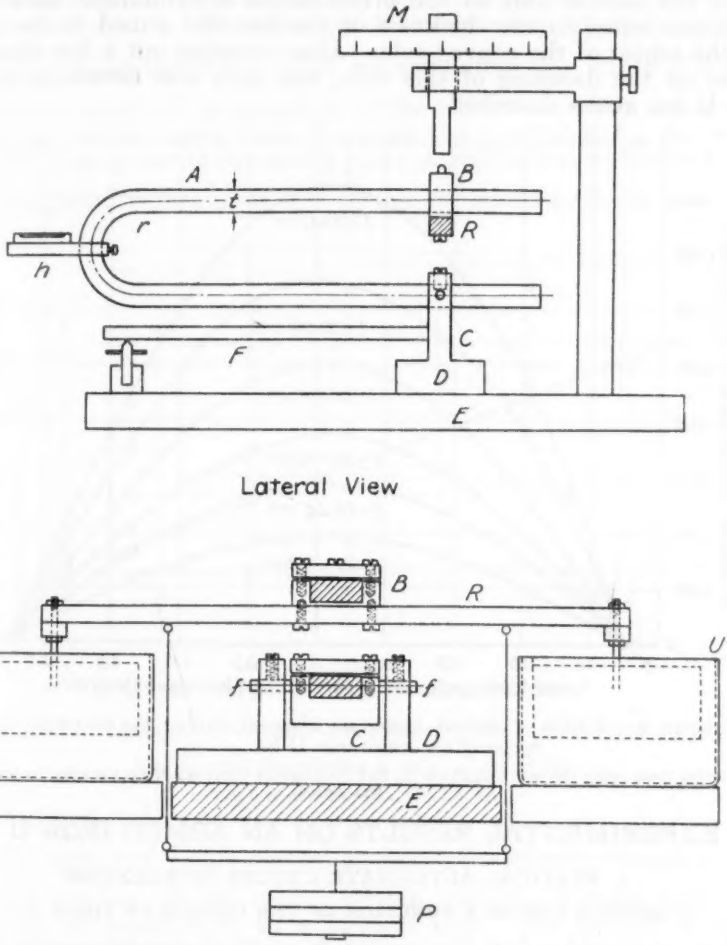

FIGURE 5.—*Diagram of the apparatus used in connection with the statical measurements*

L shows the point of application of the load; *l* is the effective length and s_1, the length.

3. DESCRIPTION OF THE U BAR

The U bar used consisted of a circular yoke and two parallel prongs as shown in Figures 4 and 5. The radius of the yoke was 1.69 cm. The total median length of the bar was 64.30 cm; that is, each arm from the center of the yoke was 32.15 cm in median length. The average thickness $2a$ of the two prongs was 0.829 and

0.825 cm, respectively. The variation in thickness from these mean values was less than ± 0.003 cm. The mean width of the bar was 1.393 cm with variations not exceeding ± 0.002 cm. In the symbols of the paper $s_1 = 32.15$ cm, $a = 0.414$ cm, $b = 1.393$ cm. The bar was made of Armco iron.

In the initital part of the investigation a cylindrical stem of a diameter equal to the thickness of the bar was joined to the yoke at the center of the convex side. After carrying out a few observations on the damping of this fork, the stem was detached, giving the U bar above described.

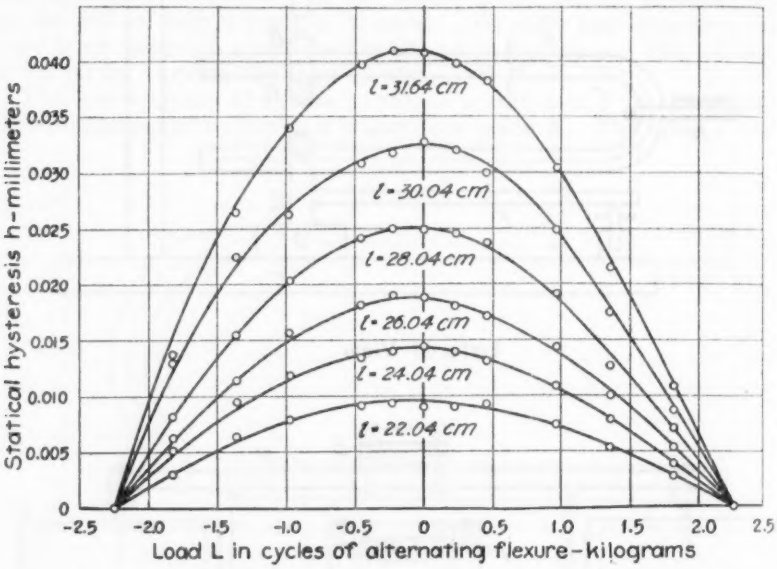

FIGURE 6.—*Values of statical hysteresis observed during the alternate flexure cycles of an armco iron* U *bar*

During these cycles the load amplitude L_m had the constant value of 2.27 kg; the effective length l was varied.

V. EXPERIMENTAL RESULTS ON AN ARMCO IRON U BAR

1. STATICAL ALTERNATE CYCLES OF FLEXURE

(a) ENERGY LOSS AS A FUNCTION OF THE LENGTH OF THE U BAR

Let us consider first the results of statical experiments in which L_m, the amplitude of the alternating load, was kept constant at 2.27 kg. The effective length l of the U-bar arms was changed from 31.64 cm to 30.04, 28.04, 26.04, 24.04, and 22.04 cm in turn.

In performing the cycle we started with $L = 0$, increasing to $L = +L_m$, then decreasing to $L = -L_m$ and finally increasing to $L = 0$. Each alternating load cycle was repeated three times. The elastic lag or "the width of the hysteresis loop" was determined as the difference of the deflections at any load L for increasing and decreasing values. It was found that the after effect, or the difference in deflection for the initial and final zero loads in these various cycles was practically zero. It was therefore considered safe to assume that the elastic lag was due almost exclusively to statical hysteresis and

that hysteresis due to elastic afterworking was practically absent. The results are given in Table 1 where the statical hysteresis h is given corresponding to each load L of the load cycle.

The data in Table 1 are plotted in Figure 6, where the circles are observed values. The areas under these curves give the loss of energy H due to statical hysteresis in the two arms of the U bar for the various load cycles. The values of H in ergs are given in Table 2.

We now need the values of W for computing $\frac{H}{W}$, where W is the maximum energy of deformation of the whole bar when L has the value L_m. It is known that W equals the product $d_m L_m$, d_m being the deflection of the U bar at the point of application of the load L_m. The calculated values of W and $\frac{H}{W}$ are also given in Table 2.

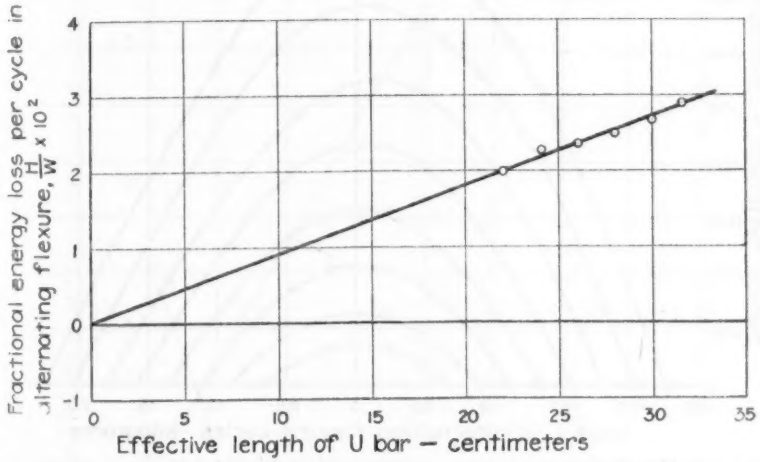

FIGURE 7.—*Variation during alternating flexure cycles of the fractional energy loss* $\frac{H}{W}$ *with the effective length l of the* U *bar*

The load amplitude L_m was 2.27 kg.

These values of $\frac{H}{W}$ are plotted against l, the effective length of the arms of the bar, in Figure 7. Within the experimental error the data can be represented by a straight line. The method of least squares gives for the equation of the line

$$\frac{H}{W} \times 10^{-2} = 0.092l - B \qquad (33)$$

$$B = 0.000$$

Owing to the great extrapolation necessary there is considerable uncertainty in the value of B, and this experiment may be said to leave its value indeterminate. Equation (33) agrees with theoretically derived equation (23) and, therefore, the results of the experiment are not inconsistent with the hysteresis law as given by equation (22).

(b) ENERGY LOSS AS A FUNCTION OF THE MAXIMUM DEFLECTION

Let us consider next the results of experiments in which the effective length l was kept constant at the value 31.64 cm, practically the length of the arms of the U bar. The load amplitude, L_m, of the alternating flexure cycles was varied from 2.268 kg to 2.041, 1.814, 1.588, 1.361, 1.134, 0.907, and 0.690 kg, respectively. For these conditions the statical hysteresis h was determined. These values are given in Table 3, for each load L of the load cycle. The data of this table are presented in the plots of Figure 8 in which the circles repre-

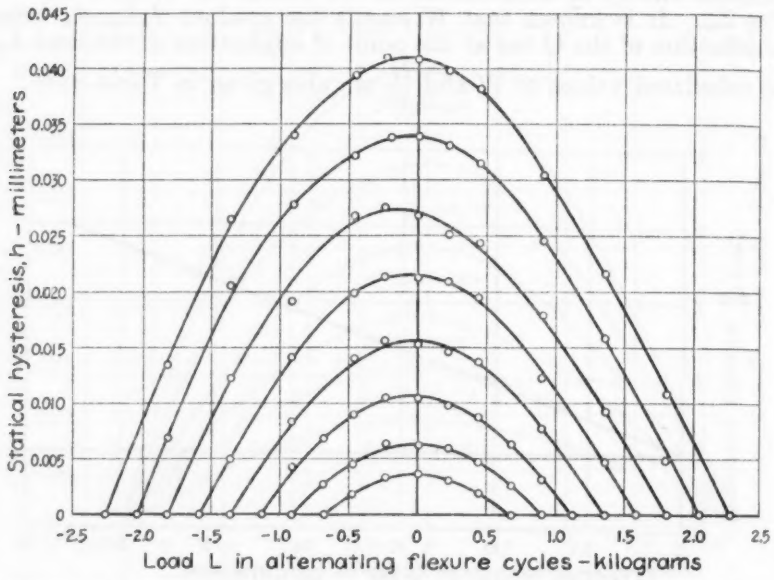

FIGURE 8.—*Experimental values of the statical hysteresis in alternate flexure cycles of an Armco iron U bar 31.64 cm in effective length for various load amplitudes* L_m

sent observed values. The values of H in ergs, as calculated from the areas under these curves are entered in Table 4 as well as the values of $d_m(=D_m$, because the load was applied at the end of the bar)L_m, and the computed values of W and $\frac{H}{W}$.

The values of $\frac{H}{W}$ given in Table 4 are plotted against D_m in Figure 9. Within the experimental error the data can be represented by a straight line which meets the axis at a deflection $D_m=D_o$. The method of least squares gives for the equation of the line

$$\frac{H}{W}\times 10^2 = 1.70\ (D_m - D_o) \tag{34}$$

$$D_o = 0.04\ mm$$

This is in agreement with the theoretical result, equation (23), and therefore the results of the experiment are consistent with the hysteresis law as given by the equation (22).

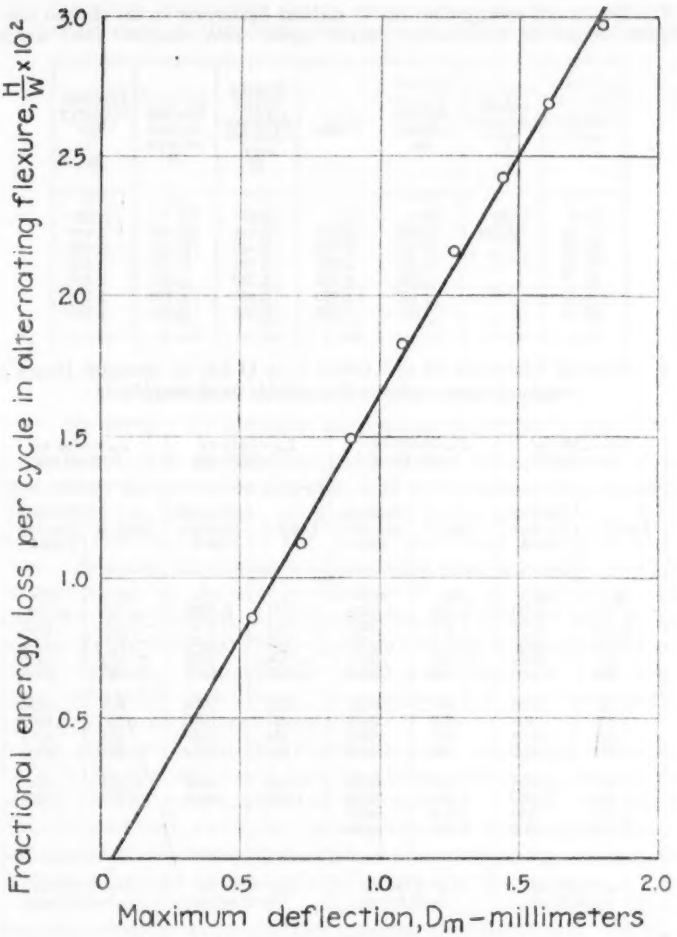

FIGURE 9.—*Variation of the fractional loss of energy* $\frac{H}{W}$ *during alternating flexure cycles of an Armco iron* U *bar 31.64 cm in effective length as a function of the maximum deflection* D_m

TABLE 1.—*Statical hysteresis in an Armco iron* U *bar of variable length in alternating flexure cycles with constant load amplitude*

L_m, kg l, cm	2.27 31.64	2.27 30.04	2.27 28.04	2.26 26.04	2.27 24.04	2.27 22.04
Load L	Statical hysteresis h					
kg	*mm*	*mm*	*mm*	*mm*	*mm*	*mm*
−2.268	0.0000	0.0000	0.0000	0.0000	0.0000	0.0000
−1.814	.0136	.0129	.0082	.0062	.0052	.0030
−1.361	.0265	.0225	.0154	.0115	.0095	.0064
−.907	.0340	.0263	.0204	.0157	.0119	.0078
−.453	.0396	.0309	.0242	.0181	.0135	.0091
−.227	.0410	.0318	.0250	.0190	.0140	.0095
.000	.0408	.0328	.0249	.0188	.0146	.0090
.227	.0398	.0321	.0246	.0181	.0140	.0091
.453	.0382	.0300	.0237	.0172	.0132	.0093
.907	.0304	.0249	.0192	.0145	.0109	.0074
1.361	.0216	.0174	.0126	.0101	.0078	.0053
1.814	.0109	.0087	.0071	.0053	.0039	.0028
2.268	.0000	.0000	.0000	.0000	.0000	.0000

TABLE 2.—*Fractional energy loss due to statical hysteresis in an Armco iron* U *bar of variable length in alternating flexure cycles with constant load amplitude*

Effective length	Load amplitude L_m	Deflection d_m	$L_m d_m$	Energy of the deformation (in ergs) W	Hysteresis loss (in ergs) H	Fractional energy loss $\frac{H}{W}$
cm	*kg*	*mm*		$\times 10^2$		$\times 10^{-2}$
31.64	2.268	1.804	4.090	4,010	11,900	2.968
30.04	----------	1.545	3.502	3,440	9,310	2.708
28.04	----------	1.257	2.850	2,791	7,130	2.555
26.04	----------	1.005	2.210	2,232	5,352	2.398
24.04	----------	.782	1.773	1,747	4,020	2.300
22.04	----------	.611	1.385	1.356	2,698	1.988

TABLE 3.—*Statical hysteresis in an Armco iron* U *bar of constant length in alternating flexure cycles with variable load amplitude*

L_m=2.268 kg l=31.54 cm		L_m=2.041 kg l=31.64 cm		L_m=1.814 kg l=31.64 cm		L_m=1.588 kg l=31.54 cm	
Load L	Statical hysteresis h	Load L	Statical hysteresis h	Load L	Statical hysteresis h	Load L	Statical hysteresis h
kg	*mm*	*kg*	*mm*	*kg*	*mm*	*kg*	*mm*
−2.268	0.0000	−2.041	0.0000	−1.814	0.0002	−1.588	0.000
−1.814	.0136	−1.814	.0068	−1.361	.0123	−1.361	.0050
−1.361	.0265	−1.361	.0206	−.907	.0192	−.907	.0131
−.907	.0340	−.907	.0278	−.454	.0268	−.454	.0198
−.453	.0396	−.454	.0322	−.227	.0275	−.227	.0213
−.227	.0410	−.227	.0337	.000	.0268	.000	.0213
.000	.0408	.000	.0339	.227	.0252	.227	.0207
.227	.0398	.227	.0331	.454	.0245	.454	.0195
.453	.0382	.454	.0315	.907	.0178	.907	.0123
.907	.0304	.907	.0246	1.361	.0093	1.361	.0047
1.361	.0216	1.361	.0159	1.814	.0000	1.588	.0000
1.814	.0109	1.814	.0049				
2.268	.0000	2.041	.0000				

L_m=1.361 kg l=31.64 cm		L_m=1.134 kg l=31.64 cm		L_m=0.907 kg l=31.64 cm		L_m=0.680 kg l=31.64 cm	
Load L	Statical hysteresis h	Load L	Statical hysteresis h	Load L	Statical hysteresis h	Load L	Statical hysteresis h
kg	*mm*	*kg*	*mm*	*kg*	*mm*	*kg*	*mm*
−1.361	0.0000	−1.134	0.0000	−0.907	0.0000	−0.680	0.0000
−.907	.0083	−.907	.0043	−.680	.0027	−.454	.0019
−.454	.0141	−.680	.0068	−.454	.0046	−.227	.0034
−.227	.0156	−.454	.0090	−.227	.0063	.000	.0036
.000	.0152	.227	.0105	.000	.0062	.227	.0032
+.227	.0146	.000	.0105	.227	.0059	.454	.0020
.454	.0138	.227	.0099	.454	.0048	.680	.0000
.907	.0078	.454	.0088	.680	.0026		
1.361	.0000	.680	.0063	.407	.0000		
		.907	.0032				
		1.134	.0000				

TABLE 4.—*Fractional energy loss due to statical hysteresis in an Armco iron* U *bar of constant length in alternating flexure cycles with variable load amplitude*

Effective length	Load amplitude L_m	Deflection $d_m(=D_m)$	$L_m d_m$	Energy of deformation (in ergs) W	Hysteresis loss (in ergs) H	Fractional energy loss $\frac{H}{W}$
cm	*kg*	*mm*		$\times 10^3$		$\times 10^{-4}$
31.64	0.680	0.542	0.368	361	303	0.838
	.907	.722	.654	641	721	1.122
	1.134	.903	1.023	1,022	1,526	1.494
	1.361	1.083	1.475	1,445	2,654	1.836
	1.588	1.262	2.002	1,961	4,221	2.150
	1.814	1.443	2.617	2,565	6,187	2.412
	2.041	1.624	3.315	3,248	8,720	2.685
	2.268	1.804	4.090	4,010	11,900	2.968

2. ENERGY LOSS DURING VIBRATION

(a) EFFECT OF METHOD OF SUPPORTING THE U BAR

In the experiments on the damping of the vibrations of the U bar it was necessary to consider the effect of the method of supporting the bar. The various methods of support were as follows: First, the stem initially forming part of the yoke was firmly clamped to a heavy rigid base. Second, the stem was inserted into a rubber bed, the bed being surrounded by a metal cylinder 5 cm in diameter, which in turn was firmly attached to a heavy base. Third, the U bar was hung vertically downward from the stem being supported by a strand of ordinary thread. Fourth, the stem was detached and the U bar was hung vertically downward by means of a narrow wooden vise gripping the yoke at its mid portion.

With the support as in the third method, damping measurements were made with the unloaded bar, and then with a 4 g weight attached successively to the extremities of the prongs. With the support as in the fourth method, damping measurements were made both before and after the statical tests discussed in the preceding section, in order to determine whether these tests affected the damping.

The double amplitudes of vibration, 2α, measured from the photographic records were plotted against the number of vibrations n. The smooth curves drawn through these plotted values were taken to represent the damping curve of the vibrations. The double amplitudes of vibration as read from these curves are given in Table 5 for the four methods of supporting the U bar. The data in columns 3a and 3b in the table headed 3, refer to the third method of support, column 3 being for the case in which the prongs were unloaded, and columns 3a and 3b for that in which the prongs were loaded. The data in columns 4 and 4a refer to the fourth method of support, the first before, and the latter after, the statical tests.

In order to obtain the fractional energy loss per cycle for any particular cycle which is

$$\frac{2}{a}\frac{d\alpha}{dn}$$

the slopes $2\frac{d\alpha}{dn}$ of the damping curves were determined graphically and were plotted against α. A smooth curve was drawn in each case, thus obtaining the curve of decrements. The curve thus

obtained from the data for the fourth method of supporting the U bar is given in Figure 10. Division of the ordinate by the abscissa of the decrement curve gives, for any desired value of the amplitude a, the fractional loss in energy. The values thus obtained are presented in Table 6.

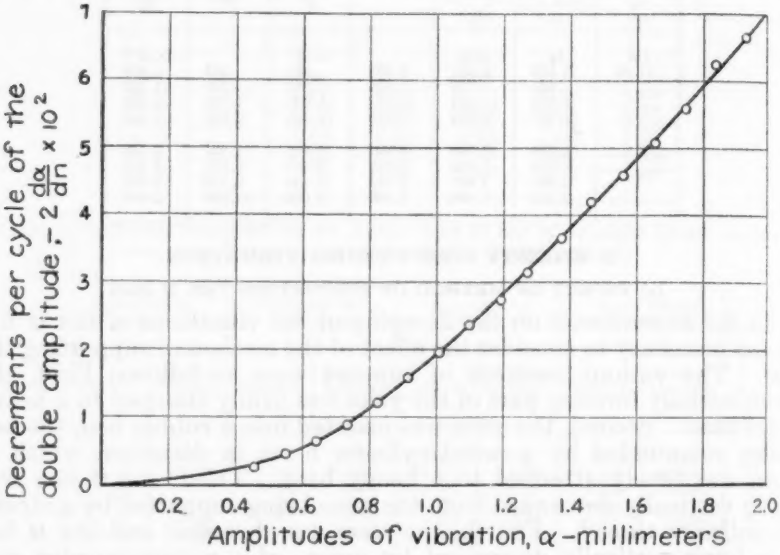

FIGURE 10.—*A typical curve showing the decrement per complete cycle at various amplitudes of vibration of the freely vibrating* U *bar*

TABLE 5.—*Double amplitudes of vibration of the Armco iron* U *bar for various methods of support*

Vibration No.	Method of support						
	1	2	3	3a	3b	4	4a
	Double amplitude of the end excursions 2a						
n	*mm*	*mm*	*mm*	*mm*	*mm*	*mm*	*mm*
0	3.200	4.520	4.480	4.065	4.305	5.310	3.995
10	2.760	3.765	3.760	3.485	3.635	4.402	3.397
20	2.432	3.250	3.265	3.033	3.132	3.712	2.950
30	2.175	2.848	2.875	2.685	2.742	3.202	2.619
40	1.972	2.543	2.570	2.400	2.450	2.809	2.345
50	1.808	2.295	2.335	2.182	2.210	2.480	2.135
60	1.670	2.090	2.140	2.003	2.018	2.248	1.940
70	1.550	1.922	1.972	1.855	1.852	2.045	1.790
80	1.452	1.782	1.832	1.730	1.718	1.880	1.665
90	1.368	1.661	1.720	1.618	1.600	1.748	1.562
100	1.295	1.560	1.615	1.520	1.520	1.632	1.462
120	1.172	1.410	1.437	1.375	1.375	1.453	1.327
140	1.072	1.293	1.310	1.255	1.252	1.320	1.222
160	.995	1.196	1.218	1.160	1.148	1.210	1.134
180	.930	1.113	1.138	1.085	1.038	1.118	1.060
200	.876	1.050	1.070	1.022	1.002	1.038	.992
220	.828	.993	1.008	.960	.948	.975	.928
240	.785	.923	.958	.905	.898	.930	.873
260	.747	.868	.913	.860	.853	----------	.823
280	----------	.819	.872	.823	.813	----------	.783
300	----------	.778	.840	.788	.775	----------	.752
320	----------	.742	.808	.760	.738	----------	.722

TABLE 6.—*Fractional loss of energy per cycle of lateral vibration of the Armco iron* U *bar*

Amplitude α	Method of support							
	1	2	3	3a	3b	4	4a	Average
	Fractional loss in energy $\frac{2}{\alpha}\frac{d\alpha}{dn}\times 10^2$							
mm								
2.0	4.20	4.02	3.72	3.68	3.68	3.60	3.76	3.84
1.9	4.00	3.72	3.52	3.50	3.54	3.46	3.60	3.62
1.8	3.78	3.50	3.30	3.32	3.38	3.32	3.42	3.44
1.7	3.54	3.28	3.08	3.14	3.22	3.16	3.28	3.24
1.6	3.30	3.06	2.86	2.94	3.04	3.00	3.08	3.04
1.5	3.04	2.82	2.66	2.74	2.88	2.84	2.88	2.84
1.4	2.80	2.62	2.44	2.56	2.68	2.68	2.68	2.64
1.3	2.56	2.32	2.26	2.36	2.48	2.52	2.50	2.42
1.2	2.32	2.18	2.04	2.16	2.30	2.32	2.30	2.22
1.1	2.06	1.96	1.86	1.94	2.08	2.14	2.08	2.02
1.0	1.84	1.76	1.64	1.76	1.76	1.80	1.86	1.78
.9	1.62	1.58	1.46	1.56	1.62	1.68	1.64	1.60
.8	1.40	1.34	1.24	1.34	1.40	1.42	1.40	1.36
.7	1.18	1.12	1.06	1.12	1.14	1.12	1.14	1.12
.6	.94	.94	.82	.86	.88	.86	.88	.88
.5	.70	.74	.62	.66	.68	.68	.64	.64
.4	.54	.54	.42	.42	.44	.44	.42	.44
.3	.30	.36	.30	.26	.30	.30	.30	.30

When the data in the various columns in Table 6 for a given amplitude α are examined one finds that individual values differ as much as 10 per cent from the average value. Since the data in column 3 were obtained with a support possessing practically no elastic coupling with the fork, it is expected that the values of the fractional loss of energy given in column 3 will be smaller than those in the other columns. Actually this is the case, but the variation is less than 4 per cent from the average value. On the other hand, the data may have errors as high as 5 per cent due to slight shifting of the vibrating U bar from experiment to experiment causing variations in the value of the magnification of the optical system from the value used in reducing the data. Since the experimental error is of about the same order of magnitude as the observed average effect of the various methods of supporting the bar, it appears reasonable to ignore the effect of the various supports on the energy loss. The average value of the energy loss is therefore used in making the final calculations.

(b) ENERGY LOSS PER CYCLE

Values of the average fractional loss in energy given in Table 6 are plotted against the amplitude α in Figure 11. For amplitudes equal to or greater than 0.9 mm, these data fall on a straight line which meets the axis at the amplitude $\alpha=\alpha_0$. The points at the smaller amplitudes are neglected in determining this line because (*a*) the experimental errors are relatively very large at these amplitudes and (*b*) primarily because the theory which has been developed applies only to large values of the stress amplitude (equation (19)). The equation of this line, determined by least squares, is as follows:

$$\frac{2}{\alpha}\frac{d\alpha}{dn}\times 10^2 = 2.02\ (\alpha-\alpha_0) \tag{35}$$

$$d_0 = 0.10\ mm$$

This is in agreement with equation (31) and therefore the results of the experiment are consistent with the hysteresis law of the equation (22).

VI. COMPARISON OF THE EXPERIMENTAL RESULTS

Thus far we have seen that the results of the three typical tests considered are qualitatively in good agreement with the theory.

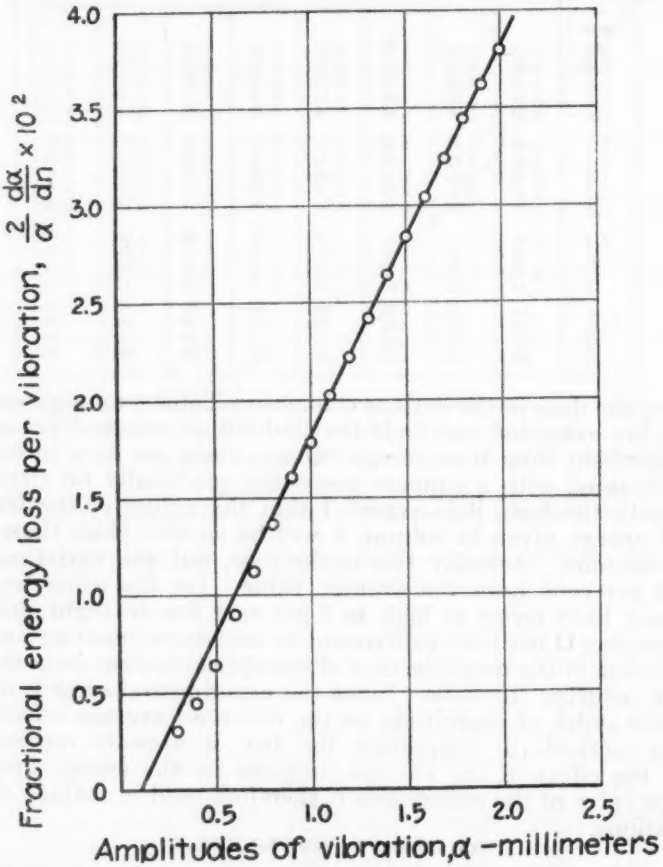

FIGURE 11.—*Variation of the fractional energy loss per complete vibration with amplitude of vibration during the lateral vibration of an Armco iron* U *bar*

That is, tests of each type are consistent with equations (22). It now remains to see how well the various results agree quantitatively.

It is seen that a comparison of equation (23) and the experimental results expressed in equation (33) gives the first of the following relations. A similar comparison of the theoretically derived equations (28) and (31) with the corresponding experimental results in equations (34) and (35) gives the last two of the relations below.

$$\frac{aL_mA}{I}=0.92\times10^{-3},\ (L_m=2.27\text{ kg})$$

$$\frac{3\ EaA}{{s_1}^2} = 1.70 \times 10^{-1} \text{ per cm}$$

$$\frac{32\ EaA}{9\ {s_1}^2} = 2.02 \times 10^{-1} \text{ per cm}$$

The first two relations are based on the two series of results obtained statically and the third on the results obtained from the vibrating U bar. Introducing the numerical values of constants

$$s_1 = 31.64 \text{ cm}$$

$$E = 2.03 \times 10^6 \text{ kg per cm}^2$$

$$a = 0.413 \text{ cm}$$

$$b = 1.393 \text{ cm}$$

$$I = 6.25 \times 10^{-2} \text{ cm}^4$$

it is found that the corresponding determinations of A are

$$\begin{aligned} A &= 0.66 \times 10^{-4} \text{ cm}^2 \text{ per kg} \\ A &= 0.68 \times 10^{-4} \text{ cm}^2 \text{ per kg} \\ A &= 0.71 \times 10^{-4} \text{ cm}^2 \text{ per kg} \end{aligned} \qquad (36)$$

Next for the determination of the small stress σ_0 below which practically no energy loss occurs, we have the three independent relations

$$\sigma_0 = \frac{B}{A};\ B = 0.00 \times 10 B^{-2}$$

$$\sigma_0 = \frac{3\ aE}{{s_1}^2} D_0;\ D_0 = 0.4 \times 10^{-2} \text{ cm}$$

$$\sigma_0 = \frac{32}{9}\ a\ \frac{E}{{s_1}^2 \alpha_0}\ \alpha_0 = 1.0 \times 10^{-2} \text{ cm}$$

These have been, respectively, obtained from the theoretical results in equations (23), (29), and (32) and the experimental results given in equations (33), (34), and (35). Calculation gives, using the constants given in the previous paragraph,

$$\begin{aligned} \sigma_0 &= 00 \text{ kg per cm}^2 \\ \sigma_0 &= 10 \text{ kg per cm}^2 \\ \sigma_0 &= 27 \text{ kg per cm}^2 \end{aligned} \qquad (37)$$

Hence, we see that the results of the three typical experiments are qualitatively in agreement, since they all give practically the same value for A. Only in the case of σ_0 is the discrepancy between the various determinations considerable. This is to be expected, since σ_0 was obtained by extrapolations of considerable uncertainty from test to test. As a probable value we suggest $\sigma_0 = 20$ kg per cm^2, ignoring the value of $\sigma_0 = 0$ since the extrapolation by which it was obtained has by far the greatest uncertainty.

We, therefore, conclude that the agreement between these three typical tests shows that the theory given furnishes an adequate basis for determining the statical hysteresis of materials of this type by measurement of the decrement of freely vibrating bars.

VII. LAW OF STATICAL HYSTERESIS IN ARMCO IRON

On the basis of the theory developed and the experimental results obtained the law of statical-hysteresis in Armco iron for stresses at least up to 600 kg per cm² appears to be of the form

$$f(\sigma)=0 \quad \sigma \leqq \sigma_0$$

$$f(\sigma)=\beta_3\sigma^3\left[1-\frac{9}{16}\frac{\sigma_0}{\sigma}-\frac{7}{16}\left(\frac{\sigma_0}{\sigma}\right)^2\right] \tag{38}$$

The value of σ_0 was found to be 20 kg per cm². From equation (22)

$$\beta_3=\frac{8}{9}\frac{A}{E}$$

With the mean value of A 0.68×10^{-4} cm² per kg, the numerical value of β_3 now becomes

$$\beta_3=2.91\times10^{-11} \text{ cm}^4 \text{ per kg}^2$$

or

$$\beta_3=2.91\times10^{-5} \text{ ergs cm}^3 \text{ per kg}^3 \tag{39}$$

The results on hysteresis loss in Armco iron as given in previous papers[16] were obtained with a bar cut from the same sample as the present one under discussion. In these papers it was assumed that

$$f(\sigma)=\frac{1}{3}\beta\sigma_r^3 \tag{40}$$

where

$$\beta=1.15\times10^{-5} \text{ ergs cm}^3 \text{ per kg}^3$$

and σ_r represents the range of stresses in the cycles, the cycles being alternate or otherwise. Putting

$$\sigma_r=2\sigma$$

it follows that

$$\beta_3=\frac{8}{3}\beta$$

or in the symbols of this report (40) becomes

$$f(\sigma)=\beta_3\sigma^3 \tag{41}$$

where

$$\beta_3=3.07\times10^{-5} \text{ ergs cm}^3 \text{ per kg}^3$$

Comparing the expressions (38, and (41), the values of β_3 are seen to be substantially equal, but the threshold stress σ_0 does not appear in equation (41). This absence of σ_0 is explained by the fact that the method of calculations adopted in the previous papers and the lack of sufficient data obscured the presence of a threshold stress in the energy loss due to statical hysteresis.

WASHINGTON, March 19, 1932.

[16] See footnotes 1 and 2, p. 635.

AN UNRECOGNIZED PROPERTY OF THE REVERSIBLE PENDULUM

By Paul R. Heyl

ABSTRACT

In a reversible pendulum which carries two planes and is supported from either plane in turn upon the same knife-edge, it is found that the correction for a circularly rounded knife-edge eliminates itself.

The time of swing t of a simple pendulum whose length is equal to the distance between the two planes of support of a reversible pendulum of times of swing T_1 and T_2 is given by the well-known formula

$$t^2 = \frac{T_1^2 h_1 - T_2^2 h_2}{h_1 - h_2} \tag{1}$$

where h_1 and h_2 are the distances from the center of gravity to the point of support in the two positions of the reversible pendulum.

The nature of this formula is such that it brings about a self-eliminating effect in the case of certain corrections to which T_1 and T_2 may be subject.

Let there be corrections ΔT_1 and ΔT_2 applied to T_1 and T_2 according to the following formulas:

$$\left.\begin{aligned} T_1' &= T_1 (1 + \Delta T_1) \\ T_2' &= T_2 (1 + \Delta T_2) \end{aligned}\right\} \tag{2}$$

What must be the form of ΔT_1 and ΔT_2 in order that the value of t shall be unaltered by applying these corrections?

The condition to be fulfilled is evidently

$$T_1^2 (1 + \Delta T_1)^2 h_1 - T_2^2 (1 + \Delta T_2)^2 h_2 = T_1^2 h_1 - T_2^2 h_2 \tag{3}$$

Expanding and neglecting the second powers of ΔT_1 and ΔT_2, and assuming that the reversible pendulum is so closely adjusted that T_1 is nearly equal to T_2, we obtain the following condition:

$$\frac{\Delta T_1}{\Delta T_2} = \frac{h_2}{h_1} \tag{4}$$

In other words, the corrections must be inversely proportional to the h distances.

Now it happens that the correction for a circularly rounded knife-edge is exactly of this form. This correction is given by the formula

$$T' = T\left(1 + \frac{\rho}{2h}\right) \tag{5}$$

where ρ is the radius of curvature of the knife-edge.

The correction for the rounded knife-edge to be applied to either T may be quite large under conditions likely to occur in practice. For example, with a seconds pendulum the values of h_1 and h_2 may be of the order of 750 and 250 mm, while a value of 0.01 mm for ρ may often be found. The corrections for T_1 and T_2 will be, respectively, about 7 and 20 parts per 1,000,000, yet the value of t remains completely unaffected.

WASHINGTON, March 26, 1932.

5 Co. F.

RP445

A METHOD FOR THE DETERMINATION OF COBALT IN MAGNET AND HIGH-SPEED TOOL STEELS

By James I. Hoffman

ABSTRACT

A method for the accurate determination of cobalt in steel is described. Most of the iron is removed by extraction with ether; chromium, vanadium, etc., are eliminated by precipitation with sodium hydroxide and peroxide; the iron still remaining and the copper are precipitated by cupferron in a dilute hydrochloric-acid solution, and the cobalt is precipitated in the filtrate by α-nitroso-β-naphthol. Cupferron does not interfere in the precipitation of cobalt by α-nitroso-β-naphthol, and a method of testing the latter reagent is given. Quantitative data are presented which show the amount of cobalt that remains with the iron in an ether extraction and in a precipitation of iron by cupferron. Copper, chromium, vanadium, and tungsten are incompletely precipitated by α-nitroso-β-naphthol. With the exception of a small part of the copper all of these are removed in the preliminary separations, and a method for the elimination of the slight interference of copper is given.

CONTENTS

	Page
I. Introduction	659
II. Method for the determination of cobalt	660
III. Discussion of the method	664
1. Extraction of the iron with ether	664
2. Precipitation with cupferron	664
3. Precipitation with α-nitroso-β-naphthol and ignition of the precipitate	665
(*a*) General discussion	665
(*b*) Testing the reagent	665
(*c*) Interfering substances	666
(*d*) Ignition of the precipitate	666
4. Possible sources of error	667
IV. Application of the method	668
V. Acknowledgment	668

I. INTRODUCTION

In 1921 the author in collaboration with Dr. G. E. F. Lundell published a method for umpire determinations of cobalt and nickel in cobalt steels.[1] Briefly stated, the following steps are involved: (1) Dissolving the sample in hydrochloric acid and oxidizing tungsten and iron by means of nitric acid; (2) removing tungstic acid and recovering any cobalt in it; (3) separating most of the iron by means of ether; (4) separating chromium and vanadium by oxidizing with potassium persulphate, twice precipitating iron, cobalt, nickel, etc., with sodium hydroxide, and filtering; (5) dissolving the precipitate, and eliminating copper by precipitation with hydrogen sulphide; (6) after expelling hydrogen sulphide from the filtrate, removing the iron which still remains, by twice precipitating it with ammonium hydroxide and filtering; (7) determining nickel and cobalt in the

[1] J. Ind. Eng. Chem., vol. 13, p. 540, 1921.

filtrate by electrolysis; (8) recovering the samll amount of cobalt which always remains in the electrolyte; and (9) separating nickel from cobalt by the use of dimethylglyoxime or α-nitroso-β-naphthol.

This method gives accurate results if properly applied, but it obviously requires too much time for use in the average laboratory excepting for standardization. Other methods, for example, those involving the basic acetate separation for the removal of iron and subsequent precipitation of nickel and cobalt by ammonuim sulphide, are equally time consuming and usually less accurate. The cyanide method is applicable in special cases but is usually employed only in routine work.

During an investigation of the zinc-oxide method for separating cobalt from iron and certain other constituents of steel,[2] it was found necessary to separate a few tenths of a milligram of cobalt from 1 to 2 g of iron. This was accomplished by extracting most of the iron with ether and then precipitating the remainder of the iron in the acid extract by the use of cupferron, which does not precipitate cobalt. Without destroying the excess of cupferron, the cobalt was precipitated in the filtrate by α-nitroso-β-naphthol and determined by igniting to the oxide, reducing in hydrogen, and weighing as the metal. This forms the basis of the following method, in which it is necessary to remove iron, copper, molybdenum, chromium, zirconium, titanium, vanadium, tin, and tungsten because these are precipitated either wholly or in part by α-nitroso-β-naphthol. (See Sec. III, 3 (c).)

II. METHOD FOR THE DETERMINATION OF COBALT

Transfer 1.000 g of sample to a 400 ml beaker, cover, add 20 ml of diluted hydrochloric acid (2 + 1),[3] and heat until solution is complete. Remove the solution from the source of heat and introduce 2 to 3 ml of diluted nitric acid (1 + 1) without uncovering the beaker. Boil gently for two to three minutes, wash and remove the cover glass and evaporate the solution to a volume of about 5 ml. Tungsten need not be removed even if some separates as tungstic acid. Transfer to a 150 to 300 ml separatory funnel, using small portions of diluted hydrochloric acid (1 + 1) to wash the beaker. The volume of the solution in the separatory funnel should not exceed 30 to 35 ml. Cool to about 5° C., add 50 ml of ether, stopper the funnel, and shake gently for one minute. Let stand in cold water for two to three minutes, and draw off the acid layer into another separatory funnel. Add 10 ml of diluted hydrochloric acid (1 + 1) to the ether extract remaining in the separatory funnel, stopper, and shake thoroughly. Allow to stand for two to three minutes, and drain the acid extract into the other separatory funnel. Add 50 ml of ether to the combined acid extracts in the second funnel, and repeat the extraction with ether and acid as before.

Allow the acid extracts to run into the original beaker, warm (gently and not over a free flame) to expel the ether, and then evaporate nearly to dryness. Add 15 ml of diluted nitric acid (2 + 1) and evaporate just to dryness. Add 50 ml of diluted hydrochloric acid (5 + 95) and heat until the salts are dissolved. If the material contains over

[2] B. S. Jour. Research, vol. 7, p. 883, 1931.

[3] This denotes 2 volumes of hydrochloric acid, specific gravity 1.18, mixed with 1 volume of water. This system of designating diluted acids is used throughout this paper. If no dilution is specified, the concentrated reagent is intended.

10 per cent of cobalt, transfer the solution to a volumetric flask, and take an aliquot portion representing approximately 0.1 g of cobalt.[4] Pour the solution into 150-ml of a 5 per cent solution of sodium hydroxide to which has been added about 2 g of sodium peroxide. Dissolve any tungstic acid that may stick to the beaker in a few drops of the solution of sodium hydroxide and add it to the main solution. Set the beaker on the steam bath and digest for one-half to one hour to destroy the excess of peroxide. Allow to cool, filter through an 11 cm S. & S. blue band or a Whatman No. 42 paper, and wash thoroughly with hot water.

Transfer the paper and precipitate from the funnel to the original beaker, and add 15 ml of diluted hydrochloric acid (2+1). Heat on the steam bath until the precipitate is in solution, stir the paper to a pulp, and add 150 ml of water. Neutralize the hydrochloric acid with ammonium hydroxide, using litmus as indicator, and then add 5 ml of hydrochloric acid. Stir thoroughly and cool to about 10° C. Add a cold 6 per cent water solution of cupferron slowly and with stirring until no further precipitation takes place. An excess of reagent is indicated by the formation of a temporary flash of a fine white precipitate of cupferron which redissolves, as contrasted with the flocculent and insoluble precipitate of the compound of cupferron with the metals. In all of the experiments described in this paper 10 ml of the 6 per cent solution of cupferron was added and found to be sufficient. Allow the precipitate to settle for 10 minutes, then filter through an 11 cm S. & S. blue band or a Whatman No. 42 paper, and wash thoroughly with cold cupferron wash solution.[5] Between 150 and 200 ml of wash solution should ordinarily be used. If more than 0.03 g of cobalt is present, wash the beaker and precipitate five times with cupferron wash solution and reserve the filtrate. Tranfer the paper and precipitate to a 200 ml Erlenmeyer flask, and add 50 ml of cupferron wash solution. Shake the paper to a pulp, filter, catch the filtrate in a separate beaker, and wash thoroughly with cupferron wash solution. This filtrate is caught in a separate beaker because occasionally the first portion is cloudy and must again be poured on the paper.

To the filtrate and washings in a volume of about 400 ml add 15 ml of hydrochloric acid and then one and one-half times as much α-nitroso-β-naphthol[6] as is required to precipitate the cobalt. Never add less than 10 ml. Heat to 60° to 70° C. by digesting on the steam bath for 20 minutes (no longer). Remove from the source of heat, allow to stand about 15 minutes, filter through a No. 589 white band or a No. 40 Whatman paper, and wash with hot diluted hydrochloric acid (1+3) and then with hot water. Transfer the wet paper and precipitate to a porcelain crucible (15 ml capacity for less than 0.05 g of cobalt and 30 ml capacity for larger amounts), heat gently at first, preferably in a muffle furnace, then ignite to constant weight at 750° to 850° C.[7] Weigh as Co_3O_4 which contains

[4] The flask should be well shaken just before withdrawing the aliquot portion so that approximately the proper proportion of tungstic acid is sucked into the pipette. About 0.1 g of cobalt is all that can be conveniently handled. This constitutes a weakness in the method when applied to materials containing high percentages of cobalt. For example, in the analysis of a steel containing 40 per cent of cobalt, a one-fourth aliquot portion, representing 0.25 g of sample, would be taken. Thus, an error of 0.1 mg in the weight of cobalt found would result in an error of 0.04 per cent. (See results Nos. 11 and 21 in Table 1.)

[5] Prepared by adding 20 ml of a 6 per cent water solution of cupferron to 1 liter of cold diluted hydrochloric acid (1+99).

[6] Prepared by dissolving 1 g of the dry reagent in 15 ml of glacial acetic acid and filtering. For the testing of the reagent, see Sec. III, 3 (*b*).

[7] See Sec. III, 3 (*d*).

73.4 per cent of cobalt. In all accurate work in which more than 0.01 g of cobalt is involved, the oxide must be reduced in hydrogen, cooled in an atmosphere of hydrogen, and the cobalt weighed as metal.

If more than 0.1 per cent of copper was present in the original material, the cobalt metal may contain a few tenths of a milligram of copper. To correct for this contamination, dissolve the cobalt metal in hydrochloric acid, dilute the solution so that it contains about 2 ml of hydrochloric acid per 100 ml, and treat with hydrogen sulphide. Filter, wash, and ignite the sulphide in a porcelain crucible. Dissolve the copper oxide in nitric acid, add an excess of ammonium hydroxide, and estimate the amount of copper colorimetrically. The standard and test solutions should be compared as nearly as possible under the same conditions, especially with respect to the concentration of ammonium hydroxide.

Results obtained by this method for the determination of cobalt are illustrated in Table 1.

TABLE 1.—*Results for cobalt obtained by the cupferron-α-nitroso-β-naphthol method*

Analysis No.	Material analyzed		Cobalt found			
	Bureau of Standards standard steels+copper	Cobalt added	Weighed as Co_3O_4	Weighed as metal	Error based on result obtained by ignition in H_2	Error based on result obtained by ignition in H_2 and assuming that exactly 1 g of sample was taken
		g	*g*	*g*	*g*	*Per cent*
1	1 g No. 50a	0.0005	0.0007			
2	do	.0483	.0481	0.0483	0.0000	0.00
3	do	.0528	.0521	.0525	−.0003	−.03
4	do	.1056	.1048	.1059	+.0003	+.03
5	do	.2640	.2640	.2648	+.0008	+.08
6	do	.2640	.2632	.2640	.0000	.00
7	do	.4226	.4216	.4228	+.0002	+.02
8	1 g No. 10d	.1056		.1054	−.0002	−.02
9	0.65 g No. 10d	.3698	.3680	.3700	+.0002	+.02
10	do	.3698	.3684	.3700	+.0002	+.02
11	do	.3698		.3688	−.0010	−.10
12	1 g No. 50a+0.005 g Cu	.0019	.0020			
13	do	.0097	.0098			
14	do	.0097	.0099			
15	do	.0483	.0479	.0483	.0000	.00
16	do	.0528	.0526	.0530	+.0002	+.02
17	do	.1322	.1322	.1326	+.0004	+.04
18	0.3 g No. 50a+0.3 g No. 73	.4226		.4224	−.0002	−.02
19	1 g No. 73+0.005 g Cu	.0097	.0098			
20	do	.0483	.0484	.0485	+.0002	+.02
21	0.3 g No. 50a+0.3 g No. 73+0.005 g Cu	.3960		.3948	−.0012	−.12
22	do	.3960		.3956	−.0004	−.04
23	do	.3960	.3936	.3960	.0000	.00
24	0.3 g No. 50a+0.3 g No. 73+0.01 g Cu	.4226		.4228	+.0002	+.02
25	do	.3698		.3692	−.0006	−.06

In analyses 5, 6, 7, 9, 10, 18, 21, 22, 23, 24, and 25 a one-fourth aliquot portion was taken for the determination. The numbers of the materials given in the second column of the table refer to Bureau of Standards standard samples which have the following percentage compositions:

No. 50a.—C, 0.66; Mn, 0.29; P, 0.02; S, 0.007; Si, 0.48; W, 18.25; Cr, 3.52; V, 0.97; Cu, 0.047; Ni, 0.045; Co, none found.

No. 10d.—C, 0.42; Mn, 0.92; P, 0.088; S, 0.03; Si, 0.063; Cu, 0.01; Ni, 0.002; Cr, 0.006; V, 0.006; Co, none found.

No. 73.—C, 0.31; Mn, 0.28; P, 0.023; S, 0.03; Si, 0.36; Cu, 0.033; Ni, 0.07; Cr, 13.9; V, 0.034; Co, none found.

The cobalt was added in the form of a solution of cobalt sulphate which was transferred to a beaker and evaporated to dryness before the steel chips were added and dissolved. The solution of cobalt sulphate is prepared and standardized as follows:

Dissolve 100 g of cobalt sulphate, $CoSO_4 \cdot 7H_2O$, in 1,500 ml of diluted hydrochloric acid (1+14), and add 250 g of potassium nitrite, KNO_2, dissolved in 500 ml of water. Allow to stand for 10 to 15 minutes, and then add 100 g more of potassium nitrite. After the precipitate has settled, decant the supernatant liquid, and transfer the potassium cobaltinitrite, $2K_3Co(NO_2)_6 \cdot 3H_2O$, to a large filter, and wash a few times with water. Transfer the potassium cobaltinitrite from the filter to the beaker in which the precipitation is made, and add 1,500 ml of diluted hydrochloric acid (1+9). Stir vigorously as the solution is heated to boiling. When the salt is dissolved, cool the solution, add 250 g of potassium nitrite dissolved in 400 ml of water and then add 200 g of potassium acetate, $KC_2H_3O_2$, dissolved in 250 ml of water. Allow the precipitate to settle, filter and wash as before. Transfer the precipitate of potassium cobaltinitrite to the beaker in which the precipitation is made, add 100 ml of diluted sulphuric acid (1+1), heat until the salt is dissolved, dilute to 2,000 ml, and treat with hydrogen sulphide. Allow to stand for four hours and filter. Add 50 ml of sulphuric acid to the filtrate, and evaporate it to a volume of about 200 ml. Add 25 ml of nitric acid, and heat until fumes of sulphuric acid are given off. Cool, dilute to 1 liter, and determine the approximate amount of cobalt in a 5 ml portion of the solution to ascertain the volume of water to be added to obtain a solution of the desired concentration. For this purpose the cobalt may be determined by precipitating it with α-nitroso-β-naphthol and igniting to the oxide, "Co_3O_4."

By following the above directions a liter of solution was obtained which was shown to contain 15.7 g of cobalt. This was diluted to 3 liters, giving a solution with a cobalt content of approximately 5 mg per milliliter. By a special test using formaldehyde and dimethylglyoxime [8] the solution was found to be free from nickel. Iron, chromium, and vanadium were also shown to be absent.

The solution was standardized (1) by electrolysis and (2) by precipitating the cobalt by α-nitroso-β-naphthol, igniting to oxide, reducing and cooling in hydrogen, and weighing as metal. By electrolysis 0.005283 g of cobalt per milliliter was obtained and by ignition in hydrogen 0.005288 g. In computing the results in Table 1 the value obtained by electrolysis was used. In the electrolysis the directions given by Lundell, Hoffman, and Bright, page 335, were followed. The cobalt remaining in the electrolyte was recovered, and correction was made for sulphur which contaminated the deposit.

[8] See F. Feigl and H. J. Kapulitzas, Z. anal. Chem., vol. 82, p. 417, 1930, or G. E. F. Lundell, J. I. Hoffman, and H. A. Bright, Chemical Analysis of Iron and Steel, p. 279. J. Wiley & Sons, New York, 1931.

III. DISCUSSION OF THE METHOD

1. EXTRACTION OF THE IRON WITH ETHER

The conditions given for the preparation of the solution for the extraction of most of the iron with ether are not so rigorous as those usually prescribed, but the separation is sufficiently complete for the purpose. The iron which remained in the acid extract when 1 g samples were used was determined in six cases and was found to average 1.1 mg per determination, with extreme values of 0.7 and 1.8 mg. By making only a single extraction with ether and acid in two similar determinations 6.6 and 7.0 mg of iron, respectively, were found in the acid extracts. In the case of steels containing tungsten it is not necessary to remove the tungstic acid, as this settles into the acid layer or remains in the beaker in which the steel was dissolved. In the subsequent precipitation by sodium hydroxide and sodium peroxide the tungstic acid is dissolved, and any cobalt retained by it is recovered without necessitating a separate operation.[9] Because of the retention of iron by tungstic acid, the iron content of the acid extract is usually slightly higher when tungsten is present than when it is absent.

In the analysis of magnet steels it may be necessary to extract the iron from solutions containing as much as 0.4 g of cobalt. It seemed advisable, therefore, to ascertain whether any cobalt is retained in the ether extract when a double extraction is made as described in the method. The ether extracts obtained in analysis No. 9 in Table 1 were combined, and the ether removed by evaporation. (In this analysis 0.65 g of iron had been separated from 0.37 g of cobalt.) Any reduced iron was oxidized by digestion with a little nitric acid. The iron was then precipitated by cupferron in a volume of 400 ml containing 20 ml of hydrochloric acid. The precipitate was removed by filtration on a large paper and the cobalt determined in the filtrate by precipitating it with α-nitroso-β-naphthol and igniting to oxide. An amount of cobalt estimated to be less than 0.3 mg was found. In a similar way the ether extract obtained in analysis No. 8 was found to contain approximately 0.1 mg of cobalt. To determine the efficacy of this method of separating such a small quantity of cobalt from such a large quantity of iron, 0.3 mg of cobalt was added to 0.6 g of iron and the latter precipitated by cupferron. A determination of cobalt in the filtrate showed between 0.2 and 0.3 mg. If much cobalt is present, more of it will be retained by the iron in the cupferron precipitate. (See Sec. III, 2.)

2. PRECIPITATION WITH CUPFERRON

Cupferron does not interfere in the precipitation of cobalt by α-nitroso-β-naphthol and is therefore a convenient reagent for removing iron and copper previous to the precipitation of cobalt. Iron is completely precipitated in solutions containing as much as 10 ml of hydrochloric acid in 100 ml, but a low concentration of acid is re-

[9] The retention of cobalt by tungstic acid is of little consequence. A magnet steel containing 36 per cent of cobalt and 3.3 per cent of tungsten and a high-speed steel containing 7 per cent of cobalt and 18 per cent of tungsten were dissolved in hydrochloric acid, oxidized with nitric acid and the solution evaporated to dryness. The residues were digested on the steam bath for one-half hour with 50 ml of diluted hydrochloric acid (5+95) and the tungstic acid removed by filtration. After thorough washing with hot diluted hydrochloric acid (5+95), the residues of tungstic acid were examined for cobalt. Less than 0.1 mg was found in either case.

quired for complete precipitation of copper. In preliminary tests it was found that copper was completely precipitated in solutions containing 0.5 ml of hydrochloric acid in 100 ml of solution, but then a little cobalt was carried down by the iron. In two experiments, in each of which the iron was precipitated by adding 10 ml of a 6 per cent water solution of cupferron to 200 ml of solution containing 2 mg of iron, 0.1 g of cobalt, 5 mg of copper and 5 ml of hydrochloric acid, less than 0.1 mg of cobalt was found in each precipitate, and 0.5 and 0.6 mg of copper in the respective filtrates. The cupferron precipitates obtained in analyses Nos. 4, 5, 6, 8, 9, and 18 of Table 1, were combined, ignited in porcelain, and dissolved in hydrochloric acid. Most of the iron was extracted with ether, and the cobalt and small quantity of iron (less than 1 mg) in the acid extract were precipitated by ammonium sulphide after the ether was removed. The sulphides were caught on a small paper, ignited, and the iron and cobalt weighed as Fe_2O_3 and Co_3O_4. The oxides were dissolved in hydrochloric acid, and the iron was precipitated with ammonium hydroxide. After filtering and washing, the iron hydroxide was dissolved in hydrochloric acid and the precipitation and filtration repeated. The precipitate was ignited, and the weight of Fe_2O_3 was subtracted from the combined $Fe_2O_3 + Co_3O_4$ previously obtained. The results showed that about 0.1 mg of cobalt was retained in each cupferron precipitate. In two similar tests in which 0.15 g of iron was precipitated by cupferron in the presence of 0.1 g of cobalt, the precipitates of iron were found to contain 0.4 and 1 mg of cobalt, respectively.

3. PRECIPITATION WITH α-NITROSO-β-NAPHTHOL, AND IGNITION OF THE PRECIPITATE

(a) GENERAL DISCUSSION

If precipitations by α-nitroso-β-naphthol are made in solutions containing cupferron, the solution should not be heated for more than 15 to 20 minutes nor at temperatures above 70° C. In almost all cases the filtrate becomes cloudy even though all of the cobalt has been precipitated. This is unfortunate because it makes it impossible to tell whether precipitation is complete unless the solution is filtered a second time and the precipitate ignited. If the specified amount of reagent has been added and the filtrate is clear when it passes through the funnel stem, no cobalt will be found in the filtrate. On standing, some of the reagent in the filtrate usually separates and adheres to the beaker. This deposit can be loosened by the continued action of hot water or by digestion with alkaline solutions.

(b) TESTING THE REAGENT

Various directions for the preparation of the solution of the reagent are given, but the solution most commonly used in this type of work is one prepared by dissolving 1 g of α-nitroso-β-naphthol in 15 ml of glacial acetic acid. For every 0.01 g of cobalt present 6 ml of the reagent is usually specified. If these directions are followed in the case of determinations involving 0.1 g of cobalt, such a large excess of reagent is added that it separates with the cobalt precipitate and makes it almost impossible to complete the ignition without loss by frothing. On the other hand, the reagent may have deteriorated to such an extent that an insufficient amount is added. The quality of

the reagent should be determined by the analyst, and a freshly prepared solution should always be used.

In this work three lots of the reagent were tested for their precipitating power as follows: Dissolve 1 g of reagent in 15 ml of glacial acetic acid, and add to it slowly and with vigorous stirring 300 ml of diluted hydrochloric acid (5+95) containing 0.25 g of cobalt. Digest, filter, wash, ignite, and weigh as described in the method for steels. One very old lot of reagent precipitated 0.048 g of cobalt, and two relatively new ones precipitated 0.068 g and 0.077 g, respectively. Theoretically 1 g should precipitate approximately 0.1 g of cobalt. Experimentally it was found that only a small excess of reagent is necessary for complete precipitation of the cobalt, and in the analysis of the steels listed in Table 1 the following procedure was adopted: First determine the precipitating power of the reagent in the manner just described, and then add one and one-half times as much as is required by the cobalt that is likely to be present. Never add less than 10 ml. In most of the work in this paper a reagent was used which precipitated 0.068 g of cobalt per gram. Approximately 35 ml of the prepared solution (1 g of reagent per 15 ml of glacial acetic acid) was thus used for 0.1 g of cobalt.

(c) INTERFERING SUBSTANCES

It is known that iron, copper, molybdenum, chromium, zirconium, titanium, vanadium, tin, and tungsten are also precipitated by α-nitroso-β-naphthol. Of these elements, all but small quantities of copper and possibly chromium are removed by the extraction with ether, by the precipitation with sodium hydroxide and sodium peroxide, or by the precipitation with cupferron. Copper, tungsten, chromium, vanadium, and molybdenum are only partially precipitated by α-nitroso-β-naphthol. Tests in which an excess of this reagent was added to a solution containing 5 ml of hydrochloric acid and 5 mg each of vanadium, tungsten, and molybdenum in 100 ml indicated that at least one-half of the vanadium, tungsten, and molybdenum passed into the filtrate. By precipitating 0.1 g of cobalt by the method outlined for steels and examining the precipitate of cobalt, 0.3 mg of copper was found in it when 1 mg of copper was present in the solution during the precipitation and 1.7 mg when 5 mg of copper was present. The final residues in analyses Nos. 15 to 25 in Table 1 were also examined for copper, and in no case was more than 0.2 mg found. This shows that interference by copper is not serious, but in very accurate work, copper in the weighed cobalt metal should be determined as described in the method. Similar tests with trivalent chromium showed that 0.4, 1.5 and 3.6 mg of chromium, respectively, were contained in the cobalt precipitates when 1.7, 9.0 and 43.0 mg of chromium were present in the solution during the precipitation of 0.1 g of cobalt with α-nitroso-β-naphthol. Nickel is not precipitated at all when alone. If cobalt is precipitated in a solution containing nickel, a little of the latter may come down with the cobalt, but this is not serious in the usual case. For example, only 0.2 mg was found in the cobalt metal in two analyses in which 0.05 g of cobalt was precipitated in the presence of 0.03 g of nickel.

(d) IGNITION OF THE PRECIPITATE

In most of this work the wet precipitate, with the filter paper folded around it, was placed in a porcelain crucible which was then put in a cold muffle furnace. The furnace was heated to a temperature of

about 750° C. in the course of two to three hours. No mechanical loss resulted, and covering the precipitate with oxalic acid to prevent volatilization of cobalt was not necessary. If the residue is to be weighed as Co_3O_4, the temperature of ignition should be held between 750° and 850° C. At temperatures above 900° C. (and even at 900° C. in the case of large amounts) the compound loses oxygen and approaches the composition CoO. By heating this oxide for one-half to one hour at 750° C. it again approaches the composition Co_3O_4. For example, a residue, which by subsequent ignition in hydrogen was shown to contain 0.1056 g of cobalt, indicated a cobalt content of 0.1053 g after igniting at 750° C. for one hour and then calculating to metal on the basis of Co_3O_4 as the composition of the oxide. The same residue, ignited at 1,000° C. for one hour, indicated 0.1020 g of cobalt by using the factor for conversion of Co_3O_4 to metal, and 0.1093 g when the factor for CoO was used. Ignition for one hour at 750° C. brought the weight back to indicate a cobalt content of 0.1053 g on the basis of Co_3O_4 as the composition of the oxide. Further ignition of this oxide for one hour at 850° C. did not cause any change in weight. In all accurate work in which more than 0.01 g of cobalt is determined the oxide should be reduced and cooled in hydrogen and the cobalt weighed as metal.

The results in Table 1 were obtained by igniting to the oxide in a muffle furnace at a temperature of 750° to 850° C., cooling, and weighing. The crucible and contents were then heated over the full heat of a Tirrill burner, and covered with a perforated quartz cover (Rose crucible cover). A slow but steady stream of hydrogen from a cylinder was introduced and the heating continued for 10 minutes. The burner was removed, the hydrogen momentarily stopped and the metal then cooled to room temperature under a stream of hydrogen. There was no evidence of any reoxidation of the metal nor any appreciable retention of hydrogen. Substituting nitrogen for hydrogen at the end of the cooling process did not affect the results. In standardizing the solution of cobalt sulphate (p. 663) the results obtained by ignition in hydrogen checked those obtained by electrolysis within 1 part in 1,000.

4. POSSIBLE SOURCES OF ERROR

1. In the analysis of materials containing 5 per cent or more of cobalt, ample time must be allowed for separation of the solution into two layers during the ether extraction, and the subsequent evaporation of the acid extract must be conducted slowly and cautiously in order to avoid loss of cobalt by spraying.

2. Very thorough washing of the precipitate obtained by cupferron is necessary to minimize retention of cobalt by the precipitate.

3. Weighing as "Co_3O_4" after ignition even under closely controlled conditions almost invariably yields slightly low results.

4. The separation of copper from cobalt by the use of cupferron is not quite perfect, and if the content of copper is high, correction should be made for copper in the final residue.

5. Blanks on the reagents should be determined. In this work steels Nos. 50a and 10d (see Table 1) were used at various times and were taken through the whole process just as if cobalt were being determined in them. A blank averaging 0.8 mg was obtained, most

of which was shown to be iron coming from the α-nitroso-β-naphthol reagent. A determination of iron in three cobalt residues and in an accompanying blank showed 0.9, 0.8, and 0.8 mg, respectively, in the cobalt residues and 0.8 mg in the blank.

IV. APPLICATION OF THE METHOD

The method serves well for the accurate determination of from a few hundredths of 1 per cent to 40 per cent of cobalt in most kinds of ferrous materials. It is especially applicable to the determination of cobalt in high-speed tool steels and in magnet steels containing as much as 40 per cent of cobalt. If the sample in which cobalt is to be determined contains more than about 0.2 g of nickel and manganese, the zinc oxide method [10] is preferable because large quantities of nickel and manganese produce bulky precipitates with sodium hydroxide and peroxide, whereas in the zinc oxide method these remain in solution and do not interfere. In ferrocobalt and cobalt metal the determination can be made more conveniently and accurately by electrolysis.

V. ACKNOWLEDGMENT

Acknowledgment is made to Dr. G. E. F. Lundell for technical advice.

WASHINGTON, March 25, 1932.

[10] B. S. Jour. Research, vol. 7, p. 883, 1931.